UNIVERSITY OF NAIROBI
INSTITUTE OF NUCLEAR SCIENCE AND TECHNOLOGY

M.Sc. Thesis Research

Computational Investigation into Development of a Prompt Gamma Neutron Activation Analysis (PGNAA) System with ^{241}Am-Be Neutron Source

BY:

TOLLAH STEPHEN

S56/74427/2012

A THESIS SUBMITTED IN PARTIAL FULFILMENT OF THE REQUIREMENTS FOR THE AWARD OF MASTER OF SCIENCE DEGREE IN NUCLEAR SCIENCE OF THE UNIVERSITY OF NAIROBI

DECLARATION

This thesis is my original work and has not been submitted in support of award of any degree or qualification of the University of Nairobi or any other University.

Signature _____ Date _____.

Tollah Stephen Owuor,
Reg. No.: S56/74427/2012
B.Sc. Physics
University of Nairobi.

This thesis has been submitted with our approval as University supervisors

Signature _____ Date _____.

Mr. D. M. Maina
Institute of Nuclear Science and Technology,
University of Nairobi.

Signature _____ Date _____.

Prof. David Chettle
Depart. Of Medical Physics and Appl. Radiation Sci.
McMaster University.

Signature _____ Date _____.

Prof. Michael J. Gatari
Institute of Nuclear Science and Technology,
University of Nairobi.

ACKNOWLEDGEMENT

First and foremost, I thank Almighty God, my family and Institute of Nuclear Science and Technology for providing me with this wonderful opportunity to grow both professionally and personally.

I wish to express my sincere gratitude to Mr. David Maina, the director of the Institute of Nuclear Science and Technology, for his time, guidance and help, and for giving me the opportunity to work on this project. My thanks goes also to my other supervisors, Prof. Chettle and Prof. Gatari for their guidance and useful suggestions during the course of this project. I am also grateful to Mr. Rotich whom provided me with the Monte Carlo MCNP-5 software.

I would also like to convey my sincere appreciation to Kenya Nuclear Electricity Board for awarding me the scholarship for this post graduate studies. My heartfelt gratitude also goes to NACOSTI for their generous funding towards my project. My appreciation is also extended to the Institute of Nuclear Science and Technology staff and the entire student fraternity for their unwavering support.

DEDICATIONS

This research is dedicated to God almighty for his mercies during the course of this project, to my father, the late James Tollah, for providing us with a strong education background. To my mother, brothers and sisters for their special support, love and patience. To my relatives, friends and colleagues for their moral support.

ABSTRACT

The purpose of this research was to conduct a computational investigation into developing a PGNAA irradiation system for elemental analysis using the Am-Be neutron source stationed at INST. The research focused on the parametric study of the variables that influence the design of the PGNAA system through Monte Carlo simulation using the MCNP5 particle transport code. The MCNP5 was used to model the PGNAA system and to generate the flux profile of fast, epithermal and thermal neutrons along the irradiation sites and the prompt gamma flux at the detector. The geometry of the facility was modeled as one cylinder with the neutron source at the center of the cylinder and paraffin wax as the moderator. The original irradiation site was modeled directly above the source while sites 2, 3 and 4 were modeled at radial distances of 5 cm, 10 cm and 15 cm from the source respectively. The study showed that the optimum thermal neutron fluxes are obtainable within the axial range of 0 cm to 6 cm along site 1 and a range of -6 cm to 6 cm along sites 2, 3 and 4 (measurement carried out with reference to the source upper surface). It was noted that the axial neutron fluxes peak near the center of the source and then reduce exponentially to very low values at the end of the channel. The percentage of the average radial thermal flux increases with the distance from the source while those of epithermal and fast neutrons decrease.

Site 2, which was simulated at 5 cm from the center of the Am-Be neutron source was selected as the ideal sample location site for PGNAA application. The thermal neutron flux of $45{,}152 \pm 388\ \mathrm{n.cm^{-2}s^{-1}}$ and the neutron ratios Φ_T/Φ_E and $(\Phi_T + \Phi_E)/\Phi_F$ of 3 and 2.8 respectively were achieved at this channel. MCNP was again used to study the response of the proposed system with an HPGe detector and sample holder added to the earlier set up. The background gamma ray spectrum was analyzed and the result showed high level of gamma-ray radiation from the construction materials. The system was used to obtain sensitivies and detection limits of pure samples of H, B, N, Si, and P. Based on the above neutron fluxes, elemental sensitivities for Hydrogen and Boron were calculated and obtained as 17.762(cps)/mg and 7.887(cps)/mg respectively. Since the simulated thermal neutron flux is very low, the sensitivity obtained for the elements are very low. Apart from hydrogen which showed discrepancy due to the interference from the high

background peak, boron had the best sensitivity. The boron sensitivity of 7.887(cps)/mg with a lower detection limit of 10 mg could be applied in analysis of boron samples.

NOMENCLATURE

PGNAA	Prompt Gamma Neutron Activation Analysis
BNCT	Boron Neutron Capture Therapy
CPGAA	Cold-Neutron Prompt Gamma-Ray Activation Analysis
FNAA	Fast Neutron Activation Analysis
INS	Isotopic Neutron Source
NAA	Neutron Activation Analysis
ENDF	Evaluated Nuclear Data File
HPGe	High- purity Germanium
MCNP	Monte Carlo for Neutron and Photons
Am	Americium
Be	Beryllium
INST	Institute of Nuclear Science and Technology
NIST	National Institute of Standards and Technology
TXRF	Total Reflection X-ray Fluorescence
ANRTC	Ankara Nuclear Research and Training Center
REGe	Reverse Electrode Coaxial Ge Detectors
EDXRF	Energy Dispersive X-ray Fluorescence
PTFE	Polytetrafluoroethylene
BGO	Bismuth germanate/ Bismuth germanium oxide

TABLE OF CONTENTS

LIST OF FIGURES

LIST OF TABLES

CHAPTER 1

INTRODUCTION

In this chapter, the introduction to this thesis is presented. Section 1.1 gives the background of the current research work. It is also dedicated to the relevant previous work and the motivation for carrying out the present work. The problem statement and justifications of the research work are provided in sections 1.2 and 1.3 respectively. Section 1.4 presents the purpose and specific objectives of the study.

1.1 Background

Neutron interactions with matter have been extensively utilized as a tool for identification and quantification of elements contained in various types of samples. The techniques that use neutrons as a tool to activate samples for analysis (Neutron Analytical Techniques) are classified into two broad groups in reference to the time of sample activation, detection and measurement of the radiation products, that is, online techniques and offline techniques. In offline, the induced radioactivity is observed after the end of irradiation while in online technique the capture gamma-rays are observed during neutron bombardment.

Delayed Gamma Neutron Activation Analysis (DGNAA), also called conventional NAA, is the most popular offline Neutron Analytical Technique (NAT) where the samples are irradiated with thermal neutrons and the induced radioactivity (β, γ) are subsequently measured for the determination of the concentrations of elements present in the sample. The energies of the gamma rays emitted during the radioactivity corresponds to specific elements present in the sample analyzed and are therefore used to identify the elements. This technique was invented back in 1930's but it became most popular in the early 1950's due to the availability of research reactors which could produce neutron fluxes in the order of $10^{12}\mathrm{n.cm^{-2}s^{-1}}$ and $10^{14}\mathrm{n.cm^{-2}s^{-1}}$ (Anderson et al., 2004). The invention of semiconductor detectors with high resolutions in the late 1960's further enhanced the scope of the technique which could then measure up to about 65 elements of the periodic table with sensitivity of the range of ppt to ppm (Perry et al., 2002). The elements which

could not be measured using NAA included those which produced a non-radioactive isotopes or very short-lived isotopes after neutron capture and those which produces only pure β – emitters e.g. phosphorus and sulfur. Such elements can only be analyzed by measuring their prompt gamma-rays which are emitted instantly during irradiation. This online neutron analytical technique in which the prompt gammas are measured during irradiation is known as Prompt Gamma Neutron Activation Analysis (PGNAA).

PGNAA is a highly sensitive non-destructive technique that can be utilized in the analysis of major, minor and trace elements in variety of samples (Bergaoui et al., 2015; Ghorbari et al., 2011). The nuclear reaction commonly utilized in PGNAA is the radiative capture (n, γ) reaction where a target nucleus absorbs a thermal neutron and the compound nucleus formed is in an excited state with energy nearly equal to the binding energy of the added neutron (Anderson et al., 2004). The compound nucleus de-excites almost instantaneously with a time scale of the order of 10^{-14}s (Shim et al., 2012) into a more stable configuration through emission of characteristic prompt gamma rays. In most cases, the new configuration yields a radioactive nucleus which also de-excites by delayed emission of a beta particle and a characteristic gamma photon. Both the delayed and prompt gamma radiations are characteristic of each element (Anderson et al., 2004), thus, their energies can be used as an identity for the emitter nuclide while their intensities are comparative to their amount hence their detection enables the determination of the constituents of the sample analyzed as well as their quantities.

In principle, PGNAA can detect almost the entire periodic table (Molnar, 2004). However, concentration of elements detected by PGNAA in a sample will vary since the detection limit for Prompt Gamma Neutron Activation Analysis depends on the capture cross-section of the specific elements contained in that sample and the background spectrum (Molnar, 2004). This technique is therefore best suitable for the analysis of light elements such as H, B, C, Si, P, S and Cl, because of their high neutron capture cross-section. Typically, PGNAA is used to complement NAA is situations where radioactive products cannot be formed.

PGNAA technique has been used at several neutron beam facilities all over the world (Howell et al., 2000; Anderson et al., 2004). In the following section, a few of the majorly known PGNAA facilities are briefly discussed including some of their applications. Detailed study of the applications of PGNAA based on isotopic neutron sources are also discussed in section 2.2.6.

One of the majorly known PGNAA facility in the world is the Centre for Neutron Research (CNR) which is situated at National Institute of Standards and Technology (NIST) in Gaithersburg, Maryland, USA. The CNR houses a 20 MW research reactor that delivers a thermal equivalent flux in the range of 10^8 n $cm^{-2}s^{-1}$ (Choi et al., 2001).

Extensive work has been performed with the PGNAA facilities at NIST. One of the key applications of the PGNAA at NIST is in the development of a PGNAA database through inter-laboratory comparison with other major PGNAA facilities (Choi et al., 2001). Other uses include the determination of the constituents of dietary supplements (Hight et al., 1993) as well as meat homogenates (Anderson, 2000). The facilities at NIST have also been used for elemental analysis including the study of ^{1}H content in doped strontium cerate ($SrCeO_3$) (Krug, 1995) and Titanium (Paul et al., 1996). The PGNAA have been used to examine trace elements in sapphire components for Laser Interferometer Gravitational Wave Observatory (McGuire et al., 2002), as well as examining the chloride distribution in concrete (Saleh et al., 2002).

The Seoul National University (SNU) and Korea Atomic Energy Research Institute (KAERI) jointly developed the SNU-KAERI PGNAA facility at the 30 MW HANARO research reactor. The facility has been in operation since 2001 (Choi et al., 2001). The facility delivers a neutron flux of 7.9×10^7 n $cm^{-2}s^{-1}$ in a 1 cm^2 area to the PGNAA sample position (Byun et al., 2000). The SNU – KAERI PGNAA facility has been used to analyze boron concentration for standard reference materials (Byun et al., 2004).

The Japan Atomic Energy Research Institute (JAERI) also operates a PGNAA facility using the Japan Research Reactor (JRR-3M) which is a 20 MW light water research reactor. The facility has both the cold and thermal neutron guides delivering 1.1×10^8 n $cm^{-2}s^{-1}$ and 2.4×10^7 n $cm^{-2}s^{-1}$ respectively (Yonezawa et al., 1993). The

JRR-3M PGNAA facility has been extensively used over a wide range of areas such as boron analysis in animal samples (Miyamoto et al., 2000), and heavy metals uptake in rats (Oura et al., 2000). It has also been applied in the analysis of marine oil, sediment, and bivalve sample (Yonezawa et al., 2001). Studies have also been done using the facility to analyze contaminants in agricultural samples (Tanoi et al., 2001).

The Institute of Isotope and Surface Chemistry in Budapest, Hungary, also operates a PGNAA facility at the Budapest 10 MW research reactor. The facility is equipped with a cold neutron source and delivers thermal equivalent neutron flux of 2×10^6 n $\mathrm{cm}^{-2}\mathrm{s}^{-1}$ at the target position (Choi et al., 2001). The Budapest Research Reactor (BRR) has been used in various research work including the developing of new prompt gamma library (Revay et al., 2000), detector calibration (Molnar et al., 2002), and hydrogen determination (Tompa et al., 2003) and also in analysis of metals (Kasztovszky et al., 2000). Other major facilities worldwide includes the PGNAA facility at the 100 MW Dhruva research reactor in India and the 500 kW Dalat Nuclear Research Reactor in Vietnam (Choi et al., 2001).

Non- reactor neutrons sources such as neutron accelerators and isotopic sources have also been used for PGNAA experiments. Isotopic sources have been used in the past mostly to develop portable PGNAA devices to perform on site analysis in cases where it is impractical to transport samples into the laboratories (Clayton et al., 1983). A common use for such portable devices is in borehole logging for the analysis of coal deposits for multiple elements (Borsaru et al., 2001). Khelifi et al. (2007) successfully used a 37Gbq Am-Be neutron source and a portable hyper pure germanium detection system in a PGNAA set up to determine detection limits for pollutants in water. The neutron source produced a flux of 2.2×10^6 ns^{-1} and was located inside a paraffin block in irradiation position. Hamed et al. (2006) also used an isotopic based PGNAA facility to estimate the percentage concentration of boron in Egyptian tomato and spinach samples as biological materials, also in one of the byproducts of one the Egyptian motor oil and glass samples as industrial materials. This system, which was set up at the Radiative Environmental Pollution Department, consisted of 252Cf source and HPGe detector which was used to

collect the gamma rays that were emitted. The neutron flux density at the target position was measured and found to be 5×10^5 n $cm^{-2}s^{-1}$.

1.2 Problem statement

Currently, the primary techniques for elemental analysis available at INST are the EDXRF, TXRF and NAA. While EDXRF and TXRF have been successfully used to identify heavier elements, analysis of light and rare earth elements has presented a special challenge to the XRF techniques. Light elements have very low fluorescent yield, i.e. fewer fluorescence are produced for every photoelectric interaction in the atom as the auger emission is favored in the low-Z elements (Cember and Johnson, 2009). Also, the characteristic X-rays emitted by the light elements are relatively of low energy and are mostly absorbed within the sample matrix. These low energy X-rays have low penetration power and are severely attenuated by the beryllium window and the air gap between the sample and the detector. The above reasons leads to very poor photon count at the detector making it very difficult to analyze light elements by XRF techniques. In addition, XRF techniques also require sample preparation which may cause contamination to sample. The traditional Neutron Activation Analysis (NAA), for which the isotopic neutron source set up at INST have been used, is restricted to delayed gamma or beta rays from radioactive daughter nuclei from about 70 elements and is not sensitive to some important elements such as H, B, C, O, N, Si, P, S and Pb (Perry et al., 2002). It is then the goal of this study to expand the experimental capabilities of the INST isotopic neutron source by characterizing and designing a proposed PGNAA facility to complement the existing analytical facilities at the institute.

1.3 Justification

PGNAA will provide a unique tool for the determination of low-Z and rare earth elements and serve as a complementary technique to NAA and on its own by allowing determination of elements with too long or too short half-life to be conveniently analyzed by NAA(e.g. carbon) (Byun et al., 2002). Following success completion of the development of the PGNAA facility, it will aid in the accurate and faster analysis of the hydrogen content in the Kenyan petroleum byproducts and also in the exploration of

minerals. The facility will also open up a new research field in medical physics at the institute by helping with the analysis of boron contents in biological materials and could also help in the future development of Boron Neutron Capture Therapy (BNCT) that can be used for cancer treatment. The facility could also be used for industrial purposes such as in the online analysis of cement products.

PGNAA has distinct advantages over other techniques in that the long ranges of neutrons and of capture gamma rays makes it possible to analyze large samples e.g. geological samples. These large samples cannot be analyzed by NAA since they are too large to be placed inside the irradiation channel as required by NAA. Also, the technique does not require special sample preparation which may cause structural damage to the material; this reduces the chances of sample contamination and furthermore since the technique is non-destructive the samples can still be used for other analytical techniques. PGNAA is capable of online sample analysis and can improve the sample turnaround time. Lastly, PGNAA is capable of simultaneously measuring major and minor elements in various types of samples.

1.4 Objectives

General objective

The main objective of this scientific study was to conduct a computational investigation into developing a PGNAA methodology for elemental analysis using the Am-Be neutron source at INST.

Specific objectives

1. To investigate the flux and energy distribution of neutrons emitted from the INST Am-Be neutron source and to optimize the flux for PGNAA applications.
2. To model the response of the proposed detection system.
3. To obtain the theoretical sensitivity and detection limits achieved by the facility for some selected elements.

CHAPTER 2

LITERATURE REVIEW

This chapter provides a general overview of the PGNAA system, its concept, design, implementation and applications. The chapter is arranged as follows: The basic overview of the PGNAA is provided in section 2.1. Section 2.2 and 2.3 deals with the theoretical concept applicable to this study while section 2.4 presents the general design of PGNAA system. Neutron sources are discussed in section 2.5 and the applications of radioisotope based PGNAA are also presented in section 2.6.

2.1 Background

The development of Prompt gamma analysis started slowly in 1934 after the first reports of gamma radiation from neutron capture reaction in hydrogenous materials (Molnar, 2004). It was observed that when neutrons are captured by hydrogenous materials, a high penetrating gamma radiation is emitted. The gamma ray observed was later identified as the 2223.2487 keV energy prompt gamma from $^{1}\mathrm{H}(\mathrm{n},\gamma)^{2}\mathrm{H}$ nuclear reaction. Later in 1936, Gyorgy Hevesy proposed the use of neutron capture reaction for the purpose of elemental analysis (Paul et al., 2000).

Proper utilization of PGNAA began in 1966 when the first reactor-based prompt gamma neutron activation analysis was carried out by Isenhour and Morrison utilizing a pulsed neutron beam from a nuclear reactor and detecting the gamma rays with a NaI scintillator detector (Anderson et al., 2004). PGNAA received a major boost in late 1960s through the development of semiconductor gamma ray detectors which had resolution more than 20 times better than the NaI scintillators (Paul et al., 2000). This superior resolution aided in the interpretation of complex spectra from neutron capture reaction, and also helped to improve the detection limit of elements analyzed by PGNAA facilities that were incorporated with the semiconductor detector. Analysis of prompt gamma rays have since become a well-established analytical tool with applications in various research fields.

2.2 The concept of PGNAA

The fundamental physical process occurring in PGNAA is the radiative neutron capture reaction (n, γ). In this type of reaction (Figure 2.1), a target nucleus (${}^{A}_{Z}X$) absorbs a neutron resulting in an excited compound nucleus (${}^{A+1}_{Z}X^{*}$) whose excitation energy is equal to the neutron binding energy plus the kinetic energy of the target neutron as is illustrated in equation (1).

$$\text{Excitation Energy} = BE_n + K.E_n \quad (1)$$

Where, BE_n is neutron binding energy.
and $K.E_n$ is the kinetic energy of the target neutron

When irradiating with neutrons whose kinetic energies are less than 0.5 eV, the capture states have well-defined values which are approximately equal the neutron binding energies. For most stable nuclei the binding energies range between 6 – 10MeV (Anderson et al., 2004). During the transition, the excitation energy of the compound nucleus formed immediately after radiative capture is rapidly shared among the many nucleons within that nucleus. The nucleons almost instantaneously de-excite through a series of discrete energy transitions in which a gamma ray is released for each transition with energy equal to the energy of the transition minus the recoil energy of the nucleus as shown by the following equations.

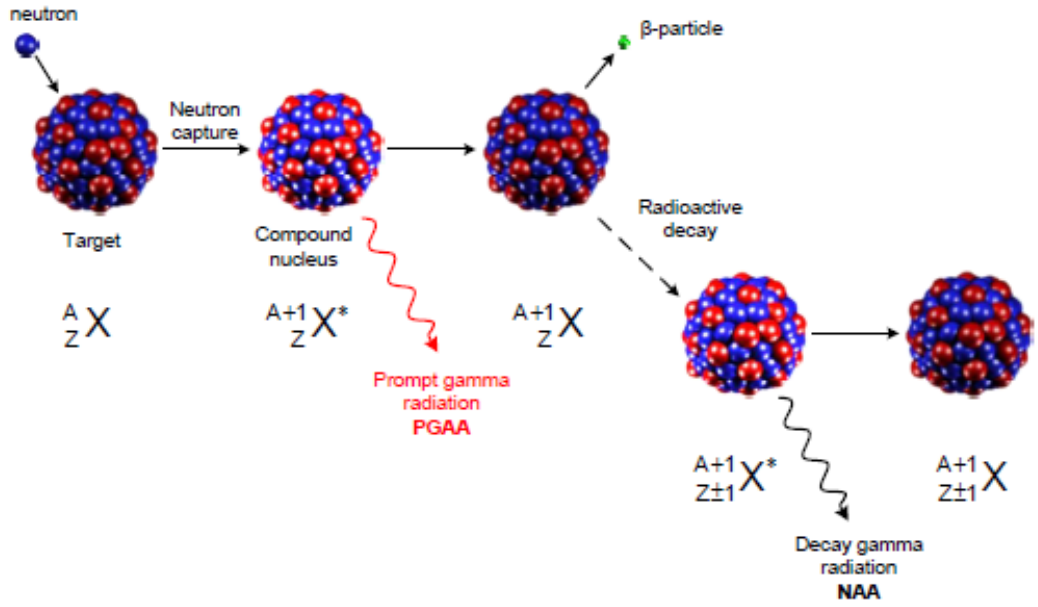

Figure 2.1 Reaction scheme of a thermal neutron impinging on a target nucleus, yielding a radioactive nucleus (adapted from Lylia et al., 2013)

$$E_\gamma = E_T - E_R \tag{2}$$

$$\text{where; } E_R = \frac{P^2}{2M} = \frac{E_\gamma^2}{2Mc^2} \tag{3}$$

$$\text{since } E^2 = P^2c^2 + m^2c^4 \tag{4}$$

and, E_γ is the energy for the released gamma ray

E_T is the energy of the transition

E_R is the recoil energy of the nucleus

P = momentum

m = mass of the nucleus

c = speed of light

As the compound nucleus de-excites, it releases gamma rays of discrete energy levels. Since the nucleus has energy levels which are distinct for each isotope of each element (as

those of atomic energy level), the gamma rays radiation released from the nucleus is thus characteristic of the emitting nuclide. Therefore, the energy value of these gamma ray radiations can be used as fingerprints for identifying the emitting nuclide and their intensities are proportional to the number of atoms of that particular element present in the sample.

If the resulting nucleus from the (n, γ) reaction is unstable as in some cases, the nucleus will further decay by β-particle emission and the subsequent de-excitation of the daughter nuclide gives rise to emission of one or more delayed gamma-ray photons. The detection of these delayed gamma radiations and radioactivity is the basis of the traditional NAA while the basis of PGNAA is the detection of mainly the prompt gamma rays.

Apart from radiative capture, capture reaction with emission of charged particles are also common reactions taking place inside PGNAA facility. Charged particles are mostly emitted when slow neutrons interact with light elements. The most relevant cases of this type of reaction includes: $^{3}He(n, p)^{3}H$ with thermal cross section equal to 5333 b; $^{6}Li(n, t)^{4}He$ (940 b), $^{14}N(n, p)^{14}C$ (1.83 b) without gamma emission and $^{10}B(n, \alpha)^{7}Li$ (3837 b).

2.3 Characteristics of PGNAA

2.3.1 Neutron properties

Neutrons are uncharged nuclear particles with a mass of approximately $1.68x10^{-27}$ kg (940 $keVc^{-2}$) (Dove, 2004). An isolated neutron is not stable but decays in beta decay with a half-life of 10.25 minutes to a proton by emitting an electron and an antineutrino.

Based on their energy spectrum, neutrons are commonly divided into three major categories: thermal/slow neutrons (<0.5 eV), Epithermal neutrons (0.5 eV- 0.5 MeV), and fast neutrons (>0.5 MeV). Since neutrons are uncharged, they are unaffected by the electrostatic fields of the electron cloud and of the protons contained inside the nucleus. Thus neutrons can penetrate the electron cloud unaffected and directly interact with the nucleus without being repelled. Furthermore, since the neutrons are uncharged, they can penetrate deep into materials without interacting and hence can be used to probe large

samples. Neutron wavelength is inversely proportional to its momentum, thus its velocity as shown in eq.5.

$$\lambda = \frac{h}{p_n} = \frac{h}{m_n v} = \frac{395.6}{v_n} \quad (5)$$

2.3.2 Neutron-nuclear reaction

Neutrons essentially interact with only the atomic nucleus. Neutron – nuclear reactions can either be inelastic scattering, elastic scattering or absorption depending on the energy of the incident neutron.

a) Elastic scattering

Neutrons at the time of their generation from isotopic neutron sources such as Am-Be are mostly fast neutrons. These fast neutrons mainly undergo elastic collision with the surrounding atoms as they penetrate through the matter. In this type of reaction, part of the neutron kinetic energy is transferred to the nucleus but the nucleus is still left in its ground state. The minimum energy E of the scattered neutron can be calculated by equation 6 (Cember and Johson, 2009).

$$E = E_0 \left[\frac{M - m}{M + m}\right]^2 \quad (6)$$

where; E_0- energy of incident neutron,

m - mass of the incident neutron, and

M - mass of the scattering nucleus.

Examining equation (6) when $M \approx m$ and when $M \gg m$ it follows that low Z elements are best suitable to moderate the neutrons. In the same way, neutrons produced by the isotopic source undergo scattering reactions with the paraffin wax and are moderated down to energies at which they are in thermal equilibrium with the atoms of the samples.

b) Inelastic scattering

In this type of neutron reaction, part of the neutron kinetic energy is absorbed by the target nucleus thereby exciting the nucleus. The excitation energy is subsequently emitted as a

photon of gamma radiation. This kind of reaction is best shown by the compound nuclear model in equation (7).

$$ {}^{1}_{0}\mathrm{n} + \left({}^{\mathrm{A}}_{\mathrm{Z}}\mathrm{X}\right) \rightarrow \left({}^{\mathrm{A+1}}_{\mathrm{Z}}\mathrm{X}\right)^{*} \rightarrow {}^{1}_{0}\mathrm{n} + \left({}^{\mathrm{A}}_{\mathrm{Z}}\mathrm{X}\right)^{*} \rightarrow {}^{1}_{0}\mathrm{n} + {}^{\mathrm{A}}_{\mathrm{Z}}\mathrm{X} + \gamma \qquad (7) $$

Where; $\left({}^{\mathrm{A}}_{\mathrm{Z}}\mathrm{X}\right)$ is the target nucleus,

$({}^{A+1}_{Z}X)^{*}$ excited compound nucleus,

$\left({}^{\mathrm{A}}_{\mathrm{Z}}\mathrm{X}\right)^{*}$ is the excited nucleus,

γ is the gamma radiation

Inelastic scattering is a threshold phenomenon and usually occurs for relatively high neutron energies (>10keV).

c) Neutron absorption reaction

Once the neutrons are in thermal equilibrium with the surrounding atoms, a neutron gets absorbed by the target nucleus and hence forms a new nucleus with a unit increase in mass number. The resulting compound nucleus can decay by either charge particle emission (n, α) or (n, p) reactions, radiative capture (n, γ), neutron producing reactions $(\mathrm{n}, \mathrm{xn})$ or by fission reaction. Of all the neutron absorption reactions, radiative neutron capture is the most significant for PGNAA technique.

2.3.3 Gamma ray

Gamma rays are high energy electromagnetic waves that originates inside the nucleus of an atom. They are produced mainly by decay of the excited nucleus or by a nuclear reaction. However, low energy gamma rays can also be formed by means of accelerating or decelerating a charged particle in a medium or during annihilation of particles and antiparticle. In this study, prompt or capture gamma rays are of most significance. Prompt gamma radiations are emitted during the capture reactions in the nucleus. These reactions take place at all incident neutron energies but have a higher probability of occurrence at thermal energies.

2.3.4 Gamma ray interaction with matter

Gamma rays can interact with matter in numerous different ways, however, for the photons of energies considered in PGNAA technique, only three processes are predominant. The first predominant method is the photoelectric effect; when a low energy gamma ray strikes an atom, the total energy of the photon is absorbed and an electron is ejected from the atom. This type of interaction mostly occurs with low energy gammas rays interacting with high Z elements and rarely occurs with gammas having energies above 1 MeV (Figure 2.2). The photoelectron ejected will deposit its energy in the material near the point of collision through ionization and excitation. As a consequence of the photoelectric effect, a vacancy is created in one of the bound shells of the atom. This vacancy is quickly filled by a free electron of the absorber material or by an electron belonging to other shells of the same atom. Therefore, one or more characteristics x-rays are generated as the atom de-excites. In some cases, the excitation energy is transferred to an outer electron which is then ejected from the atom carrying away the atomic excitation energy with it. This Auger electron production dominates for low atomic number elements while characteristic X-rays is favored for high atomic number elements.

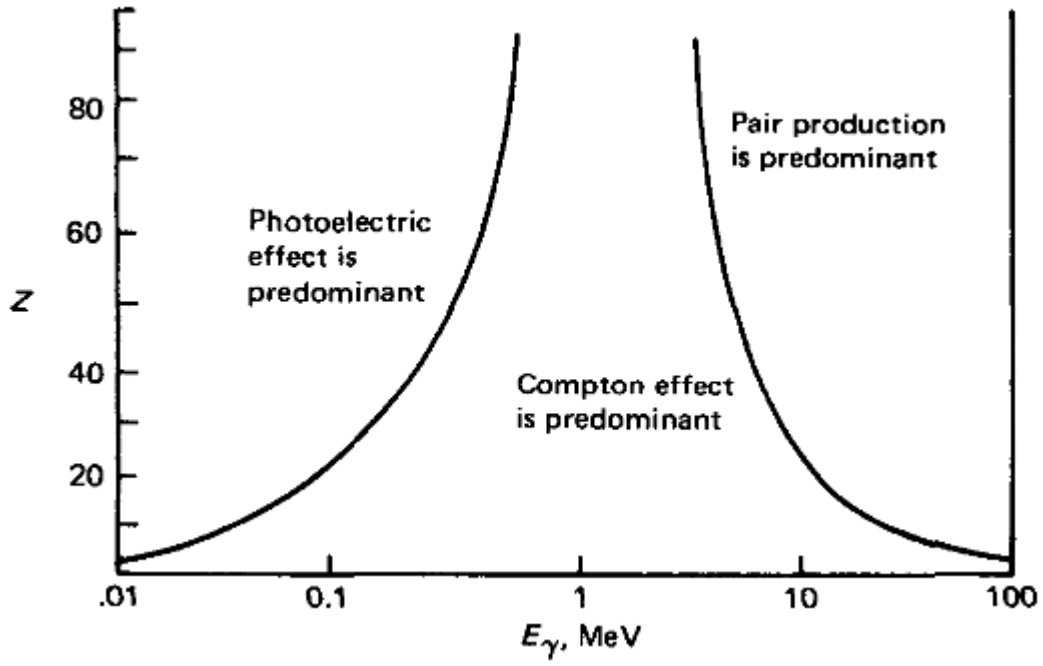

Figure 2.2 The relative importance of the three major gamma interactions (extracted from Nicholas, 1995)

The second mode of interaction, Compton scattering, is the predominant mechanism by which the photon interacts with low Z-elements (Figure 2.2). Here, the incoming gamma radiation interacts with the orbital or free electron transferring part of its energy to the electron (Figure 2.3). This process occurs mostly at a higher energy than the photoelectric effect i.e. energy of about 0.1 MeV and higher (Cember and Johnson, 2009).

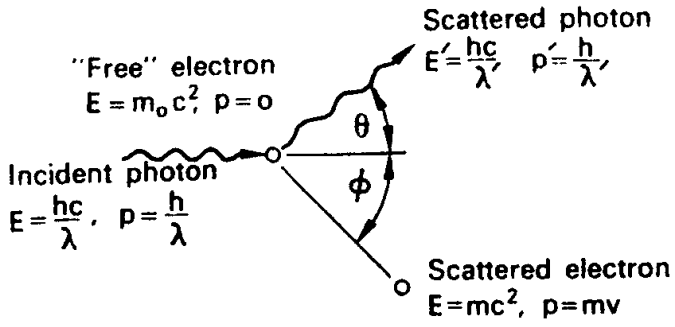

Figure 2.3. Compton scattering reaction (adapted from Cember and Johnson, 2009)

The other predominant process is the pair production. In this type of interaction, the photon energy is entirely absorbed by an atom, and an electron-positron pair is produced (Figure 2.4). This type of reaction takes place at much higher energy, that is, for the reaction to take place, the original gamma ray must have at least 1.02 MeV of energy. This threshold energy is used to produce the pair of particles while the excess energy becomes the kinetic energy of the emitted particles.

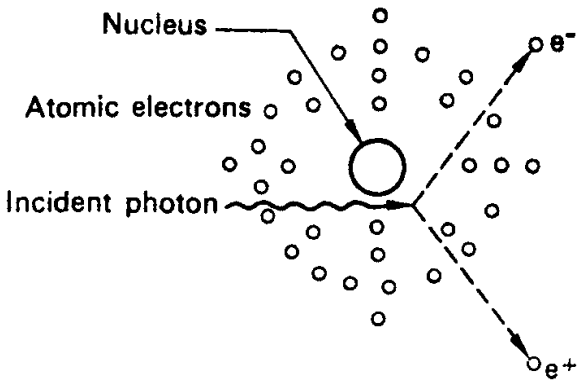

Figure 2.4 . Pair production reaction (adapted from Cember and Johnson, 2009)

2.3.5 Fundamental quantities

One of the fundamental quantities considered in PGNAA technique is the neutron cross section, σ, which characterizes the probability of interaction between the neutron and the target nucleus. For a given nuclear target and reaction, the cross section strongly depends on the projectile velocity, ν. In the slow neutron range the dependence follows the $1/\nu$ law. The thermal neutron cross sections, σ_0, for PGNAA neutron data library are usually tabulated for 2200 $\mathrm{m\,s^{-1}}$ monochromatic neutrons. The cross section can therefore be determined for any other neutron velocity as shown by equation (8).

$$\sigma(\nu) = \sigma_o \frac{\nu}{\nu_0} \tag{8}$$

where ν_0 = 2200$\mathrm{m\,s^{-1}}$.

Another important quantity in PGNAA is the partial gamma ray production cross section, σ_γ, which is given by equation (9):

$$\sigma_\gamma = \theta \sigma P_\gamma \tag{9}$$

where θ and P_γ are the natural isotope abundance of the given nuclide and the gamma emission probability respectively. This quantity characterizes the probability of production of a given gamma ray for one atom of the examined element.

The gamma peak count rate, ρ_γ, at a given energy of the spectrum can therefore be written as:

$$\rho_\gamma = \varepsilon(E_\gamma) n \sigma_\gamma \phi \tag{10}$$

where n is the number of target atoms, $\varepsilon(E_\gamma)$ is the counting efficiency at a given gamma ray energy and ϕ is the neutron flux.

2.3.6 Sensitivity and detection limit

The capability of a PGNAA facility for elemental analysis is partially considered in terms of the sensitivity and the detection limit (Byun and Choi, 2000). The analytical sensitivity, S, for a specific element is defined by equation (11) below:

$$S = \frac{\rho_\gamma}{m} = \frac{N_A}{M} \sigma_\gamma \phi \varepsilon(E) \tag{11}$$

Where S is the sensitivity, ρ_γ is the gamma peak count rate, m is the mass of the sample analyzed, N_A is Avogadro's number, M is the atomic mass, σ_γ is the partial gamma ray production cross section, ϕ is the neutron flux, and $\varepsilon(E)$ is the counting efficiency at a given gamma ray energy.

From the practical point of view;

$$S = \frac{N_G - N_B}{t \times m} \tag{4}$$

Where N_G and N_B are respectively the total and background count under the peak of a particular energy, t is the detection period while m is the mass of the sample analyzed. The counts are obtained from samples of pure elements, thus, the sensitivity does not

depend on the sample but depends on the experimental setup i.e. the neutron flux at sample position, the geometry and the detection system.

The analytical detection limit (DL) decision is usually based on hypothesis testing. In this case, the type I (α) and type II (β) errors of the hypothesis have to be specified. The type I error refers to the rejection of the null hypothesis when it is true i.e. to conclude that a sample contains the analyte when it actually does not. Type II error occurs if one fails to reject the null hypothesis when it is false. The decision in favor of the alternate hypothesis is based on a particular concentration, the decision limit, CL, chosen to keep type I error at a specified desired level. The analytical detection limit is usually calculated with $\alpha = \beta = 0.05$ and CL=0.5DL (Curie, 1999).

Thus,

$$\mathrm{DL} = 2 \times \mathrm{CL} = 2 \times \mathrm{Z}_{.95} \times \mathrm{S} \tag{5}$$

$$\mathrm{DL} = 2 \times 1.645 \times \mathrm{SD} = 3.29\mathrm{SD} \tag{6}$$

Where SD is the standard deviation of the probability distribution of making type I error.

$$\mathrm{SD} = \frac{\sqrt{\mathrm{N_B}}}{\mathrm{S} \times \mathrm{t}} \tag{7}$$

Thus, the detection limit is calculate from equation (16) shown below.

$$\mathrm{DL} = \frac{3.29 \times \sqrt{\mathrm{N_B}}}{\mathrm{S} \times \mathrm{t}} \tag{8}$$

The actual sensitivity and detection limit may vary between experimental setups and depends on several factors including;-

1. Thermal neutron flux at the sample position (Asamoah et al., 2011).
2. The distance between the sample and the detector (Paul et al., 2000).
3. Gamma ray contribution from the construction materials (Curie, 1999).
4. The detector arrangement (Khelifi, 2007).

2.3.7 Multi-elemental PGNAA capability of isotopic source based facility

Isotopic source based PGNAA facilities have not been extensively utilized and much of the available data for PGNAA are either from reactor based or generator based facilities. The sensitivity and detection limits of elements shown in table 2.2. (Perry et al., 2002) were calculated by Yonezawa based on the cross section yields of the most intense gamma rays, with the Japan Atomic Energy Research Institute (JAERI) cold neutron beam facility. The D attached to a particular gamma energy indicates that the gamma rays are from short-lived radioisotopes produced during the PGNAA measurement.

Turhan et al. (2004) have shown the feasibility of using AmBe based PGNAA system for determining the sensitivity and detection limit for standard boric acid samples. The set up installed at Ankara Nuclear Research and Training Center (ANRTC) consisted of a 22.6% Reverse Electrode Coaxial Ge Detectors (REGe) detector and a 740 GBq $^{241}\mathrm{Am}-\mathrm{Be}$ source moderated with water and paraffin. They observed a thermal fluence rate of $2.36\times10^{4}\mathrm{n.\,cm^{-2}s^{-1}}$at the sample irradiation position and a corresponding Cd ratio of 22 for gold. Using this system, the detection limit for boron in standard boric acid was found to be 43mg for a counting time of 60,000 seconds.

Ramanjaneyulu et al. (2007) determined boron concentration in ground water samples by PGNAA using the reflected beam from the DHRUVA reactor which delivered a neutron flux of $10^{6}\mathrm{n.\,cm^{-2}s^{-1}}$ at the sample holder. The boron sensitivity of the PGNAA facility was found as 18.83 cps $\mathrm{mg^{-1}}$ and a detection limit of 0.2μg $\mathrm{g^{-1}}$.

Table 2.1 Sensitivity and detection limit for selected gamma rays calculated by Yonezawa, with JAERI cold neutron beam.

Element	E_γ(KeV)	Sensitivity (cps/mg)	Detection limit (μγ/g)	Element	E_γ(MeV)	Sensitivity (cps/mg)	Detection limit (μγ/g)
H	2223	3.14	1.3	Ru	540	0.278	11
Li	2032	0.0467	24	Pd	717	0.169	19
Be	6809	0.00566	49	Ag	198	5.21	1.7
B	478	2300	0.0025	Cd	558	403	0.0108
C	1262	0.0029	807	In	273	13.5	0.39
N	5269	0.007	115	Sn	1293	0.0178	110
F	1634 D	0.0272	267	Sb	283	0.108	40
Na	473	0.867	4.7	Te	603	0.609	11
Mg	3918	0.00752	73	I	134	1.04	10
Al	1779 D	0.11	15	Ba	1436	0.0311	41
Si	3540	0.0298	23	La	218	0.338	22
P	513	0.0909	54	Ce	662	0.0956	29
S	841	0.253	15	Pr	177	0.548	14
Cl	1165	3.6	0.79	Nd	697	7.99	0.68
K	770	0.574	3.1	Sm	334	749	0.0071

Table2.1 (continued)

Element	E_γ(keV)	Sensitivity (cps mg^{-1})	Detection limit ($\mu\gamma$/g)	Element	E_γ(keV)	Sensitivity (cps mg^{-1})	Detection limit ($\mu\gamma$/g)
Ca	1942	0.0546	18	Eu	90 D	740	0.047
Sc	228	14.9	0.65		221	25.7	0.34
Ti	1381	1.9	0.79	Gd	182	1564	0.0064
V	125	285	3.9	Tb	352	0.11	24
	1434 D	1.69	0.7	Dy	186	67.4	0.11
Cr	835	0.688	3.9	Ho	137	7.2	1.8
Mn	212	2.67	2.7	Er	816	4.55	0.35
Fe	352	0.229	28	Tm	205	3.17	1.9
Co	556	2.92	0.94	Yb	515	2.53	1.8
Ni	465	0.558	5.1		636	0.277	5.9
Cu	278	0.789	6.4	Lu	458	1.1	2.7
Zn	1078	0.107	15	Hf	214 D	14	0.57
Ga	508	0.174	28	Ta	270	1.29	4.3
Ge	596	0.393	13	W	146	0.583	18
As	165	1.13	8.7	Re	208	1.2	5.7
Se	614	0.796	4.4	Ir	352	0.144	19
Br	245	0.919	6.5	Pt	356	1.22	3
Sr	1837	0.134	7	Au	215	1.36	4.5
Y	777	0.167	11	Hg	368	53.7	0.055
Zr	934	0.0261	71	Tl	348	0.0691	46
Nb	256	0.0795	53	Pb	7368	0.00147	240
Mo	778	0.465	3.8	Bi	320	0.00172	2200

2.4 Components of the PGNAA.

The major components of PGNAA system include a neutron source, a gamma ray detector, nuclear signal-processing electronics, and software for gamma spectroscopy. Since the measurement of the prompt gamma is done during irradiation, the complete PGNAA detection system is incorporated with HPGe detector and a multichannel analyzer system integrated with a computer (Figure 2.5). The detector collects the signals which are then taken through the electronic acquisition system for processing.

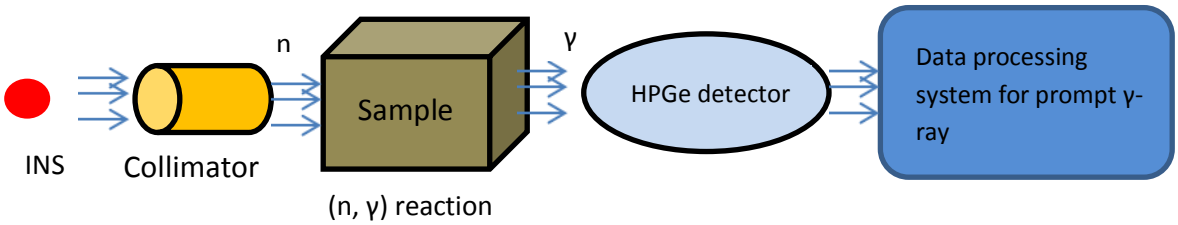

Figure 2.5 Schematic structure for a PGNAA system based on INS

2.5 Neutron sources

Neutrons can be produced by various sources. Large fluxes of neutrons are produced by neutron reactors and neutron generators (up to10^{15} ns^{-1}). But small neutron fluxes (up to10^{8} ns^{-1}) can also be produced by isotopic neutron sources (INS) e.g. ^{241}Am-Be, ^{252}Cf etc. Despite their small output fluxes, these isotope sources can still be utilized since they are relatively inexpensive for low neutron emission (usually $<10^{8}ns^{-1}$) or due to their compact size, which facilitate some unique applications such as building portable PGNAA systems. Isotopic neutron sources such as Am-Be source have the advantage of producing relatively stable neutrons fluxes for several years i.e. there is temporal stability of the neutron fluxes; this makes them suitable for calibration purposes in neutron dosimeters.

Some of the disadvantages of INS include their broad spectra. Also their neutron output cannot be pulsed and they cannot be turned off, hence they must be contained within bulky shielding at all times.

2.6 Applications of radioisotope based PGNAA

A wide variety of elements have been analyzed by neutron activation analysis techniques (PGNAA and NAA) in laboratories and in the field using the isotopic neutron sources. PGNAA is especially suitable for determining elements in geological, biological and environmental samples in which light elements form a good fraction of the matrix. Many applications utilizing isotopic sources have been quoted in material science (Nirmal, 2011), environmental studies (Zhao et al., 2007), biology (Ghorbari et al., 2012), industrial applications (Samir, 1993; Saleh et al., 2000), chemistry, geology (Gozani et al., 1978) and archaeology (Kasztovszky et al., 2005). Some of the most common applications are discussed below.

2.6.1 Measurement of coal or oil quantities

Geological measurements often require portable PGNAA devices since it is impractical to bring geological formations into the reactor facilities. In-situ elemental analysis is the most common application of isotopic neutron sources utilizing PGNAA techniques. In this way PGNAA is used for ore mining in mineral industries and oil explorations as an environmental friendly technique. Borsaru et al. (2004) demonstrated PGNAA technique using ^{252}Cf isotopic neutron source for in-situ determination of Ash, Fe, Si, Al and density of coal in water filled boreholes. In another study, several elements including C, H, N, S, Al, Si, Ca, Ti, Fe, Na, K and Cl were detected in coal samples with ^{252}Cf source irradiation (Gozani et al., 1978).

2.6.2 Environmental pollution studies

Toxic environmental pollutants such as Cd and Hg have good response in prompt gamma spectra, hence PGNAA, alone or in combination with other methods, can be used to analyze environment samples. Determination of buried materials such as landmines, heavy metals etc. and the determination of the concentration of such materials or contaminants in soil can also be conveniently done by PGNAA using portable isotopic based instruments (Shue et al., 1998). The fast neutrons from the radioisotope on the surface irradiates the soil and in the process are thermalized by the soil. The thermal neutrons are then captured by the normal soil constituents and also by the soil

contaminants. A collimated radiation detector place above the soil then measures the intensities of the characteristic gamma rays released by the elements in the soil that captured the neutrons.

2.6.3 Medical applications

PGNAA is a very useful technique in the field of medicine. Analysis of boron concentration in biological samples is a major challenge using other analytical techniques, but its high cross-section for producing the 478 keV prompt gamma lines when irradiated with neutrons provides a very sensitive non-destructive analysis (Ghorbari et al., 2012). Many applications have been carried out in BNCT to evaluate the ^{10}B concentration in biological samples (Choi et al., 2001). $^{10}\mathrm{B}\ (\mathrm{n}, \propto)^{7}\mathrm{Li}$ reaction is used in boron neutron capture therapy, and the alpha particles emitted are used to kill cancerous cells selectively leading to the elimination or reduction of the tumor.

2.6.4 Determination of chemical weapons, explosives and various narcotics

Nuclear techniques based on neutron and gamma rays from radioisotope sources e.g. ^{241}Am-Be, ^{252}Cf etc. can be used to locate and identify explosives and contraband hidden in cargo containers. Almost all explosives and illicit materials are made from the light elements hydrogen, carbon, nitrogen and oxygen in varying ratios (Shue et al., 1998). Light elements are characterized by large cross-sections for neutron reaction hence neutron technique is an ideal tool for detecting the contrabands.

2.6.5 Industrial applications of isotopic systems

Several industrial applications also require portable PGAA devices. Corrosion in iron pipes can be detected by prompt gamma emission rapidly, and without regard to pipe temperature or surface conditioning. Organic scales, which may be missed by more conventional techniques, can also be detected by PGAA. Samir (1993), successfully applied the PGNAA technique in thickness gauging of iron pipes to determine the changes in wall thickness that might have occurred due to corrosion and also to analyze the type and quantity of scale that may accumulate inside pipes at desalination plants.

Prompt gamma measurements have also shown promise for the analysis of "green liquor", an aluminum formed during the refinement processing, and is an alternative to atomic absorption spectroscopy techniques (Gardner et al., 1997). Gardner et al. (1997) found out that PGNAA is very sensitive to chlorine and somewhat to sodium contained in green liquor. On the other hand, they also found that NAA is very sensitive to aluminum and slightly sensitive to sodium but not to chlorine. The two techniques can therefore complement one another to great effect in the analysis of green liquor.

CHAPTER 3

MODELLING AND SIMULATION OF THE PGNAA EXPERIMENT.

This chapter provides the description of the computation investigation part of the thesis. First and foremost, the description of the Am-Be neutron system at INST is provided in section 3.1. The computational tool in this work is the Monte Carlo (MC) particle/radiation transport simulation; a brief introduction to MC technique is provided in section 3.2. Section 3.3 gives the description of the MCNP code used and finally section 3.4 presents the guidelines on how to code MCNP-5 input files and how to obtain the results from the output. The irradiation system as modelled in MCNP-5 are also provide in this section.

3.1 The Am-Be irradiation source at INST

The irradiating facility (Figure 3.1) station at the Institute of Nuclear Science and Technology consists of a single 370 GBq ^{241}AmBe neutron source, with neutron emission rate of $2.2 \times 10^{7}\ \mathrm{ns}^{-1} \pm 10\%$ as per the source certificate. The neutron source, a cylindrical capsule of dimensions 3.0 cm diameter and 5.0 cm overall length, is placed at the center of a moderating solid paraffin block of dimensions 50 cm diameter and height of 55 cm. An axial cylindrical cavity of dimensions 3.2 cm diameter and 23.5 cm height is bored perpendicularly at the center of the paraffin block.

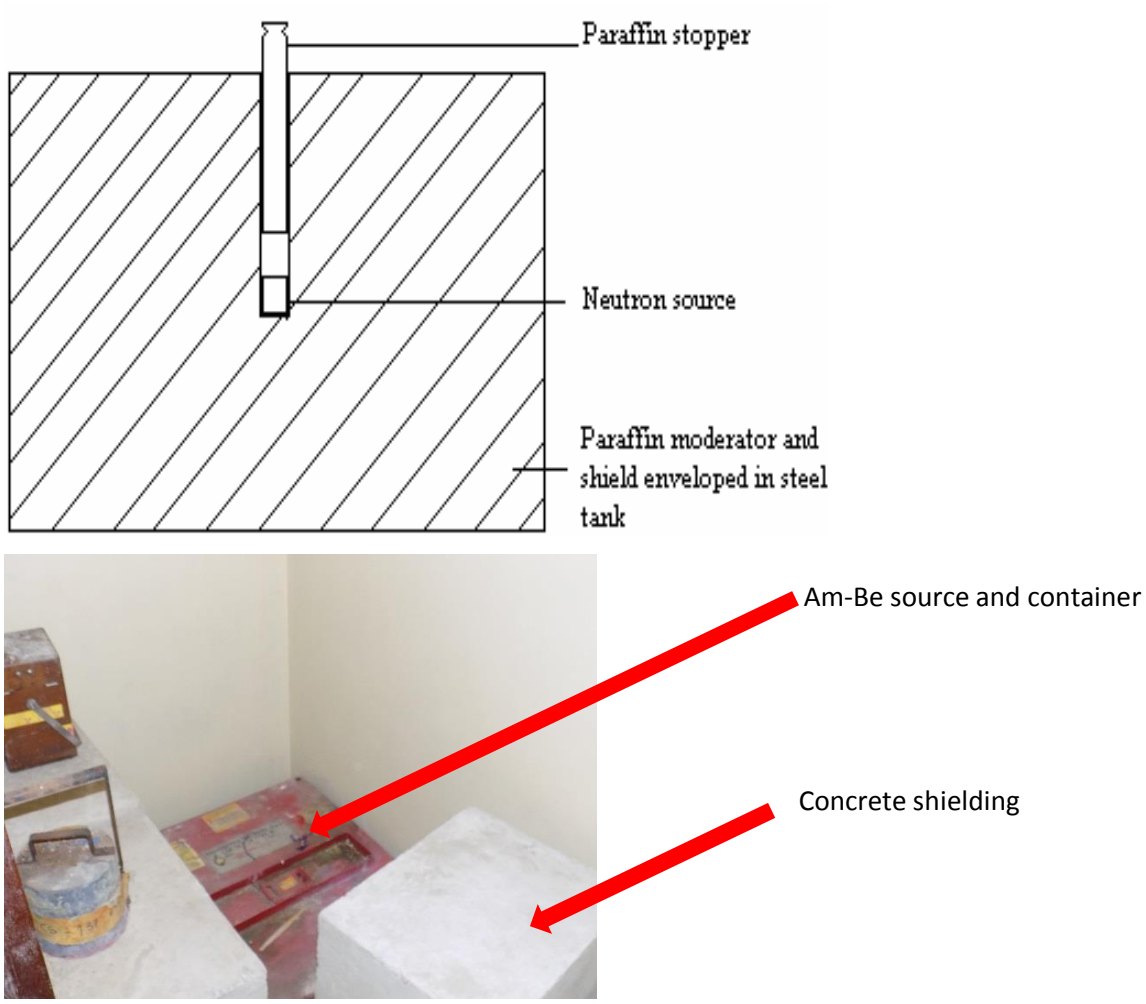

Figure 3.1 A schematic and a photo of Am-Be neutron source facility and housing

In this source, alpha particles (^{4}He) from ^{241}Am is absorbed by beryllium (^{9}Be) and upon radioactive capture interaction, carbon (^{12}C) is formed as the product nucleus and neutron as a recoil particle with kinetic energies ranging from 0 MeV to about 11 MeV (Figure. 3.2). The reaction has a positive Q-value of 5.71 MeV (Equation. 17).

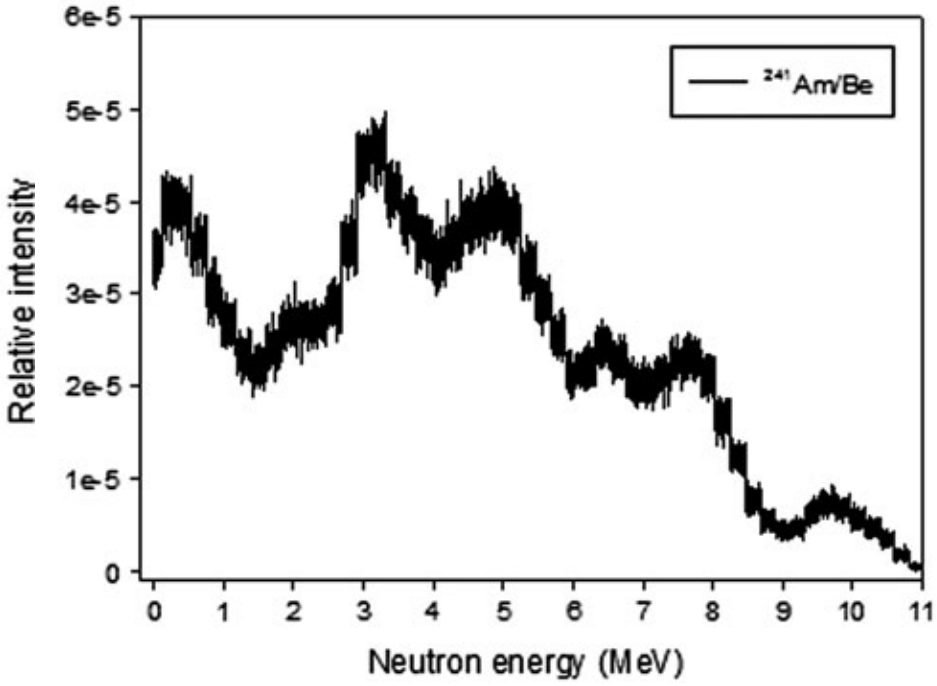

Figure 3.2 Normalized neutron energy spectrum from the Am-Be source (Adapted from Fantidis et al., 2011)

$$^{4}\mathrm{He} + {}^{9}\mathrm{Be} \rightarrow {}^{12}\mathrm{C} + \mathrm{n} + 5.71\mathrm{MeV} \quad (9)$$

The fast (recoil) neutrons from the source are moderated (slowed down) by its nearly 4π immersion within the volume of paraffin wax. The slow neutron beam can then be used to illuminate the sample.

3.2 Monte Carlo technique

Computer modelling and simulation is a cost and time effective way for optimizing laboratory set ups without risk of radiation exposure to the workers. Monte Carlo (MC) is the most used technique for simulating nuclear particles and to model radiation facilities. MC is a numerical method that uses random numbers to simulate a physical process where the underlying probabilities are known but the results are too complex to be determined by mathematical analysis (X-5 Monte Carlo Team, 2003). MC simulation has been widely applied since it can deal with complex geometries of actual interest as opposed to deterministic models which oversimplify the geometry and use approximation and

assumptions. With MC, it is easy to construct a model of the system and experiment with the model to draw inferences of the real system behavior when adjustments are made with a view of finding optimum conditions.

3.3 MCNP code

The MCNP code is a general purpose Monte Carlo N-particle code that is developed and maintained by the Los Alamos Laboratory in USA (X-5 Monte Carlo Team, 2003). The code can be used to track the transport of neutrons, photons and other elementary nuclear particles from source to their death (i.e. absorption, escape, etc.) (Howell et al., 2000; Shim et al., 2002; Thi et al., 2007; Tuffour-Achampong et al., 2012). The tracking and recording of the particle histories allows the tallying of events such as particle fluxes, absorbed dose and reaction rates as desired by the user.

The use of MCNP as a transport code requires a deep knowledge of the radiation source, the geometry of the problem, the composition of the materials used plus the physical data e.g. cross-section of different reactions involved in the problem. The user supplies the code with an input file that contains this information; the MCNP input file is divided into 3 main blocks: 1) Cell card; 2) Surface card; 3) Data card. The first two correspond to the geometry definition while the third block contains all information associated with the specification of the neutron source, the definition of the materials used, the cross sections, the type of tallies preferred and the variance reduction that are used to improve efficiency.

The greatest advantage of using the Monte Carlo technique to simulate radiation transport is its ability to handle complicated geometries thus avoiding simplifications and approximations. MCNP5 utilizes ENDF6 cross-section which contains more current continuous energy cross-section libraries hence contains more information than most codes thus allowing neutron and photon interactions with matter to be modelled in far more detail. The Monte Carlo method also helps to minimize the time of system optimization and of assessing detection limits of the facility.

3.4 MCNP-5 input files.

MCNP5 is operated by user-defined parameters in the input file. All the input lines in the input file are limited to 80 columns. The code however is case insensitive as upper, lower or mixed cases are accepted. A $ (dollar sign) is used to terminate data entry and any entry written after the dollar sign is taken as a comment. Blank lines are used as delimiters and as an optional terminator. The data inputs are divided by one or more delimiters. Comment cards can be used anywhere in the input file after the problem title card and before the optional blank terminator card. The comment lines must have a "C" somewhere in column 1-5 followed by at least one blank and can be a total of 80 columns long. Cells, surfaces, and data cards must all begin within the first five columns of the line. A blank filling of the first five columns indicates a continuation of the last named card. Entries within the cards are separated by one or more blanks.

An input file generally takes the following format;
Message Block (optional)
Blank Line Delimiter (optional)
One Line Problem Title Card
Cell Cards
…
Blank Line Delimiter
Surface Cards
…
Blank Line Delimiter
Data Cards
…
Blank Line Terminator (optional)

3.4.1 Neutron flux distribution in the Am-Be irradiator channels

In this work, MCNP5 was used to model and to simulate the Am-Be neutron source facility. The geometry of the facility was modelled as described in section (3.1). Figure 3.3 shows the diagram that was generated from the MCNP5 input file that was used to

describe the geometry. The numbers in red indicate the cell numbers while those in blue indicate the surface numbers.

The source was coded using the sdef card, where neutron emission starting point is centered in the source (cell 1). The uniform particle position sampling was provided by the EXT variable and a built-in power law function $P(x) = C\,|x|^{a}$ was used for the source radius value (RAD) with $a = 1$. This ensured that starting particles in the source volume were uniformly distributed. The starting energy spectrum used was that of an Am-Be emitter ranging from 0.414 eV to 11.03 MeV. Small cylindrical cells were created along the irradiation sites and were used to tally the neutron flux. The neutron flux was estimated using the F4 tally with MODE N; this calculated the average neutron flux over the tally cells ($particle.\,cm^{-2}$). 5million source particles were run creating 5 million histories. The range of energies considered in the tally card were thermal neutron (below 0.5eV), epithermal neutrons (between 0.5 eV to 0.5 MeV) and fast neutrons (above 0.5 MeV).

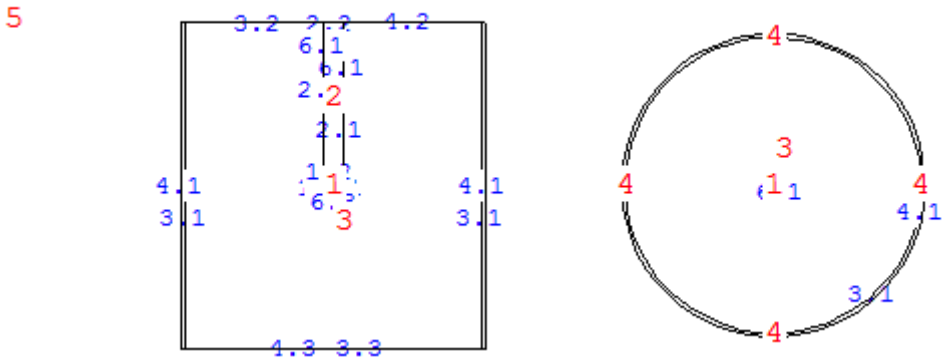

(a) **(b)**

igure 3.3 Schematic vertical (a) and horizontal (b) cross sectional view of the Am-Be neutron source facility as modelled in MCNP5

No variance-reduction technique was used and all the parts of the geometry were registered as similarly important as far as particle transport was concerned. Only the outside space (outside world) of the geometry has a zero neutron importance. This was

important for the termination of neutron histories so as not to spend much time simulating neutrons outside the facility. Figure 4.6 also indicates that very minimal neutrons are escaping the drum container hence simulating neutrons outside the drum will have no major effect on the neutron flux. The ENDF6 cross-section data library built in MCNP-5 were used for the radiative capture reactions.

The MNCP5 input files were prepared for three more irradiation sites (site 2, 3 and 4) in addition to the original site (site1). The original irradiation site was modeled directly above the source while sites 2, 3 and 4 were modeled at 5 cm, 10 cm and 15 cm from the source center respectively. These additional sites were proposed in order to monitor the neutron flux if the irradiation sites were located in different places in the paraffin wax. The following figures show the geometries of the facility filled with materials for site1 (Figure 3.4), site 2 (Figure.3.5) and site3 (Figure 3.6) for illustrations. A typical MCNP5 file for flux profiling is shown in Appendices.

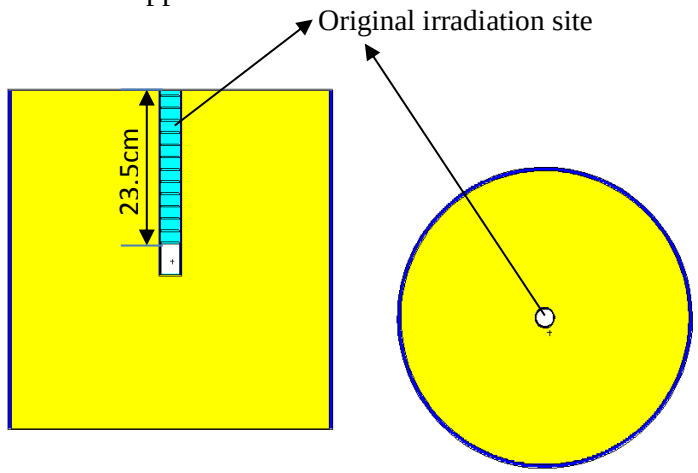

Figure 3.4 MCNP5 geometry for irradiation site1 (showing (a) vertical and (b) horizontal cross sectional view)

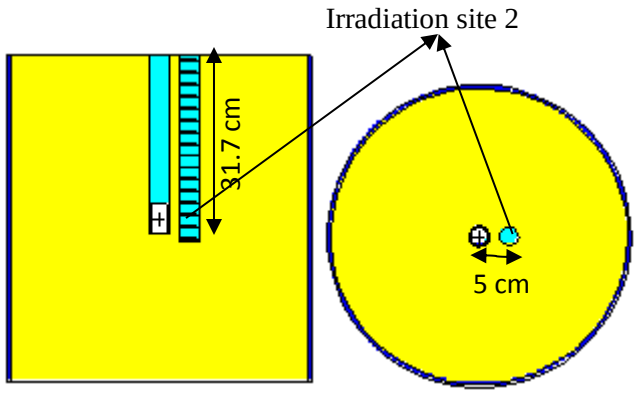

(a) **(b)**

Figure 3.5 MCNP5 geometry for irradiation site2 (showing (a) vertical and (b) horizontal cross sectional view)

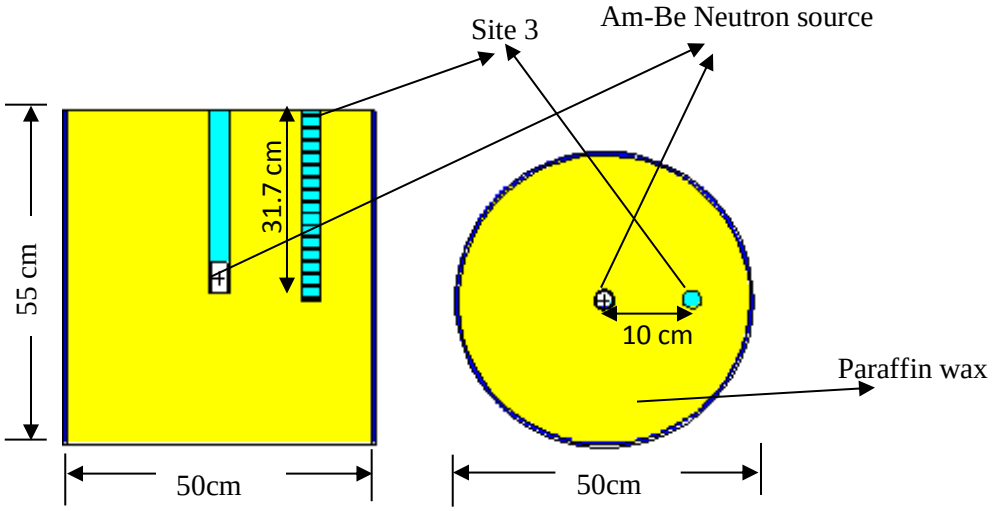

(a) **(b)**

Figure 3.6 MCNP5 geometry for irradiation site 3 (showing (a) vertical and (b) horizontal cross sectional view).

3.4.2 Modelling and simulation of the proposed detection system

The basic design objective for the PGNAA facility was to achieve the best possible sensitivity and detection limits within the engineering constraints. Equation (10) shows that to obtain a better sensitivity and minimal detection limit we need to maximize the thermal flux at the sample position and also to minimize the sample to detector position. The choice of geometry affects the neutron flux and gamma ray background at the

detector. The internal target geometry is the most preferred since the neutron flux is higher within the irradiation channels. While the external sample geometry has very low flux, the gamma ray transmission factor is higher and is most preferred when irradiating large samples.

The geometry of the system was modelled as in the section 3.2.1 with the inclusion of HPGe detector, sample holder and sample. For the detector, only the active volume (covered with 0.5 mm of aluminum) was modeled. The germanium reaction cross section was not available in the MCNP-5 cross-section data library hence the detector was modelled as gallium crystal since gallium is close to germanium in the periodic table. The elements chosen for this study are; H, B, C, N, Si, and P. This choice mainly comprises light elements which are hard to measure or have low sensitivity in off line NAA.

On the basis of the discussion from the results obtained for the flux monitoring, irradiation site2 was used as the preferred site for PGNAA since it had the highest thermal flux and better neutron ratios, Φ_T/Φ_E and $(\Phi_T + \Phi_E)/\Phi_F$, of 3 and 2.8 respectively. The samples were modelled closer to the source within the high flux regions as was obtained from the flux monitoring results.

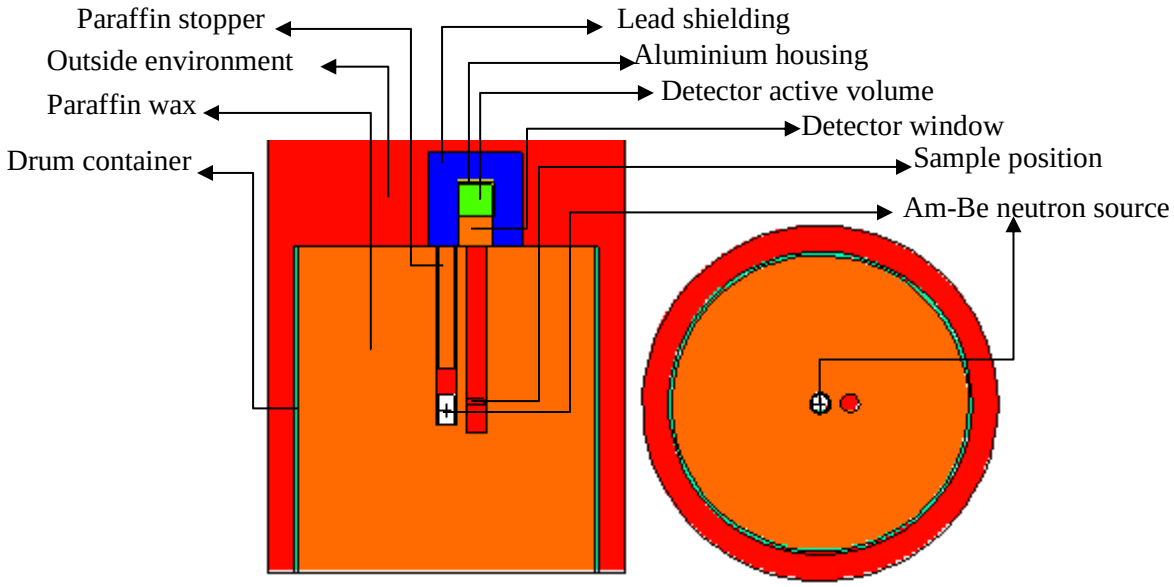

Figure 3.7 MCNP5 schematic diagram of the PGNAA set up for detector configuration A. (showing vertical and horizontal cross-sections respectively).

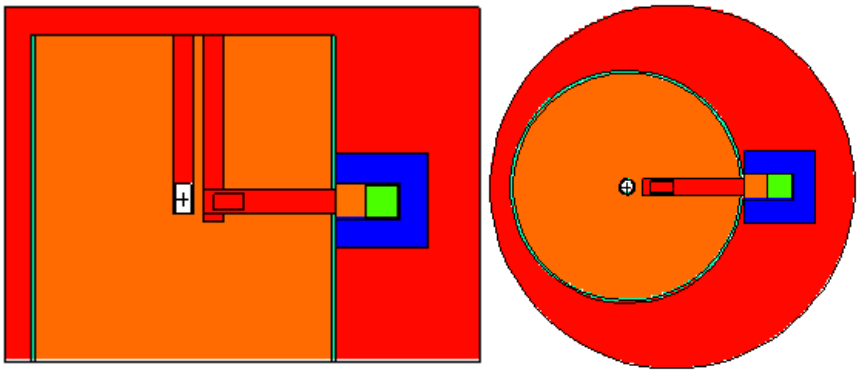

Figure 3.8 MCNP5 schematic diagram of the PGNAA set up for detector configuration B. (showing vertical and horizontal cross-sections respectively).

CHAPTER 4

RESULTS AND DISCUSSIONS

This chapter presents the results and discussions of the simulation in the form of neutron flux, sensitivity and detection limit. The neutron flux within the irradiation sites are presented in section 4.1. The analysis of the background gamma ray spectrum is also presented in section 4.2. Section 4.3 presents the sensitivities and detection limit of some selected elements as simulated in MCNP5.

4.1 Neutron flux profile in the irradiation sites

In the first part of this work, the MCNP5 simulation was run to estimate the distribution of neutron flux in the original irradiation site and the three additional proposed irradiation sites. Thermal (< 0.5 eV), epithermal (0.5 eV – 0.5 MeV) and fast neutrons (> 0.5 MeV) were tallied in each channel and the flux multiplied by the source strength since MCNP normalizes the tally per source neutron.

Table 4.1 Average neutron flux in each irradiation channels as obtained from MCNP-5.

Irradiation. sites	Average thermal flux (Φ_T)/(n $cm^{-2}s^{-1}$)		Average epithermal (Φ_E)/(n $cm^{-2}s^{-1}$)		Average fast neutron (Φ_F)/(n $cm^{-2}s^{-1}$)	
	Flux	**% flux**	Flux	**%flux**	Flux	**%flux**
Site 1(0cm)	34,540 ± 328	**31.3**	19,316 ±290	**17.5**	56,320 ±422	**51.1**
Site2 (5cm)	45,152 ±388	**55.3**	14,899 ±268	**18.3**	21,556 ±287	**26.4**
Site3(10cm)	20,243 ±247	**69.3**	4,248 ± 127	**14.5**	4,732 ±122	**16.2**
Site4 (15cm)	6,910 ±133	**71.3**	1,329 ±65	**13.7**	1,446 ±61	**14.9**

Tables 4.1 shows the mean neutron flux yield in each of the irradiation sites from 1 to 4. The percentage flux (% flux) was calculated as a fraction of the total flux of each neutron category multiplied by a hundred. The result corresponds to five million of neutron initial histories. In all cases the relative error estimated was less than 5%, passing all the MCNP5 statistical checks.

As is evident from the table 4.1 that average neutron flux levels are greater in the channels nearer to the neutron source than in the further channels except for thermal flux which is highest at the second site and thereafter decreases as the other fluxes, that is, as the radial distance from the source inside the paraffin wax increases, the neutron flux level decreases. This observed decrease in flux level can be attributed to neutron leakage and absorption in the paraffin wax. Also, as the distance from the source increases the percentage of the average thermal neutron rises whereas that of epithermal and fast neutron drops due to moderation of the fast neutrons by the wax. Asamoah et al. (2011) also performed a similar MCNP simulation on a water moderated Am-Be neutron source at NNRI to determine the radial and axial neutron fluxes on two irradiation sites that were 13.1cm and 4.2cm from the source. Their results compare well with this research work as can be seen in table 4.2.

Table 4.2 The average thermal, epithermal and fast neutron flux in the irradiation sites (adapted from Asamoah et al., 2011)

Irrad. Sites	Thermal (n $cm^{-2}s^{-1}$)	Epithermal (n $cm^{-2}s^{-1}$)	Fast (n $cm^{-2}s^{-1}$)
1 (13.1cm)	4,476 ± 7	657 ± 2	370 ± 2
2 (4.2cm)	19,839 ± 14	5,945 ± 7	2,611 ±4

The neutron flux distribution evaluated for irradiation sites 1, 2, 3 and 4 are presented in figures. 4.1 to 4.4 respectively. The graphs reveal that optimum thermal neutron fluxes are obtainable within the range of 0 cm to 6 cm for site 1 and a range of -6 cm to 6 cm for sites 2, 3 and 4. The thermal neutron flux reaches its maximum near the neutron source. This is due to the moderation effect by the hydrogenous paraffin wax. An earlier experimental study on the same source by Olando (2005) also stated that the maximum flux is within 6 cm from the source surface in the original irradiation site.

As observed from the above results, thermal neutron flux was higher in the sites closer to the neutron source. Better thermal plus epithermal to flux ratio, $(\Phi_T + \Phi_E)/\Phi_F$, and thermal to epithermal flux ratio (Φ_T/Φ_E) can be achieved in the sites farther from the source (table 4.3). Site 1 is characterized by high thermal flux, however, it is not suitable for PGNAA since both ratios are very low; that is, the fast neutron component is very

large and any solution used to stop these fast neutrons would cause reduction of the thermal neutrons. While sites 3 and 4 have better ratios, their thermal flux is very low compared to sites 1 and 2. Site 2 provided the highest thermal flux and a better Φ_T/Φ_E ratio of 3 implies that the gamma rays obtained from irradiation of samples as a result of thermal neutron interaction will dominate those from epithermal interaction. For these reasons, site 2 was chosen for the development of the proposed PGNAA facility.

Table 4.3 Summary of the neutron flux of the facility

Irradiation sites	Φ_T/Φ_E	$(\Phi_T + \Phi_E)/\Phi_F$
Site 1(0cm)	1.8	1.0
Site2 (5cm)	3.0	2.8
Site3(10cm)	4.8	5.2
Site4 (15cm)	5.2	5.7

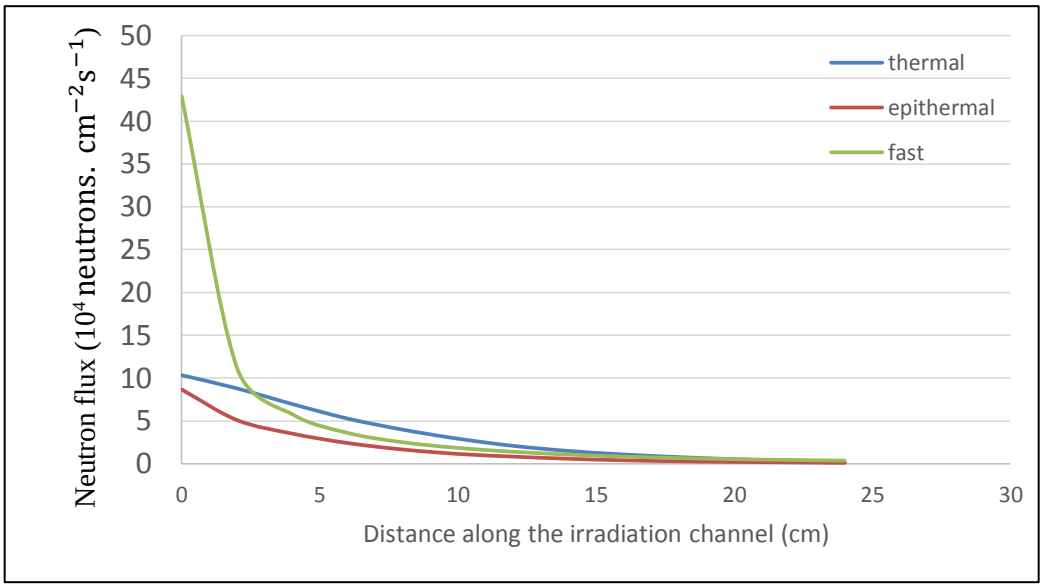

Figure 4.1. Neutron flux distribution along irradiation site 1

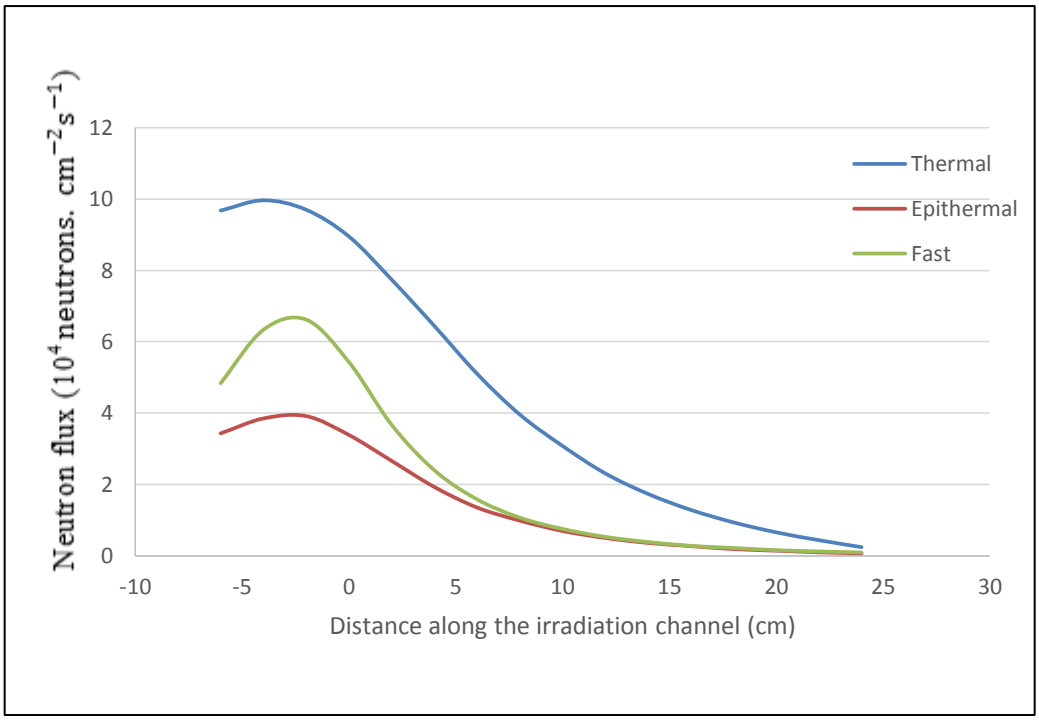

Figure 4.2. Neutron flux distribution along irradiation site 2

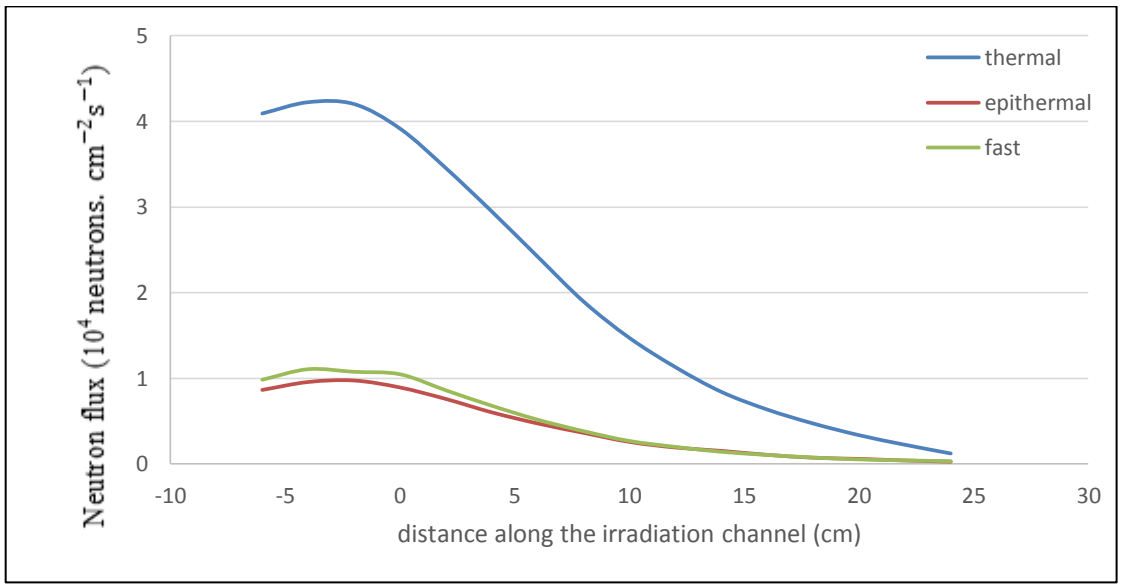

Figure 4.3. Neutron flux distribution along irradiation site 3

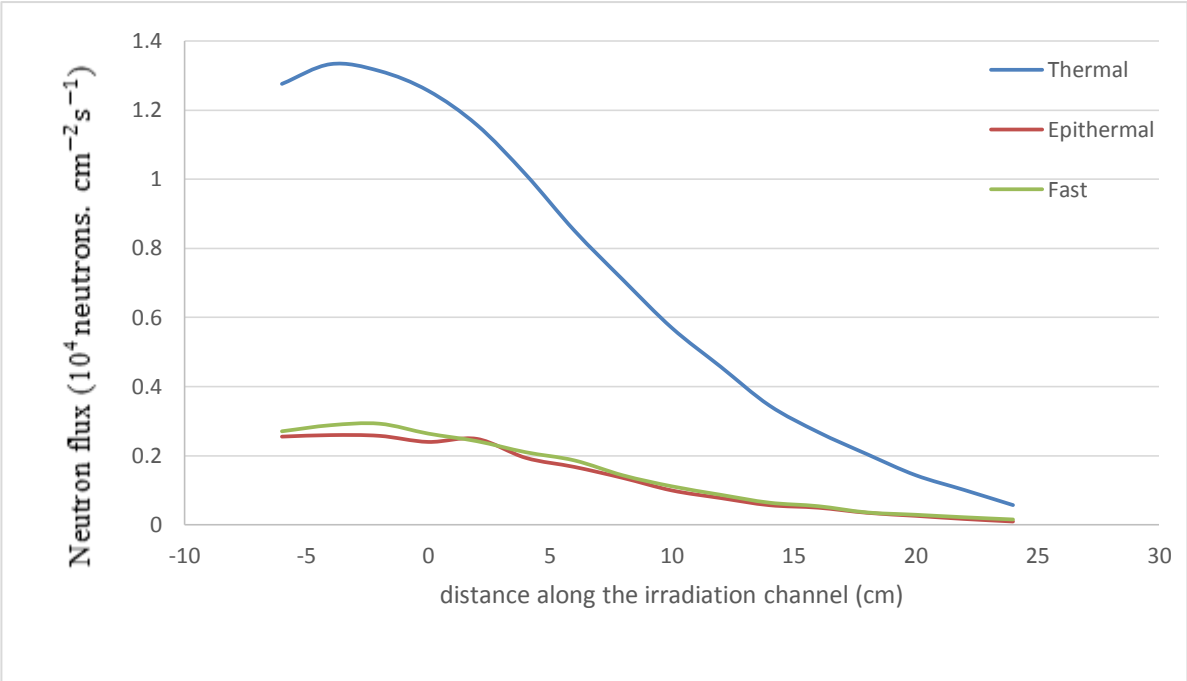

Figure 4.4. Neutron flux distribution along irradiation site 4.

4.2 Gamma ray background spectrum

The construction material background spectrum was collected in 10 keV energy bins. The background spectrum measured with empty Teflon bag and simulated for 5 million neutron histories is shown in figure 4.5 below. The values are as per source neutron per unit energy interval. Most of the identified peaks were those of the construction materials, that is, hydrogen, boron, lead, and annihilation peak.

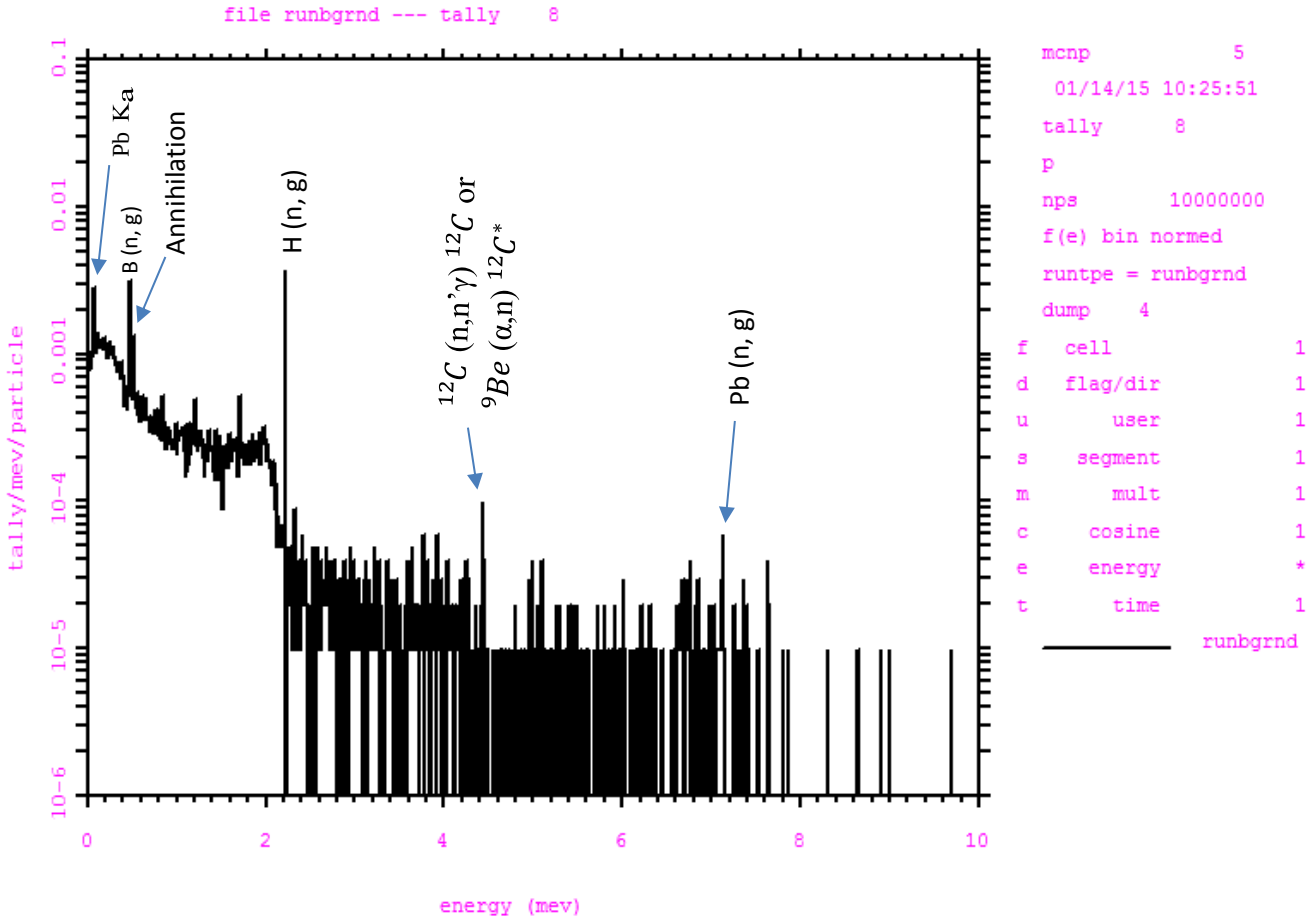

Figure. 4.5 PGNAA background flux at the detector as obtained from MCNP simulation. The values are per source neutron per unit interval energy. Note: the vertical axis should read "tally/MeV/particle" and the horizontal axis should read "energy (MeV)"

The most significant disadvantage of the isotopic PGNAA facilities is the high level of the background counts coming from different origins within the facility. The major

background peaks identified in the assembled Am/Be PGNAA facility are discussed in the following section;

The 2.22 MeV prompt peak of hydrogen is the most intense peak with about 3.66E-5 counts. The boron prompt peak at 0.48 MeV is also prominent with count rate of 3.14E-5. The hydrogen and boron peaks originate from the paraffin wax used for neutron moderation and from the borated polyethylene material used for neutron shielding at the detector window respectively. The photopeak at 4.45 MeV is due to the gamma ray counts from the first excited state of carbon-12 (4.43 MeV). The presence of the 4.43 MeV photons maybe due to the photons emitted by neutron source during ^{9}Be (α, n) $^{12}C^{*}$ nuclear reaction where the carbon-12 nuclide is left in excited state, or due to ^{12}C (n, n'γ) ^{12}C elastic scattering reaction in the paraffin wax. Gamma rays from lead (at 7.368 MeV) and activation products of the gallium crystal in the detector (at 0.69 MeV) as well as the prompt gamma from the aluminum material housing the detector (7.724 MeV) are not as prominent in the spectra. The low gamma contribution from this part of the model maybe an indication that the stray neutrons hitting the detector are very minimal. This can be verified by the simulated particle display in the figure 4.6 below showing points of neutron collisions. The less intense lead peak may also be due to the uncertainties in Pb radiative capture cross-section. Table 4.3 shows the summary of the most prominent peaks of the gamma ray background spectra.

Table 4.4 Background peak count rate with beam incident on an empty Teflon bag

Energy (MeV)	**Element or nuclide identification**	**Count rate (cps)**
0.08	Pb Ka	617
0.48	Boron (n, γ)	691
0.52	Annihilation	296
2.23	Hydrogen (n, γ)	806
4.45	^{12}C (n,n'γ) ^{12}C or ^{9}Be (α,n) $^{12}C^{*}$	8.69
7.37	Pb (n, γ)	6.52

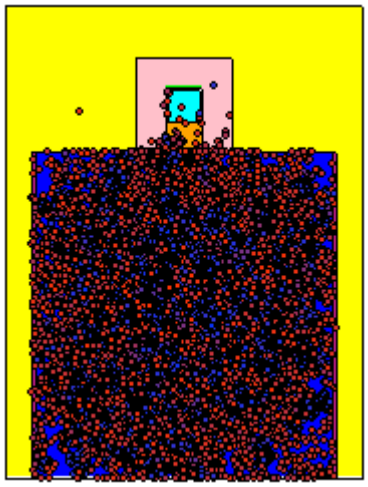

Figure 4.6. Particle displays at points of neutron collisions (358977 points plotted. Minimum energy used = 0.1003E-08. Maximum energy used = 0.1102E+02. Minimum energy found>1.e-9 = 0.1003E-08 maximum energy found = 0.1102E+02. Minimum blue maximum red.)

4.3 Sensitivities and detection limits for selected elements

The analysis presented includes those of light elements H, B, N, Si, and P which can hardly be analyzed by NAA. The values of sensitivities obtained by Monte Carlo simulation of the PGNAA system are presented in table 4.4.

Table 4.5 Sensitivity for different nuclides obtained from the irradiation of pure samples

Nuclide	E_γ(MeV)	Sensitivity (cps mg^{-1})	
		Configuration A	Configuration B
Hydrogen	2.223	7.9912	17.762
Boron	0.478	3.1429	7.887
Carbon	1.261	0.0002	0.0006
Nitrogen	1.885	0.1086	0.1281
Silicon	3.539	0.0005	0.0003
Phosphorus	0.638	0.0029	0.0034

The detection sensitivities for the elements were obtained by irradiating pure elements placed inside Teflon bags. The analytical sensitivities are defined by the gradient of a straight line representing the variation of the count rate (in cps) of a full energy peak as a function of the element mass (in mg) shown in appendix B. The masses of the elements were selected so as the graphs obtained to remain as straight lines. From the results obtained, the boron showed a better response when compared with other related research results. From the slopes of calibration plot, the sensitivity for boron at the full peak energy of 478 keV was found to be 3.14 cpsmg^{-1} for configuration A and 7.87 cpsmg^{-1} for configuration B. The difference is acceptable since the sensitivity and detection limits vary depending on the elementals present in the sample being irradiated and also due to the difference in thermal flux at sample position.

Generally, the results obtained for sensitivity in this work are very low due to the low thermal flux at the sample position. Uncertainties in the cross-sections could have also contributed to the sensitivity of the detector system. Table 4.4 shows that for sensitivity, only Si was worse in position B than in position A. However, table 4.5 shows that the detection limits were better in position B for the first three elements and worse for the other three. The sensitivity obtained for hydrogen was higher compared to the results obtained from reactor based facilities.

An estimation of the detection limit is calculated by the formula (15) in section 2.2.6. It was noted that the detection limit for boron is as small as 10.0 mg. The results obtained in this section corresponds to a total neutron source output of 2.2×10^7 neutrons which is the Am-Be source neutron output per second. Therefore, irradiating the sample for 1000 second would drastically lower the detection limit with a factor of 31.62 i.e. for Boron the detection limit will improve to 0.316 mg.

Table 4.6 Detection limits for different nuclides obtained from the irradiation of pure samples

Elements	Detection limit (mg)	
	Configuration A	Configuration B
Hydrogen	10.71	5.48
Boron	21.96	10.0
Carbon	50,691	10,911
Nitrogen	142.2	215.5
Silicon	19,518.99	26,107
Phosphorus	8,243.7	9,077

CHAPTER 5

CONCLUSION AND RECOMMENDATION

In this chapter, the conclusion and recommendation is presented, based on the analysis of the results, for further studies.

5.1 Conclusions

These simulation results describe the possibility of setting up a PGNAA system for multi-elemental analysis at INST. The system consists of a single 370 GBq ^{241}AmBe isotopic neutron source, with emission rate of 2.2×10^7 $\mathrm{ns}^{-1} \pm 10\%$. The source emits mostly fast neutrons which are then moderated by paraffin wax encasing the source. An axial cylindrical cavity of dimensions 3.2 cm diameter and 23.5 cm height is bored perpendicularly at the center of the paraffin block. Three more cavities are simulated at a radial position of 5 cm, 10 cm and 15 cm from the source. The following are the conclusions from the research work.

- Investigation of the flux and energy distribution of the neutrons revealed that maximum thermal flux is achieved within -6 cm to 6 cm position along the irradiation channels. Site 2, which was bored at a radial distance of 5 cm from the neutron source, had the highest average thermal flux and best optimal thermal ratios hence was chosen for internal sample configuration. The thermal neutron flux of $45{,}152 \pm 388\ \mathrm{n.cm^{-2}s^{-1}}$ and the neutron ratios Φ_T/Φ_E and $(\Phi_T + \Phi_E)/\Phi_F$ of 3 and 2.8 respectively were achieved at this channel.
- In the second part, an HPGe detector and sample holder were included to model for the simulation of the whole detection system and to obtain theoretical sensitivity and detection limits for some selected elements. The background counts obtained mostly includes the gamma ray energy from the building materials such hydrogen, lead and boron.
- As obtained from the results, the estimated thermal neutron flux ($10^4\mathrm{n.cm^{-2}s^{-1}}$) was very low hence the sensitivity obtained for the selected elements were also very

low. Apart from hydrogen which showed discrepancy due to the interference from the high background peak, boron had the best sensitivity. The boron sensitivity of 7.887 $\mathrm{cpsmg}^{-1}$with a lower detection limit of 10 mg could be applied in analysis of boron samples.

5.2 Recommendations

Isotopic neutron sources have potentials for multi-element analysis and other applications as outlined in section 2.6, however, for the paraffin wax moderated 370 GBq ^{241}AmBe neutron source to be utilized for PGNAA, necessary modifications must be made to improve the sensitivity and also to eliminate the high peak background counts. Such modifications may include replacing the paraffin moderator with a non-hydrogenous moderator in order to eliminate the intense hydrogen background counts. The background counts may also be reduced by enhancing the detection system with a Compton suppressor. The results from the facility may also be improved by including collimators in the irradiation channels to enhance thermal neutron flux at the sample position. The sample-detector geometry and also shielding materials may need adjustments in order to increase the flux at sample position. The proposed detector system should then be subjected to the experimental analysis of the sensitivity.

REFERENCES

Anderson D.L. (2000). **Neutron Capture Prompt Gamma-ray Activation Analysis of Meat Homogenates**. Journal of Radioanalytical and Nuclear Chemistry, 244(1), pp 225-229.

Anderson D. L., Richard M. L., Tamas B., Gabor L. M., Richard B. F., Zsolt R., Zsolt K.,Chushiro Y. (2004). **Handbook of prompt gamma activation analysis with neutron beam**. Kluwer academics publishers, Dordrecht.

Anyenda O. E. (2009). **Characterization and application of Neutron Flux of a 370 GBq 241Am-Be irradiating systems.** MSc Thesis., University of Nairobi.

Asamoah, M., Nyarko, B.J.B., Fletcher, J.J., Sogbadji, R.M.B., Yamoah, S., Agbemava, S.E., Mensimah, E. (2011). **Neutron flux distribution in the irradiation channels of Am–Be neutron source irradiation facility**. Analytical Nuclear Energy 38 (6), 1219-1224.

Bergaoui, K., Reguigui, N., Gary, C. K., Brown, C., Cremer, J. T., Vainionpaa, J. H., & Piestrup, M. A. (2014)**. Development of a new deuterium–deuterium (D–D) neutron generator for prompt gamma-ray neutron activation analysis.** Applied Radiation and Isotopes, 94(1), 319-327.

Bergaoui K., Reguigui N., Gary C.K., Brown C., Cremer J.T., Vainionpaa J.H., Piestrup M.A.(2015) **Prompt gamma-ray neutron activation analysis of boron using Deuterium–Deuterium (D–D) neutron generator. Journal of** Radioanalytical and Nuclear Chemistry, 303 (1) 115-121.

Borsaru M., Berry M., Biggs M., Rojc A. (2004). **In situ determination of Sulphur in coal seams and overburden rock by PGNAA**. Nuclear Instruments and Methods in Physics Research Section B: Beam Interactions with Materials and Atoms 213, 530-534. http://library.seg.org/doi/abs/10.1190/1.1442165 .

Briesmeister JF, Editor. (2003). **MCNP—A general Monte Carlo n-particle transport code**. LA-UR-03-1987, Version 5, Los Alamos National Laboratory.

Byun S. H., Choi H.D. (2000). **Design features of a prompt gamma neutron activation analysis system at HANARO**. Journal of Radioanalytical and Nuclear Chemistry, 244(2) 413-416.

Byun S. H., Sun G. M., Choi H. D. (2004). **Prompt gamma activation analysis of boron in reference materials using diffracted polychromatic neutron beam.** . Nuclear instruments and methods in physics Research, 213(B) 535-539.

Byun S. H., Sun G. M., Choi H. D. (2002). **Development of a prompt gamma activation analysis facility using diffracted polychromatic neutron beam**. Nuclear instruments and methods in physics Research, 487 (A) 521-529.

Cember H., and Johnson T. E. (2009) Introduction to Health Physics: 4 Ed. McGraw-Hill Companies, New York.

Choi H.D, Firestone R.B., Lindstrom R.M., Molnar G.L., Reddy V.R.A., Tan V.H., Zhou C.M., Paviotti- Corcuera R. and Trkov A. (2001), **Development of a Database for Prompt Gamm-ray Neutron Activation Analysis**. Journal of Nuclear Science and Technology, 39(2), 1372-1375.

Choi H., Firestone R. (2006) **Database of prompt gamma ray from slow Neutron capture for elemental analysis.** Neutron capture for elemental analysis IAEA, Vienna.

Dove, E. L. (2004). **Physics of Medical Imaging -An Introduction.** Biomedical Engineering the University of Iowa, Iowa.

Fantidis, J.; Nicolaou, G.; Potolias, C.; Vordos, N.; Bandekas, D. (2011).**The comparison of four neutron sources for Prompt Gamma Neutron Activation Analysis (PGNAA) in vivo detections of boron.** Journal of Radioanalytical & Nuclear Chemistry, 290 (2), p289-295.

Gardner R. P., Guo P., Wang Y. Y., Sood A., Lee S. H., Dobbs C. L. (1997). **Feasibility of Neutron Activation Methods for Measurement of Sodium and Aluminum in Green Liquor.** Applied Radiation and Isotopes, 48, 1355-1372.

Ghorbari P., Sardari, D., Doostmohammade K. (2012) **Neutron beam preparation with Am-Be source for analysis of biological samples with PGNAA method**. Journal of Radioanalytical and nuclear chemistry, 291(3) 839-842.

Gozani, T., Bozorgmanesh, H., Brown, D., Elias, E., Maung, T., and Reynolds, G. (1978). **Coal elemental analysis by prompt-neutron activation analysis**. Transactions of the American Nuclear Society; (Vol. 28). United States.

Hamed A., and Hassan A.M (2006**). Estimation of boron in some local materials by Prompt gamma ray neutron activation analysis Technique**. Proceedings of the 2nd Environmental Physics Conference, Alexandria, Egypt

Hight S. C., Anderson D. L., Cunningham W. C., Capar S. G., Lamont W. H. and Sinex S. A. (1993). **Analysis of dietary supplements for nutritional, toxic and other elements**. Journal of Food Composition and Analysis 6(2), 121-139

Howell S. L., Sigg R. A., Moore F. S. and Devol T. A. (2000). **Calibration and validation of Monte Carlo model for PGNAA of chlorine in soil**. Journal of Radioanalytical and Nuclear Chemistry, 244(1), 173-178.

Idiri Z., Mazroa H., Amokrane A., Beddek S. (2009**). Methodology for qualitative and quantitative analysis of large liquid samples with prompt gamma neutron activation analysis using Am-Be source**. Physicsegypt .org. proceedings of the 7th conference on nuclear particle physics 11-15 Nov. 2009, Egypt.

Kasztovszky, Zs., Panczyk, E., Fedorowicz, W., Révay, Zs. (2005) **Comparative archaeometrical study of Roman silver coins by prompt gamma activation analysis and SEM-EDX**. Journal of Radioanalytical and Nuclear Chemistry, 265(2), pp 193-199.

Kasztovszky Zs., Revay Zs., Belgya T., Molnar G.L. (2000). **Nondestructive analysis of metals by PGAA at the Budapest Research Reactor**. Journal of Radioanalytical and Nuclear Chemistry, 244 (2), pp 379-382.

Khelifi R.,Amokrane A., and Bode P. (2007). **Detection limits of pollutants in water for PGNAA using Am-Be source.** Nuclear instruments and methods in physics research section B: Beam interaction with material and atoms, 262(2) 329-332.

Khelifi, R., Idiri, Z., Omari, L., Seghir, M. (1999). **Prompt gamma neutron activation analysis of bulk concrete samples with an Am–Be neutron source**. Application Radiation Isotopes. 51, 9.

Krug F., Schober T., Paul R. and Springer T. (1995). **Investigation of the Hydrogen Uptake of Doped SrCeO3 by TEM, Thermogravimetry, and Cold Neutron Prompt Gamma Activation Analysis (CNPGAA)**, Solid State Ionics, 77, pp 185-188

Lloyd A. Curie (1999). **Detection limits. Origin and historical overview**. Analytica chimica Acta. 391(1999), 127-134.

Lylia H., Hocine S., Tarik A., and Boussaad Z. (2013). **Concepts, Instrumentation and Techniques of Neutron Activation Analysis**, Imaging and Radioanalytical Techniques in Interdisciplinary Research - Fundamentals and Cutting Edge Applications, Dr. Faycal Kharfi (Ed.), http://www.intechopen.com/books/imaging-and-radioanalytical-techniques-in-interdisciplinary-research-fundamentals-and-cutting-edge-applications/concepts-instrumentation-and-techniques-of-neutron-activation-analysis.

McGuire S.C., Lamaze G.P., Mackey E.A. (2002).**Trace Element Search in Synthetic Sapphire for Advanced LIGO**, Transactions of the American Nuclear Society, 87, p 484

Miyamoto S., Sutoh M., Shlomoto A., Yamazaki S., Nishimura K., Yonezawa C., Matuse H., Hoshi M. (2000). **Determination of Boron in Animals by Reactor Neutron Induced Prompt Gamma-ray Analysis**. Journal of Radioanalytical and Nuclear Chemistry, 244 (2), pp 307-309.

Molnar, G. L. (2004). **Hand Book of Prompt Gamma Activation Analysis**. Boston/ London: Kluwer Academic Publishers.

Molnar G. L., Revay Z, Belgya T, Firestone RB. (2000).**The new prompt gamma-ray catalogue for PGAA.** Applied Radiation and Isotopes, 53(4-5), 527-533.

Molnar G.L., Revay Zs., Belgya T. (2002). **Wide Energy Range Efficiency Calibration Method for Ge Detectors**. Nuclear Instruments and Methods in Physics Research A, 489 (1-3), pp 140-159

Nicholas T. (1995). **Measurement and Detection of Radiation**. 2nd Ed. Taylor and Francis, Washington, DC.

Nirmal S. (2011). **Radioisotopes – Applications in physical science**. Janeza Trdine, Croatia.

Oura Y., Enomoto S., Nakahara H., Matsue H., Yonezawa C. (2000). **Prompt Gamma-ray Analysis of Rats**. Journal of Radioanalytical and Nuclear Chemistry, 244 (2), pp 311-315.

Paul R. L. and Lindstrom R. M. (2000). **Prompt gamma-ray activation analysis: Fundamentals and applications**. Journal of Radioanalytical and Nuclear Chemistry, 243 (1), 181-189.

Paul R L., Privett H M., Lindstrom R M., Richards W. J., and Greenberg R R. (1996). **Determination of Hydrogen in Titanium Alloys by Cold Neutron Prompt Gamma Activation Analysis**. Metallurgical and Materials Transactions, 27 (11), pp 3682-3687

Perry D. L., Firestone R. B, Molnar G. L., Revay Zs., Kasztovszky Zs., Gatti R. G., and Wilde P. (2002**). Neutron-induced prompt gamma activation analysis (PGAA) of metals and non-metals in ocean floor geothermal vent-generated samples.** Journal of analytical atomic spectroscopy, 2002(17) 32-37.

Pinault J.L., Daudu, F. (1991). **Borehole logging in a bauxite mine by use of prompt gamma neutron activation analysis** (Proceedings Symposium. Vienna, 1990), IAEA,Vienna 203–214.

Prask, H. J. , Rowe, J. M. , Rush, J. J. , Schröder, I. G.(1993). **The NIST Cold Neutron Research Facility.** Journal of Research of the National Institute of Standard and Technology, 98 (1), 1–14.

Ramanjaneyulu P.S., Sayi Y. S., Newton N. T., Reddy A. V. R., and Ramakumar K. L. (2007). **Determination of boron in water samples by chemical prompt gamma neutron activation analysis.** Journal of Radioanalytical and Nuclear Chemistry, 273 (2), 411-414.

Révay Zs., Molnár G. L., Belgya T., Kasztovszky Zs., Firestone R. B.(2000). **A new gamma-ray spectrum catalog and library for PGAA.** Journal of Radioanalytical and Nuclear Chemistry, 248(2), pp 395-399.

Saleh H. H., Lavingston R. A. (2000). **Experimental evaluation of a portable neutron-based gamma-spectroscopy system for chlorine measurements in reinforced concrete**. Journal of Radioanalytical and Nuclear Chemistry, 244(2), 367-371.

Samir Abdul-Majid (1993). **Corrosion and Scale Measurements in Iron Pipes by Prompt Gamma-ray Analysis**. Nuclear Instruments and Methods in physics Research, section, B73, 398-402.

Shim H., Hong B., Lee k., Lee S., Cha H. (2012). **Monte Carlo simulation of the prompt gamma neutron activation analysis system with femtosecond laser**. Journal of the Korean physical society, 61(5), 702-709.

Shue, S.L., Faw, R.E., Shultis, J.K. (1998). **Thermal-neutron intensities in soils irradiated by fast neutrons from point sources**. Chemisrty Geology, 144, 47.

Spyrou N. M., Awotwi-Pratt J.B., and Williams A.M. (2004). **Monte Carlo calculations and neutron spectrometry in quantitative prompt gamma neutron activation analysis (PGNAA) of bulk samples using an isotopic neutron source.** Journal of Radioanalytical and Nuclear Chemistry, 259(2) 287-291.

Tanoi K., Iikura H., Nakanishi T. M. (2001). **Elemental Analysis in Cultured Cells, Tobacco and Grape, Treated with Aluminum**. Journal of Radioanalytical and Nuclear Chemistry, 249(2), pp 519-522.

Thi T., Loan H., Phuong D. N.,Thanh T. T., Khanh T.A., and Nhon M. (2007). **Monte Carlo simulations of HPGe detector response function with MCNP code**. Communication in physics, 17 (1), 59-64.

Tompa K., Bánki P., Bokor M., Lasanda G. and Vasáros L. (2003) **Diffusible and residual hydrogen in amorphous Ni (Cu)–Zr–H alloys**. Journal of Alloys and Compounds, Journal of Alloys and Compounds, 350[1-2], 52-55.

Tuffour-Achampong K., Nyarko B.J.B., Akaho E.H.K., Asamoah,M., Sogbadji R.M.B., Abrefah R.G., Boffie J. (2012).**Re-design of 241Am–Be neutron source irradiator facility at NNRI using MCNP-5 code**. Annals of Nuclear Energy, 40 (1), 60-64.

Turhan S., Yucel H., and Demirbas A. (2004). **Prompt gamma neutron activation analysis of boron with a Am-Be neutron source**. Journal of Radioanalytical and Nuclear chemistry, 262 (3), 661-664.

X-5 Monte Carlo Team (2003). **MCNP – A general Monte Carlo N-Particle transport code,** Version 5, vol.1. Overview and theory, Los Alamos National Laboratory, University of California, USA.

Yonezawa C., Khalik A., Wood H., Hoshi M., Ito Y., Tachikawa E. (1993). **The Characteristics of the prompt Gamma-ray Analyzing System at the Neutron Beam Guides of JRR-3M**. Nuclear instruments and methods in physics Research, A329, pp 207-216.

Yonezawa C., Matsue H., McKay K., Povinec P. (2001). **Analysis of Marine Samples by Neutron-induced Prompt Gamma-ray Technique and ICP-MS**. Journal of Radioanalytical and Nuclear Chemistry, 248 (3), pp 719-725.

Zevallos-Chávez J.Y. & Zamboni C.B. (2005). **Evaluation of the Neutron Flux Distribution in an Am-Be Irradiator using the MCNP-4C code.** Brazilian Journal of Physics, 35(3B), 797-800.

Zhao, L., Robinson, L., Paul, R.L., Greenberg, R.R., Miao S.L. (2007). **Application of cold neutron prompt-gamma activation analysis in environmental studies of aquatic plants**. Journal of Radioanalytical and Nuclear Chemistry, 271(3), pp 777-782.

APPENDICES

Appendix A

The following are the input files used for flux profiling at the irradiation site 1, site 2, site 3 and site 4 respectively.

```
MCNP5 AmBe input deck, flux profiling
c the irradiation channel modelled in the center of the paraffin block.
 c =========define cells================
 1   0        -1  $source
 2   5 -0.001205 -2 #1 #6 #8 #9 #10 #11 #12 #13 #14 #15 #16 #17 #18 #19
 3   3   -0.93 -3 6  $moderator material
 4   2   -7.85 -4 3  $drum container
 5   0        4  $define outside world
 6   5 -0.001205 -5  $tally at source contact
 7   2   -7.85 -6 2  $tally port
 8   5 -0.001205 -7  $ tally at 2cm from source
 9   5 -0.001205 -8  $tally at 4cm
10   5 -0.001205 -9  $tally at 6cm
11   5 -0.001205 -10  $tally at 8cm
12   5 -0.001205 -11  $tally at 10cm
13   5 -0.001205 -12  $tally at 12cm
14   5 -0.001205 -13  $tally at 14cm
15   5 -0.001205 -14  $tally at 16cm
16   5 -0.001205 -15  $tally at 18cm
17   5 -0.001205 -16  $tally at 20cm
18   5 -0.001205 -17  $tally at 22cm
19   5 -0.001205 -18  $tally at 24cm
 c =============define surfaces================
 1    rcc 0.0 0.0 -2.5 0.0 0.0 5 1.5  $  ambe source
 2    rcc 0.0  0.0  -2.52 0.0  0.0  30 1.6  $ port inner surface
 3    rcc 0.0  0.0  -27.5 0.0  0.0  55 25  $inner container
 4    rcc 0.0  0.0 -27.65 0.0  0.0 55.3 25.635  $outer container
 5    rcc 0.0  0.0  2.51 0.0  0.0  0.3 1.5  $tally1
 6    rcc 0.0 0.0 -2.67 0.0 0.0 30.15 1.75  $port outer surface
 7    rcc 0.0 0.0 4.51 0.0 0.0 0.3 1.50  $tally2
 8    rcc 0.0 0.0 6.51 0.0 0.0 0.3 1.50  $tally3
 9    rcc 0.0 0.0 8.51 0.0 0.0 0.3 1.50  $tally4
10    rcc 0.0 0.0 10.51 0.0 0.0 0.3 1.50  $tally5
11    rcc 0.0 0.0 12.51 0.0 0.0 0.3 1.50  $tally6
12    rcc 0.0 0.0 14.51 0.0 0.0 0.3 1.50  $tally7
13    rcc 0.0 0.0 16.51 0.0 0.0 0.3 1.50  $tally8
```

```
  14      rcc 0.0 0.0 18.51 0.0 0.0 0.3 1.50  $tally9
  15      rcc 0.0 0.0 20.51 0.0 0.0 0.3 1.50  $tally10
  16      rcc 0.0 0.0 22.51 0.0 0.0 0.3 1.50  $tally11
  17      rcc 0.0 0.0 24.51 0.0 0.0 0.3 1.50  $tally12
  18      rcc 0.0 0.0 26.51 0.0 0.0 0.3 1.50  $tally13
mode  n
c   ========== define materials==================
m1    95241.            0.08  $AmO2Be
     8016.           0.001 4009.           0.909
m2    26056.             -1  $ iron (steel)
m3    1001.        -0.148605  $paraffin wax
     6000.        -0.851395
m4    49000.             -1  $Indium
m5    6000.        -0.000124  $Air
     7014.        -0.755268 8016.        -0.231781 18000.       -0.012827
imp:n           1 3r                 0          1 13r          $ 1, 19
c
c
c ===========source definition====================
sc1   Am-Be SPECTRUM (ISO 8529)
sdef. Par =n erg.=d1 cell.=1 rad.=d2 ext.=d3 axs.=0 0 1
si1   H  0.414E-06 1.1e-1 3.3e-1 5.4e-1 7.5e-1 9.7e-1 0.118e1 0.14e1 0.161e1 0.182e1 0.204e1
     0.225e1 0.247e1 0.268e1 0.29e1 0.311e1 0.332e1 0.354e1 0.375e1 0.397e1 0.418e1 0.439e1 0.461e1
     0.482e1 0.504e1 0.525e1 0.547e1 0.568e1 0.589e1 0.611e1 0.632e1 0.654e1 0.675e1 0.696e1 0.718e1
     0.739e1 0.761e1 0.782e1 0.803e1 0.825e1 0.846e1 0.868e1 0.889e1 0.911e1 0.932e1 0.953e1 0.975e1
     0.996e1 0.1018e2 0.1039e2 0.106e2 0.1082e2 0.1103e2
sp1   D  0.00      0.00144  0.00334  0.00313  0.00281  0.00250
       0.00214  0.00198  0.00175  0.00192  0.00223  0.00215
       0.00225  0.00228  0.00295  0.00356  0.00369  0.00346
       0.00307  0.00300  0.00269  0.00286  0.00318  0.00307
       0.00333  0.00304  0.00274  0.00233  0.00206  0.00182
       0.00177  0.00204  0.00183  0.00163  0.00167  0.00168
       0.00188  0.00184  0.00169  0.00144  0.000968  0.000652
       0.000426  0.000367  0.000381  0.000506  0.000625  0.000552
       0.000468  0.000370  0.000278  0.000151  0.0000363
si2  0 1.5
sp2 -21 1
si3  3
sp3 -21 0
f4:n  6 8 9 10 11 12 13 14 15 16 17 18 19   $tally neutrons
e4    5e-7 .5 12
```

```
mt3 poly.01t $thermal treatment card
Print
nps 5000000
```

site2, irradiation channel at 5cm from the center of the paraffin block.

```
MCNP5 AmBe input deck, flux profiling
c the irradiation channel modelled at 5cm from the center of paraffin block.
  c =========define cells================
  1    0        -1  $source
  2    5 -0.001205 -2 #1
  3    3   -0.93 -3 6 19  $moderator material
  4    2   -7.85 -4 3  $drum container
  5    0        4  $define outside world
  7    2   -7.85 -6 2  $tally port
 21    5 -0.001205 -20  $ tally at -3.5 from source centre
 22    5 -0.001205 -21  $tally at -1.5 frm src centre
 23    5 -0.001205 -22  $tally at 0.5 frm src centre
  6    5 -0.001205 -5  $tally at source contact
  8    5 -0.001205 -7  $ tally at 4.5cm from source centre
  9    5 -0.001205 -8  $tally at 6.5cm
 10    5 -0.001205 -9  $tally at 8.5cm
 11    5 -0.001205 -10  $tally at 10.5cm
 12    5 -0.001205 -11  $tally at 12.5cm
 13    5 -0.001205 -12  $tally at 14.5cm
 14    5 -0.001205 -13  $tally at 16.5cm
 15    5 -0.001205 -14  $tally at 18.5cm
 16    5 -0.001205 -15  $tally at 20.5cm
 17    5 -0.001205 -16  $tally at 22.5cm
 18    5 -0.001205 -17  $tally at 24.5cm
 19    5 -0.001205 -18  $tally at 26.5cm
c --------------site2 cell-----------------
 20    5 -0.001205 -19 #6 #8 #9 #10 #11 #12 #13 #14 #15 #16 #17 #18 $port
        #19 #21 #22 #23

  c =============define surfaces================
  1     rcc 0.0 0.0 -2.5 0.0 0.0 5 1.50  $  ambe source
  2     rcc 0.0 0.0 -2.52 0.0 0.0 30 1.60  $port inside surface
  3     rcc 0.0 0.0 -27.5 0.0 0.0 55 25  $inner container
  4     rcc 0.0 0.0 -27.65 0.0 0.0 55.3 25.635  $outer container
  6     rcc 0.0 0.0 -2.67 0.0 0.0 30.15 1.75  $port outer surface
```

```
  20      rcc 5.0 0.0 -3.5 0.0 0.0 0.3 1.50
  21      rcc 5.0 0.0 -1.5 0.0 0.0 0.3 1.50
  22      rcc 5.0 0.0 0.5 0.0 0.0 0.3 1.50
   5      rcc 5.0 0.0 2.51 0.0 0.0 0.3 1.50  $tally1
   7      rcc 5.0 0.0 4.51 0.0 0.0 0.3 1.50  $tally2
   8      rcc 5.0 0.0 6.51 0.0 0.0 0.3 1.50  $tally3
   9      rcc 5.0 0.0 8.51 0.0 0.0 0.3 1.50  $tally4
  10      rcc 5.0 0.0 10.51 0.0 0.0 0.3 1.50  $tally5
  11      rcc 5.0 0.0 12.51 0.0 0.0 0.3 1.50  $tally6
  12      rcc 5.0 0.0 14.51 0.0 0.0 0.3 1.50  $tally7
  13      rcc 5.0 0.0 16.51 0.0 0.0 0.3 1.50  $tally8
  14      rcc 5.0 0.0 18.51 0.0 0.0 0.3 1.50  $tally9
  15      rcc 5.0 0.0 20.51 0.0 0.0 0.3 1.50  $tally10
  16      rcc 5.0 0.0 22.51 0.0 0.0 0.3 1.50  $tally11
  17      rcc 5.0 0.0 24.51 0.0 0.0 0.3 1.50  $tally12
  18      rcc 5.0 0.0 26.51 0.0 0.0 0.3 1.50  $tally13
c ----------site2 surfaces--------------------
  19      rcc 5 0 -4 0 0 31.5 1.6  $site2 surface
mode  n
c  ==========define materials==================
m1    95241.            0.08  $AmO2Be
     8016.           0.001 4009.           0.909
m2    26056.             -1  $ iron (steel)
m3    1001.        -0.148605  $paraffin wax
     6000.        -0.851395
m4    49000.             -1  $Indium
m5    6000.        -0.000124  $Air
     7014.        -0.755268 8016.        -0.231781 18000.        -0.012827
imp:n           1 2r                  0          1 18r          $ 1, 20
c
c
c ===========source defination====================
sc1   Am-Be SPECTRUM (ISO 8529)
sdef par=n erg=d1 cell=1 rad=d2 ext=d3 axs=0 0 1
si1   H  0.414E-06 1.1e-1 3.3e-1 5.4e-1 7.5e-1 9.7e-1 0.118e1 0.14e1 0.161e1 0.182e1 0.204e1
     0.225e1 0.247e1 0.268e1 0.29e1 0.311e1 0.332e1 0.354e1 0.375e1 0.397e1 0.418e1 0.439e1 0.461e1
     0.482e1 0.504e1 0.525e1 0.547e1 0.568e1 0.589e1 0.611e1 0.632e1 0.654e1 0.675e1 0.696e1 0.718e1
     0.739e1 0.761e1 0.782e1 0.803e1 0.825e1 0.846e1 0.868e1 0.889e1 0.911e1 0.932e1 0.953e1 0.975e1
     0.996e1 0.1018e2 0.1039e2 0.106e2 0.1082e2 0.1103e2
sp1   D  0.00      0.00144  0.00334  0.00313  0.00281  0.00250
      0.00214  0.00198  0.00175  0.00192  0.00223  0.00215
```

```
      0.00225  0.00228  0.00295  0.00356  0.00369  0.00346
      0.00307  0.00300  0.00269  0.00286  0.00318  0.00307
      0.00333  0.00304  0.00274  0.00233  0.00206  0.00182
      0.00177  0.00204  0.00183  0.00163  0.00167  0.00168
      0.00188  0.00184  0.00169  0.00144  0.000968  0.000652
      0.000426  0.000367  0.000381  0.000506  0.000625  0.000552
      0.000468  0.000370  0.000278  0.000151  0.0000363
si2  0 1.5
sp2 -21 1
si3  3
sp3 -21 0
f4:n  6 8 9 10 11 12 13 14 15 16 17 18 19   $tally neutrons
e4    5e-7 .5 12
mt3 poly.01t $thermal treatment card
print
nps 5000000
```

site3, irradiation channel modeled at 10cm from the block center.

```
 MCNP5 Am-Be input deck, flux profiling
c the irradiation channel Shifted 10cm from the center of the paraffin block.
   c =========define cells================
   1    0        -1  $source
   2    5 -0.001205 -2 #1
   3    3   -0.93 -3 6 19  $moderator material
   4    2   -7.85 -4 3  $drum container
   5    0        4  $define outside world
   7    2   -7.85 -6 2  $tally port
  21    5 -0.001205 -20  $ tally at -3.5 from source centre
  22    5 -0.001205 -21  $tally at -1.5 frm src centre
  23    5 -0.001205 -22  $tally at 0.5 frm src centre
   6    5 -0.001205 -5  $tally at source contact
   8    5 -0.001205 -7  $ tally at 4.5cm from source centre
   9    5 -0.001205 -8  $tally at 6.5cm
  10    5 -0.001205 -9  $tally at 8.5cm
  11    5 -0.001205 -10  $tally at 10.5cm
  12    5 -0.001205 -11  $tally at 12.5cm
  13    5 -0.001205 -12  $tally at 14.5cm
  14    5 -0.001205 -13  $tally at 16.5cm
  15    5 -0.001205 -14  $tally at 18.5cm
  16    5 -0.001205 -15  $tally at 20.5cm
  17    5 -0.001205 -16  $tally at 22.5cm
```

```
  18     5 -0.001205 -17  $tally at 24.5cm
  19     5 -0.001205 -18  $tally at 26.5cm
c ----------site2 cell----------
  20     5 -0.001205 -19 #6 #8 #9 #10 #11 #12 #13 #14 #15 #16 #17 #18 #19 #21
          #22 #23
   c =============define surfaces================
   1       rcc 0.0 0.0 -2.5 0.0 0.0 5 1.50  $  ambe source
   2       rcc 0.0 0.0 -2.52 0.0 0.0 30 1.60  $port inside surface
   3       rcc 0.0 0.0 -27.5 0.0 0.0 55 25  $inside container
   4       rcc 0.0 0.0 -27.65 0.0 0.0 55.3 25.635  $outer container
   6       rcc 0.0 0.0 -2.67 0.0 0.0 30.15 1.75  $port outer surface
  20       rcc 10 0.0 -3.50 0.0 0.0 0.3 1.50
  21       rcc 10 0.0 -1.5 0.0 0.0 0.3 1.50
  22       rcc 10 0.0 0.5 0.0 0.0 0.3 1.50
   5       rcc 10 0.0 2.51 0.0 0.0 0.3 1.50  $tally1
   7       rcc 10 0.0 4.51 0.0 0.0 0.3 1.50  $tally2
   8       rcc 10 0.0 6.51 0.0 0.0 0.3 1.50  $tally3
   9       rcc 10 0.0 8.51 0.0 0.0 0.3 1.50  $tally4
  10       rcc 10 0.0 10.51 0.0 0.0 0.3 1.50  $tally5
  11       rcc 10 0.0 12.51 0.0 0.0 0.3 1.50  $tally6
  12       rcc 10 0.0 14.51 0.0 0.0 0.3 1.50  $tally7
  13       rcc 10 0.0 16.51 0.0 0.0 0.3 1.50  $tally8
  14       rcc 10 0.0 18.51 0.0 0.0 0.3 1.50  $tally9
  15       rcc 10 0.0 20.51 0.0 0.0 0.3 1.50  $tally10
  16       rcc 10 0.0 22.51 0.0 0.0 0.3 1.50  $tally11
  17       rcc 10 0.0 24.51 0.0 0.0 0.3 1.50  $tally12
  18       rcc 10 0.0 26.51 0.0 0.0 0.3 1.50  $tally13
c -----------site2 surfaces--------------------
  19       rcc 10 0 -4 0 0 31.5 1.6  $site2 surface
mode  n
c   ==========define materials==================
m1    95241.            0.08  $AmO2Be
      8016.           0.001 4009.           0.909
m2    26056.             -1  $ iron (steel)
m3    1001.        -0.148605  $paraffin wax
      6000.        -0.851395
m4    49000.             -1  $Indium
m5    6000.        -0.000124  $Air
      7014.        -0.755268 8016.        -0.231781 18000.       -0.012827
imp:n           1 3r                  0          1 17r          $ 1, 20
c
```

```
c
c ===========source defination====================
sc1   Am-Be SPECTRUM (ISO 8529)
sdef par=n erg=d1 cell=1 rad=d2 ext=d3 axs=0 0 1
si1   H  0.414E-06 1.1e-1 3.3e-1 5.4e-1 7.5e-1 9.7e-1 0.118e1 0.14e1 0.161e1 0.182e1 0.204e1
     0.225e1 0.247e1 0.268e1 0.29e1 0.311e1 0.332e1 0.354e1 0.375e1 0.397e1 0.418e1 0.439e1 0.461e1
     0.482e1 0.504e1 0.525e1 0.547e1 0.568e1 0.589e1 0.611e1 0.632e1 0.654e1 0.675e1 0.696e1 0.718e1
     0.739e1 0.761e1 0.782e1 0.803e1 0.825e1 0.846e1 0.868e1 0.889e1 0.911e1 0.932e1 0.953e1 0.975e1
     0.996e1 0.1018e2 0.1039e2 0.106e2 0.1082e2 0.1103e2
sp1   D  0.00      0.00144  0.00334  0.00313  0.00281  0.00250
       0.00214  0.00198  0.00175  0.00192  0.00223  0.00215
       0.00225  0.00228  0.00295  0.00356  0.00369  0.00346
       0.00307  0.00300  0.00269  0.00286  0.00318  0.00307
       0.00333  0.00304  0.00274  0.00233  0.00206  0.00182
       0.00177  0.00204  0.00183  0.00163  0.00167  0.00168
       0.00188  0.00184  0.00169  0.00144  0.000968  0.000652
       0.000426  0.000367  0.000381  0.000506  0.000625  0.000552
       0.000468  0.000370  0.000278  0.000151  0.0000363
si2  0 1.5
sp2 -21 1
si3  3
sp3 -21 0
f4:n  21 22 23 6 8 9 10 11 12 13 14 15 16 17 18 19   $tally neutrons
e4    5e-7 .5 12
mt3 poly.01t $thermal treatment card
print
nps 5000000
```

Site 4, irradiation channel modeled at 15 cm from the block center

```
MCNP5 AmBe input deck, flux profiling
c the irradiation channel Shifted 15cm from the centre of the paraffin block.
   c =========define cells================
   1     0         -1  $source
   2     5 -0.001205 -2 #1
   3     3   -0.93 -3 6 19  $moderator material
   4     2   -7.85 -4 3  $drum container
   5     0         4  $define outside world
   7     2   -7.85 -6 2  $tally port
  21     5 -0.001205 -20  $ tally at -3.5 from source centre
  22     5 -0.001205 -21  $tally at -1.5 frm src centre
  23     5 -0.001205 -22  $tally at 0.5 frm src centre
```

```
   6     5 -0.001205 -5  $tally at source contact
   8     5 -0.001205 -7  $ tally at 4.5cm from source centre
   9     5 -0.001205 -8  $tally at 6.5cm
  10     5 -0.001205 -9  $tally at 8.5cm
  11     5 -0.001205 -10  $tally at 10.5cm
  12     5 -0.001205 -11  $tally at 12.5cm
  13     5 -0.001205 -12  $tally at 14.5cm
  14     5 -0.001205 -13  $tally at 16.5cm
  15     5 -0.001205 -14  $tally at 18.5cm
  16     5 -0.001205 -15  $tally at 20.5cm
  17     5 -0.001205 -16  $tally at 22.5cm
  18     5 -0.001205 -17  $tally at 24.5cm
  19     5 -0.001205 -18  $tally at 26.5cm
c ----------site2 cell----------
  20     5 -0.001205 -19 #6 #8 #9 #10 #11 #12 #13 #14 #15 #16 #17 #18 #19 #21
         #22 #23
   c ============define surfaces===============
   1      rcc 0.0 0.0 -2.5 0.0 0.0 5 1.50  $  ambe source
   2      rcc 0.0 0.0 -2.52 0.0 0.0 30 1.60  $port inside surface
   3      rcc 0.0 0.0 -27.5 0 0 55 25  $inner container
   4      rcc 0.0 0.0 -27.65 0.0 0.0 55.3 25.635  $outer container
   6      rcc 0.0 0.0 -2.67 0.0 0.0 30.15 1.75  $port outer surface
  20      rcc 15 0.0 -3.50 0.0 0.0 0.3 1.50
  21      rcc 15 0.0 -1.50 0.0 0.0 0.3 1.50
  22      rcc 15 0.0 0.5 0.0 0.0 0.3 1.50
   5      rcc 15 0.0 2.51 0.0 0.0 0.3 1.50  $tally1
   7      rcc 15 0.0 4.51 0.0 0.0 0.3 1.50  $tally2
   8      rcc 15 0.0 6.51 0.0 0.0 0.3 1.50  $tally3
   9      rcc 15 0.0 8.51 0.0 0.0 0.3 1.50  $tally4
  10      rcc 15 0.0 10.51 0.0 0.0 0.3 1.50  $tally5
  11      rcc 15 0.0 12.51 0.0 0.0 0.3 1.50  $tally6
  12      rcc 15 0.0 14.51 0.0 0.0 0.3 1.50  $tally7
  13      rcc 15 0.0 16.51 0.0 0.0 0.3 1.50  $tally8
  14      rcc 15 0.0 18.51 0.0 0.0 0.3 1.50  $tally9
  15      rcc 15 0.0 20.51 0.0 0.0 0.3 1.50  $tally10
  16      rcc 15 0.0 22.51 0.0 0.0 0.3 1.50  $tally11
  17      rcc 15 0.0 24.51 0.0 0.0 0.3 1.50  $tally12
  18      rcc 15 0.0 26.51 0.0 0.0 0.3 1.50  $tally13
c ----------site2 surfaces----------
  19      rcc 15 0 -4 0 0 31.5 1.6  $site2 surface
mode  n
```

```
c   ==========define materials==================
m1    95241.            0.08  $AmO2Be
      8016.           0.001 4009.           0.909
m2    26056.             -1  $ iron (steel)
m3    1001.        -0.148605  $paraffin wax
      6000.        -0.851395
m4    49000.             -1  $Indium
m5    6000.        -0.000124  $Air
      7014.        -0.755268 8016.        -0.231781 18000.       -0.012827
imp:n           1 3r                  0          1 17r          $ 1, 20
c
c
c ===========source defination====================
sc1   Am-Be SPECTRUM (ISO 8529)
sdef par=n erg=d1 cell=1 rad=d2 ext=d3 axs=0 0 1
si1   H  0.414E-06 1.1e-1 3.3e-1 5.4e-1 7.5e-1 9.7e-1 0.118e1 0.14e1 0.161e1 0.182e1 0.204e1
      0.225e1 0.247e1 0.268e1 0.29e1 0.311e1 0.332e1 0.354e1 0.375e1 0.397e1 0.418e1 0.439e1 0.461e1
      0.482e1 0.504e1 0.525e1 0.547e1 0.568e1 0.589e1 0.611e1 0.632e1 0.654e1 0.675e1 0.696e1 0.718e1
      0.739e1 0.761e1 0.782e1 0.803e1 0.825e1 0.846e1 0.868e1 0.889e1 0.911e1 0.932e1 0.953e1 0.975e1
      0.996e1 0.1018e2 0.1039e2 0.106e2 0.1082e2 0.1103e2
sp1   D  0.00      0.00144  0.00334  0.00313  0.00281  0.00250
        0.00214  0.00198  0.00175  0.00192  0.00223  0.00215
        0.00225  0.00228  0.00295  0.00356  0.00369  0.00346
        0.00307  0.00300  0.00269  0.00286  0.00318  0.00307
        0.00333  0.00304  0.00274  0.00233  0.00206  0.00182
        0.00177  0.00204  0.00183  0.00163  0.00167  0.00168
        0.00188  0.00184  0.00169  0.00144  0.000968  0.000652
        0.000426  0.000367  0.000381  0.000506  0.000625  0.000552
        0.000468  0.000370  0.000278  0.000151  0.0000363
si2  0 1.5
sp2 -21 1
si3  3
sp3 -21 0
f4:n  21 22 23 6 8 9 10 11 12 13 14 15 16 17 18 19   $tally neutrons
e4    5e-7 .5 12
mt3 poly.01t $thermal treatment card
print
nps 5000000
```

Sample mcnp5 output file for flux profiling at the irradiation site 2. The input file for site 2 has been echoed within the results generated from MCNP.

Note: Due to the bulkiness of the Monte Carlo output, only the tally sections of the output for site 1, 3 and 4 have been included.

```
      Thread Name & Version = mcnp5VE_RSICC, 1.40

                                 _
         ._ _    _  ._   ._    |_
         | | |  (_  | |  |_)    _)
                        |
 +---------------------------------------------------------------------+
 |   This program was prepared by the Regents of the University of     |
 |California at Los Alamos National Laboratory (the University) under  |
 |  contract number W-7405-ENG-36 with the U.S. Department of Energy   |
 |(DoE).  The University has certain rights in the program pursuant to|
 |  the contract and the program should not be copied or distributed   |
 | outside your organization.  All rights in the program are reserved  |
 |by the DoE and the University.  Neither the U.S. Government nor the  |
 | University makes any warranty, express or implied, or assumes any   |
 |     liability or responsibility for the use of this software.       |
 +---------------------------------------------------------------------+

1mcnp     version 5     ld=11112005                      09/03/14 13:58:22
 ***********************************************************************                probid =  09/03/14 13:58:22
  outp = output21 runtpe = runtp21

     1-       MCNP5 AmBe input deck, flux profiling
     2-       c the irradiation channel modelled at 5cm from the center of paraffin block.
     3-           c =========define cells================
     4-            1     0         -1  $source
     5-            2     5 -0.001205 -2 #1
     6-            3     3   -0.93 -3 6 19  $moderator material
     7-            4     2   -7.85 -4 3  $drum container
     8-            5     0         4  $define outside world
     9-            7     2   -7.85 -6 2  $tally port
    10-           21     5 -0.001205 -20  $ tally at -3.5 from source centre
    11-           22     5 -0.001205 -21  $tally at -1.5 frm src centre
    12-           23     5 -0.001205 -22  $tally at 0.5 frm src centre
    13-            6     5 -0.001205 -5  $tally at source contact
    14-            8     5 -0.001205 -7  $ tally at 4.5cm from source centre
    15-            9     5 -0.001205 -8  $tally at 6.5cm
    16-           10     5 -0.001205 -9  $tally at 8.5cm
    17-           11     5 -0.001205 -10  $tally at 10.5cm
    18-           12     5 -0.001205 -11  $tally at 12.5cm
```

```
 19-          13     5 -0.001205 -12  $tally at 14.5cm
 20-          14     5 -0.001205 -13  $tally at 16.5cm
 21-          15     5 -0.001205 -14  $tally at 18.5cm
 22-          16     5 -0.001205 -15  $tally at 20.5cm
 23-          17     5 -0.001205 -16  $tally at 22.5cm
 24-          18     5 -0.001205 -17  $tally at 24.5cm
 25-          19     5 -0.001205 -18  $tally at 26.5cm
 26-       c --------------site2 cell-----------------
 27-          20     5 -0.001205 -19 #6 #8 #9 #10 #11 #12 #13 #14 #15 #16 #17 #18 #19 #21
 28-                    #22 #23
 29-
 30-           c =============define surfaces================
 31-           1       rcc 0 0 -2.5 0 0 5 1.5  $  ambe source
 32-           2       rcc 0 0 -2.52 0 0 30 1.6  $port inner surface
 33-           3       rcc 0 0 -27.5 0 0 55 25  $inner drum
 34-           4       rcc 0 0 -27.65 0 0 55.3 25.635  $outer drum
 35-           6       rcc 0 0 -2.67 0 0 30.15 1.75  $port outer surface
 36-          20       rcc 5 0 -3.5 0 0 0.3 1.5
 37-          21       rcc 5 0 -1.5 0 0 0.3 1.5
 38-          22       rcc 5 0 0.5 0 0 0.3 1.5
 39-           5       rcc 5 0 2.51 0 0 0.3 1.5  $tally1
 40-           7       rcc 5 0 4.51 0 0 0.3 1.5  $tally2
 41-           8       rcc 5 0 6.51 0 0 0.3 1.5  $tally3
 42-           9       rcc 5 0 8.51 0 0 0.3 1.5  $tally4
 43-          10       rcc 5 0 10.51 0 0 0.3 1.5  $tally5
 44-          11       rcc 5 0 12.51 0 0 0.3 1.5  $tally6
 45-          12       rcc 5 0 14.51 0 0 0.3 1.5  $tally7
 46-          13       rcc 5 0 16.51 0 0 0.3 1.5  $tally8
 47-          14       rcc 5 0 18.51 0 0 0.3 1.5  $tally9
 48-          15       rcc 5 0 20.51 0 0 0.3 1.5  $tally10
 49-          16       rcc 5 0 22.51 0 0 0.3 1.5  $tally11
 50-          17       rcc 5 0 24.51 0 0 0.3 1.5  $tally12
 51-          18       rcc 5 0 26.51 0 0 0.3 1.5  $tally13
 52-       c -----------site2 surfaces--------------------
 53-          19       rcc 5 0 -4 0 0 31.5 1.6  $site2 surface
 54-
 55-       mode  n
 56-       c   ==========define materials==================
 57-       m1    95241.             0.08  $AmO2Be
warning. material   1 is not used in the problem.
 58-             8016.            0.001 4009.            0.909
 59-       m2    26056.               -1  $ iron (steel)
 60-       m3    1001.         -0.148605  $paraffin wax
 61-             6000.         -0.851395
 62-       m4    49000.               -1  $Indium
```

```
warning. material   4 is not used in the problem.
  63-       m5    6000.         -0.000124  $Air
  64-             7014.         -0.755268 8016.         -0.231781 18000.        -0.012827
  65-       imp:n             1 3r                      0            1 17r           $ 1, 20
  66-       c
  67-       c
  68-       c ===========source defination====================
  69-       sc1   Am-Be SPECTRUM (ISO 8529)
  70-       sdef par=n erg=d1 cell=1 rad=d2 ext=d3 axs=0 0 1
  71-       si1   H  4.14E-07 0.11 0.33 0.54 0.75 0.97 1.18 1.4 1.61 1.82 2.04
  72-             2.25 2.47 2.68 2.9 3.11 3.32 3.54 3.75 3.97 4.18 4.39 4.61
  73-             4.82 5.04 5.25 5.47 5.68 5.89 6.11 6.32 6.54 6.75 6.96 7.18
  74-             7.39 7.61 7.82 8.03 8.25 8.46 8.68 8.89 9.11 9.32 9.53 9.75
  75-             9.96 10.18 10.39 10.6 10.82 11.03
  76-       sp1   D  0.00      1.44E-02  3.34E-02  3.13E-02  2.81E-02  2.50E-02
  77-               2.14e-02  1.98E-02  1.75E-02  1.92E-02  2.23E-02  2.15E-02
  78-               2.25e-02  2.28E-02  2.95E-02  3.56E-02  3.69E-02  3.46E-02
  79-               3.07e-02  3.00E-02  2.69E-02  2.86E-02  3.18E-02  3.07E-02
  80-               3.33e-02  3.04E-02  2.74E-02  2.33E-02  2.06E-02  1.82E-02
  81-               1.77e-02  2.04E-02  1.83E-02  1.63E-02  1.67e-02  1.68E-02
  82-               1.88e-02  1.84E-02  1.69E-02  1.44E-02  9.68E-03  6.52E-03
  83-               4.26e-03  3.67E-03  3.81E-03  5.06E-03  6.25E-03  5.52E-03
  84-               4.68e-03  3.70E-03  2.78E-03  1.51E-03  3.63E-04
  85-       si2  0 1.5
  86-       sp2 -21 1
  87-       si3  3
  88-       sp3 -21 0
  89-       f4:n  21 22 23 6 8 9 10 11 12 13 14 15 16 17 18 19   $tally neutrons
  90-       e4    5e-7 .5 12
  91-       mt3 poly.01t $thermal treatment card
  92-       print
  93-       nps 5000000

surface      2.2 and surface      6.2 are the same.      6.2 will be deleted.
surface      3.2 and surface     19.2 are the same.     19.2 will be deleted.
surface     20.1 and surface     21.1 are the same.     21.1 will be deleted.
surface     20.1 and surface     22.1 are the same.     22.1 will be deleted.
surface     20.1 and surface      5.1 are the same.      5.1 will be deleted.
surface     20.1 and surface      7.1 are the same.      7.1 will be deleted.
surface     20.1 and surface      8.1 are the same.      8.1 will be deleted.
surface     20.1 and surface      9.1 are the same.      9.1 will be deleted.
surface     20.1 and surface     10.1 are the same.     10.1 will be deleted.
surface     20.1 and surface     11.1 are the same.     11.1 will be deleted.
surface     20.1 and surface     12.1 are the same.     12.1 will be deleted.
surface     20.1 and surface     13.1 are the same.     13.1 will be deleted.
```

```
 surface     20.1 and surface     14.1 are the same.     14.1 will be deleted.
 surface     20.1 and surface     15.1 are the same.     15.1 will be deleted.
 surface     20.1 and surface     16.1 are the same.     16.1 will be deleted.
 surface     20.1 and surface     17.1 are the same.     17.1 will be deleted.
 surface     20.1 and surface     18.1 are the same.     18.1 will be deleted.

 comment.   17 surfaces were deleted for being the same as others.
1source                                                                    print table 10
 values of defaulted or explicitly defined source variables

    cel        1.0000E+00
    sur        0.0000E+00
    tme        0.0000E+00
    dir        isotropic
    pos        0.0000E+00   0.0000E+00   0.0000E+00
    x          0.0000E+00
    y          0.0000E+00
    z          0.0000E+00
    axs        0.0000E+00   0.0000E+00   1.0000E+00
    vec        0.0000E+00   0.0000E+00   0.0000E+00
    ccc        0.0000E+00
    nrm        1.0000E+00
    ara        0.0000E+00
    wgt        1.0000E+00
    eff        1.0000E-02
    par        1.0000E+00
    tr         0.0000E+00

 probability distribution   2 for source variable rad
 power law 21:     f(x)=c*abs(x)**k          k = 1.0000E+00

 probability distribution   3 for source variable ext
 power law 21:     f(x)=c*abs(x)**k          k = 0.0000E+00

 probability distribution   1 for source variable erg
           Am-Be SPECTRUM (ISO 8529)
 unbiased histogram distribution

 source        source           cumulative          probability
  entry         value           probability           of bin
    1       4.14000E-07        0.000000E+00        0.000000E+00
    2       1.10000E-01        1.439708E-02        1.439708E-02
    3       3.30000E-01        4.779030E-02        3.339322E-02
    4       5.40000E-01        7.908395E-02        3.129365E-02
    5       7.50000E-01        1.071782E-01        2.809430E-02
```

6	9.70000E-01	1.321732E-01	2.499493E-02
7	1.18000E+00	1.535688E-01	2.139566E-02
8	1.40000E+00	1.733648E-01	1.979598E-02
9	1.61000E+00	1.908613E-01	1.749645E-02
10	1.82000E+00	2.100574E-01	1.919610E-02
11	2.04000E+00	2.323528E-01	2.229547E-02
12	2.25000E+00	2.538485E-01	2.149564E-02
13	2.47000E+00	2.763439E-01	2.249543E-02
14	2.68000E+00	2.991393E-01	2.279537E-02
15	2.90000E+00	3.286333E-01	2.949401E-02
16	3.11000E+00	3.642261E-01	3.559277E-02
17	3.32000E+00	4.011186E-01	3.689251E-02
18	3.54000E+00	4.357116E-01	3.459298E-02
19	3.75000E+00	4.664053E-01	3.069377E-02
20	3.97000E+00	4.963992E-01	2.999391E-02
21	4.18000E+00	5.232938E-01	2.689454E-02
22	4.39000E+00	5.518880E-01	2.859420E-02
23	4.61000E+00	5.836815E-01	3.179355E-02
24	4.82000E+00	6.143753E-01	3.069377E-02
25	5.04000E+00	6.476685E-01	3.329324E-02
26	5.25000E+00	6.780624E-01	3.039383E-02
27	5.47000E+00	7.054568E-01	2.739444E-02
28	5.68000E+00	7.287521E-01	2.329527E-02
29	5.89000E+00	7.493479E-01	2.059582E-02
30	6.11000E+00	7.675442E-01	1.819631E-02
31	6.32000E+00	7.852406E-01	1.769641E-02
32	6.54000E+00	8.056365E-01	2.039586E-02
33	6.75000E+00	8.239327E-01	1.829629E-02
34	6.96000E+00	8.402294E-01	1.629669E-02
35	7.18000E+00	8.569260E-01	1.669661E-02
36	7.39000E+00	8.737226E-01	1.679659E-02
37	7.61000E+00	8.925188E-01	1.879618E-02
38	7.82000E+00	9.109151E-01	1.839627E-02
39	8.03000E+00	9.278117E-01	1.689657E-02
40	8.25000E+00	9.422087E-01	1.439708E-02
41	8.46000E+00	9.518868E-01	9.678035E-03
42	8.68000E+00	9.584054E-01	6.518677E-03
43	8.89000E+00	9.626646E-01	4.259135E-03
44	9.11000E+00	9.663338E-01	3.669255E-03
45	9.32000E+00	9.701431E-01	3.809227E-03
46	9.53000E+00	9.752020E-01	5.058973E-03
47	9.75000E+00	9.814508E-01	6.248732E-03
48	9.96000E+00	9.869696E-01	5.518880E-03
49	1.01800E+01	9.916487E-01	4.679050E-03
50	1.03900E+01	9.953479E-01	3.699249E-03

```
   51       1.06000E+01        9.981274E-01        2.779436E-03
   52       1.08200E+01        9.996371E-01        1.509694E-03
   53       1.10300E+01        1.000000E+00        3.629263E-04

     the mean of source distribution   1 is  4.1576E+00

 order of sampling source variables.
 cel axs rad ext pos erg tme
1tally   4                                                                                    print table 30
          tally type 4    track length estimate of particle flux.
          tally for  neutrons
 cells    21 22 23 6 8 9 10 11 12 13 14 15 16 17 18 19

 energy bins
      0.00000E+00  to  5.00000E-07 mev
      5.00000E-07  to  5.00000E-01 mev
      5.00000E-01  to  1.20000E+01 mev
      total bin
1material composition                                                                         print table 40

 material
  number     component nuclide, atom fraction

     2           26056, 1.00000E+00
     3            1001, 6.75342E-01       6000, 3.24658E-01
 associated thermal s(a,b) data sets:    poly.01t
     5            6000, 1.50147E-04       7014, 7.84428E-01       8016, 2.10752E-01      18000, 4.66992E-03
 material
  number     component nuclide, mass fraction

     2           26056, 1.00000E+00
     3            1001, 1.48605E-01       6000, 8.51395E-01
     5            6000, 1.24000E-04       7014, 7.55268E-01       8016, 2.31781E-01      18000, 1.28270E-02

1cell volumes and masses                                                                      print table 50

        cell     atom          gram         input       calculated                              reason volume
                density       density       volume        volume         mass       pieces    not calculated

     1     1  0.00000E+00   0.00000E+00   0.00000E+00   3.53429E+01   0.00000E+00      1
     2     2  4.98948E-05   1.20500E-03   0.00000E+00   2.05931E+02   2.48147E-01      1
     3     3  1.22279E-01   9.30000E-01   0.00000E+00   0.00000E+00   0.00000E+00      0      asymmetric
     4     4  8.45143E-02   7.85000E+00   0.00000E+00   6.17503E+03   4.84740E+04      1
     5     5  0.00000E+00   0.00000E+00   0.00000E+00   0.00000E+00   0.00000E+00      0      infinite
     6     7  8.45143E-02   7.85000E+00   0.00000E+00   4.88027E+01   3.83101E+02      1
```

7	21	4.98948E-05	1.20500E-03	0.00000E+00	2.12058E+00	2.55529E-03	1
8	22	4.98948E-05	1.20500E-03	0.00000E+00	2.12058E+00	2.55529E-03	1
9	23	4.98948E-05	1.20500E-03	0.00000E+00	2.12058E+00	2.55529E-03	1
10	6	4.98948E-05	1.20500E-03	0.00000E+00	2.12058E+00	2.55529E-03	1
11	8	4.98948E-05	1.20500E-03	0.00000E+00	2.12058E+00	2.55529E-03	1
12	9	4.98948E-05	1.20500E-03	0.00000E+00	2.12058E+00	2.55529E-03	1
13	10	4.98948E-05	1.20500E-03	0.00000E+00	2.12058E+00	2.55529E-03	1
14	11	4.98948E-05	1.20500E-03	0.00000E+00	2.12058E+00	2.55529E-03	1
15	12	4.98948E-05	1.20500E-03	0.00000E+00	2.12058E+00	2.55529E-03	1
16	13	4.98948E-05	1.20500E-03	0.00000E+00	2.12058E+00	2.55529E-03	1
17	14	4.98948E-05	1.20500E-03	0.00000E+00	2.12058E+00	2.55529E-03	1
18	15	4.98948E-05	1.20500E-03	0.00000E+00	2.12058E+00	2.55529E-03	1
19	16	4.98948E-05	1.20500E-03	0.00000E+00	2.12058E+00	2.55529E-03	1
20	17	4.98948E-05	1.20500E-03	0.00000E+00	2.12058E+00	2.55529E-03	1
21	18	4.98948E-05	1.20500E-03	0.00000E+00	2.12058E+00	2.55529E-03	1
22	19	4.98948E-05	1.20500E-03	0.00000E+00	2.12058E+00	2.55529E-03	1
23	20	4.98948E-05	1.20500E-03	0.00000E+00	2.19409E+00	2.64388E-01	1

1surface areas print table 50

surface	input area	calculated area	reason area not calculated
2	1.1	0.00000E+00	4.71239E+01	
3	1.2	0.00000E+00	7.06858E+00	
4	1.3	0.00000E+00	7.06858E+00	
6	2.1	0.00000E+00	3.01593E+02	
7	2.2	0.00000E+00	9.62113E+00	
8	2.3	0.00000E+00	8.04248E+00	
10	3.1	0.00000E+00	8.63938E+03	
11	3.2	0.00000E+00	0.00000E+00	asymmetric
12	3.3	0.00000E+00	1.96350E+03	
14	4.1	0.00000E+00	8.90714E+03	
15	4.2	0.00000E+00	2.06451E+03	
16	4.3	0.00000E+00	2.06451E+03	
18	6.1	0.00000E+00	3.31517E+02	
20	6.3	0.00000E+00	9.62113E+00	
22	20.1	0.00000E+00	4.52389E+01	
23	20.2	0.00000E+00	7.06858E+00	
24	20.3	0.00000E+00	7.06858E+00	
27	21.2	0.00000E+00	7.06858E+00	
28	21.3	0.00000E+00	7.06858E+00	
31	22.2	0.00000E+00	7.06858E+00	
32	22.3	0.00000E+00	7.06858E+00	
35	5.2	0.00000E+00	7.06858E+00	
36	5.3	0.00000E+00	7.06858E+00	

39	7.2	0.00000E+00	7.06858E+00
40	7.3	0.00000E+00	7.06858E+00
43	8.2	0.00000E+00	7.06858E+00
44	8.3	0.00000E+00	7.06858E+00
47	9.2	0.00000E+00	7.06858E+00
48	9.3	0.00000E+00	7.06858E+00
51	10.2	0.00000E+00	7.06858E+00
52	10.3	0.00000E+00	7.06858E+00
55	11.2	0.00000E+00	7.06858E+00
56	11.3	0.00000E+00	7.06858E+00
59	12.2	0.00000E+00	7.06858E+00
60	12.3	0.00000E+00	7.06858E+00
63	13.2	0.00000E+00	7.06858E+00
64	13.3	0.00000E+00	7.06858E+00
67	14.2	0.00000E+00	7.06858E+00
68	14.3	0.00000E+00	7.06858E+00
71	15.2	0.00000E+00	7.06858E+00
72	15.3	0.00000E+00	7.06858E+00
75	16.2	0.00000E+00	7.06858E+00
76	16.3	0.00000E+00	7.06858E+00
79	17.2	0.00000E+00	7.06858E+00
80	17.3	0.00000E+00	7.06858E+00
83	18.2	0.00000E+00	7.06858E+00
84	18.3	0.00000E+00	7.06858E+00
86	19.1	0.00000E+00	3.16673E+02
88	19.3	0.00000E+00	8.04248E+00

1cells print table 60

	cell	mat	atom density	gram density	volume	mass	pieces	neutron importance
1	1	0	0.00000E+00	0.00000E+00	3.53429E+01	0.00000E+00	1	1.0000E+00
2	2	5	4.98948E-05	1.20500E-03	2.05931E+02	2.48147E-01	1	1.0000E+00
3	3	3s	1.22279E-01	9.30000E-01	0.00000E+00	0.00000E+00	0	1.0000E+00
4	4	2	8.45143E-02	7.85000E+00	6.17503E+03	4.84740E+04	1	1.0000E+00
5	5	0	0.00000E+00	0.00000E+00	0.00000E+00	0.00000E+00	0	0.0000E+00
6	7	2	8.45143E-02	7.85000E+00	4.88027E+01	3.83101E+02	1	1.0000E+00
7	21	5	4.98948E-05	1.20500E-03	2.12058E+00	2.55529E-03	1	1.0000E+00
8	22	5	4.98948E-05	1.20500E-03	2.12058E+00	2.55529E-03	1	1.0000E+00
9	23	5	4.98948E-05	1.20500E-03	2.12058E+00	2.55529E-03	1	1.0000E+00
10	6	5	4.98948E-05	1.20500E-03	2.12058E+00	2.55529E-03	1	1.0000E+00
11	8	5	4.98948E-05	1.20500E-03	2.12058E+00	2.55529E-03	1	1.0000E+00
12	9	5	4.98948E-05	1.20500E-03	2.12058E+00	2.55529E-03	1	1.0000E+00
13	10	5	4.98948E-05	1.20500E-03	2.12058E+00	2.55529E-03	1	1.0000E+00
14	11	5	4.98948E-05	1.20500E-03	2.12058E+00	2.55529E-03	1	1.0000E+00

15	12	5	4.98948E-05	1.20500E-03	2.12058E+00	2.55529E-03	1	1.0000E+00
16	13	5	4.98948E-05	1.20500E-03	2.12058E+00	2.55529E-03	1	1.0000E+00
17	14	5	4.98948E-05	1.20500E-03	2.12058E+00	2.55529E-03	1	1.0000E+00
18	15	5	4.98948E-05	1.20500E-03	2.12058E+00	2.55529E-03	1	1.0000E+00
19	16	5	4.98948E-05	1.20500E-03	2.12058E+00	2.55529E-03	1	1.0000E+00
20	17	5	4.98948E-05	1.20500E-03	2.12058E+00	2.55529E-03	1	1.0000E+00
21	18	5	4.98948E-05	1.20500E-03	2.12058E+00	2.55529E-03	1	1.0000E+00
22	19	5	4.98948E-05	1.20500E-03	2.12058E+00	2.55529E-03	1	1.0000E+00
23	20	5	4.98948E-05	1.20500E-03	2.19409E+02	2.64388E-01	1	1.0000E+00

total 6.71845E+03 4.88576E+04

1surfaces print table 70

surface	trans	type	surface coefficients			
1	1	rcc				
2	1.1	cz	1.5000000E+00			
3	1.2	pz	2.5000000E+00			
4	1.3	p	0.0000000E+00	0.0000000E+00	-1.0000000E+00	2.5000000E+00
5	2	rcc				
6	2.1	cz	1.6000000E+00			
7	2.2	pz	2.7480000E+01			
8	2.3	p	0.0000000E+00	0.0000000E+00	-1.0000000E+00	2.5200000E+00
9	3	rcc				
10	3.1	cz	2.5000000E+01			
11	3.2	pz	2.7500000E+01			
12	3.3	p	0.0000000E+00	0.0000000E+00	-1.0000000E+00	2.7500000E+01
13	4	rcc				
14	4.1	cz	2.5635000E+01			
15	4.2	pz	2.7650000E+01			
16	4.3	p	0.0000000E+00	0.0000000E+00	-1.0000000E+00	2.7650000E+01
17	6	rcc				
18	6.1	cz	1.7500000E+00			
20	6.3	p	0.0000000E+00	0.0000000E+00	-1.0000000E+00	2.6700000E+00
21	20	rcc				
22	20.1	c/z	5.0000000E+00	0.0000000E+00	1.5000000E+00	
23	20.2	pz	-3.2000000E+00			
24	20.3	p	0.0000000E+00	0.0000000E+00	-1.0000000E+00	3.5000000E+00
25	21	rcc				
27	21.2	pz	-1.2000000E+00			
28	21.3	p	0.0000000E+00	0.0000000E+00	-1.0000000E+00	1.5000000E+00
29	22	rcc				
31	22.2	pz	8.0000000E-01			
32	22.3	p	0.0000000E+00	0.0000000E+00	-1.0000000E+00	-5.0000000E-01
33	5	rcc				
35	5.2	pz	2.8100000E+00			

```
     36      5.3             p     0.0000000E+00   0.0000000E+00  -1.0000000E+00  -2.5100000E+00
     37      7               rcc
     39      7.2             pz    4.8100000E+00
     40      7.3             p     0.0000000E+00   0.0000000E+00  -1.0000000E+00  -4.5100000E+00
     41      8               rcc
     43      8.2             pz    6.8100000E+00
     44      8.3             p     0.0000000E+00   0.0000000E+00  -1.0000000E+00  -6.5100000E+00
     45      9               rcc
     47      9.2             pz    8.8100000E+00
     48      9.3             p     0.0000000E+00   0.0000000E+00  -1.0000000E+00  -8.5100000E+00
     49     10               rcc
     51     10.2             pz    1.0810000E+01
     52     10.3             p     0.0000000E+00   0.0000000E+00  -1.0000000E+00  -1.0510000E+01
     53     11               rcc
     55     11.2             pz    1.2810000E+01
     56     11.3             p     0.0000000E+00   0.0000000E+00  -1.0000000E+00  -1.2510000E+01
     57     12               rcc
     59     12.2             pz    1.4810000E+01
     60     12.3             p     0.0000000E+00   0.0000000E+00  -1.0000000E+00  -1.4510000E+01
     61     13               rcc
     63     13.2             pz    1.6810000E+01
     64     13.3             p     0.0000000E+00   0.0000000E+00  -1.0000000E+00  -1.6510000E+01
     65     14               rcc
     67     14.2             pz    1.8810000E+01
     68     14.3             p     0.0000000E+00   0.0000000E+00  -1.0000000E+00  -1.8510000E+01
     69     15               rcc
     71     15.2             pz    2.0810000E+01
     72     15.3             p     0.0000000E+00   0.0000000E+00  -1.0000000E+00  -2.0510000E+01
     73     16               rcc
     75     16.2             pz    2.2810000E+01
     76     16.3             p     0.0000000E+00   0.0000000E+00  -1.0000000E+00  -2.2510000E+01
     77     17               rcc
     79     17.2             pz    2.4810000E+01
     80     17.3             p     0.0000000E+00   0.0000000E+00  -1.0000000E+00  -2.4510000E+01
     81     18               rcc
     83     18.2             pz    2.6810000E+01
     84     18.3             p     0.0000000E+00   0.0000000E+00  -1.0000000E+00  -2.6510000E+01
     85     19               rcc
     86     19.1             c/z   5.0000000E+00   0.0000000E+00   1.6000000E+00
     88     19.3             p     0.0000000E+00   0.0000000E+00  -1.0000000E+00   4.0000000E+00
1  identical surfaces                                                                          print table 70

   master surface     identical surfaces
        2.2               6.2
        3.2              19.2
```

```
      20.1             21.1      22.1       5.1       7.1       8.1       9.1      10.1      11.1      12.1      13.1
                       14.1      15.1      16.1      17.1      18.1


   surface coefficients for identical surfaces not used.

         surface     trans  type   surface coefficients

    19      6.2              pz    2.7480000E+01
    87     19.2              pz    2.7500000E+01
    26     21.1              c/z   5.0000000E+00   0.0000000E+00   1.5000000E+00
    30     22.1              c/z   5.0000000E+00   0.0000000E+00   1.5000000E+00
    34      5.1              c/z   5.0000000E+00   0.0000000E+00   1.5000000E+00
    38      7.1              c/z   5.0000000E+00   0.0000000E+00   1.5000000E+00
    42      8.1              c/z   5.0000000E+00   0.0000000E+00   1.5000000E+00
    46      9.1              c/z   5.0000000E+00   0.0000000E+00   1.5000000E+00
    50     10.1              c/z   5.0000000E+00   0.0000000E+00   1.5000000E+00
    54     11.1              c/z   5.0000000E+00   0.0000000E+00   1.5000000E+00
    58     12.1              c/z   5.0000000E+00   0.0000000E+00   1.5000000E+00
    62     13.1              c/z   5.0000000E+00   0.0000000E+00   1.5000000E+00
    66     14.1              c/z   5.0000000E+00   0.0000000E+00   1.5000000E+00
    70     15.1              c/z   5.0000000E+00   0.0000000E+00   1.5000000E+00
    74     16.1              c/z   5.0000000E+00   0.0000000E+00   1.5000000E+00
    78     17.1              c/z   5.0000000E+00   0.0000000E+00   1.5000000E+00
    82     18.1              c/z   5.0000000E+00   0.0000000E+00   1.5000000E+00
1  cell temperatures in mev for the free-gas thermal neutron treatment.                                    print table 72

   all non-zero importance cells with materials have a temperature for thermal neutrons of 2.5300E-08 mev.

    minimum source weight = 1.0000E+00    maximum source weight = 1.0000E+00

 ***************************************************
 * Random Number Generator  =                    1 *
 * Random Number Seed       =       19073486328125 *
 * Random Number Multiplier =       19073486328125 *
 * Random Number Adder      =                    0 *
 * Random Number Bits Used  =                   48 *
 * Random Number Stride     =               152917 *
 ***************************************************

         2 warning messages so far.
1physical constants                                                                                      print table 98
   name                     value     description

   huge      1.0000000000000E+36     infinity
```

```
    pie      3.1415926535898E+00     pi
  euler      5.7721566490153E-01     euler constant
 avogad      6.0220434469282E+23     avogadro number (molecules/mole)
  aneut      1.0086649670000E+00     neutron mass (amu)
  avgdn      5.9703109000000E-01     avogadro number/neutron mass (1.e-24*molecules/mole/amu)
  slite      2.9979250000000E+02     speed of light (cm/shake)
 planck      4.1357320000000E-13     planck constant (mev shake)
  fscon      1.3703930000000E+02     inverse fine structure constant h*c/(2*pi*e**2)
 gpt(1)      9.3958000000000E+02     neutron mass (mev)
 gpt(3)      5.1100800000000E-01     electron mass (mev)

 fission q-values:     nuclide    q(mev)   nuclide    q(mev)
                         90232    171.91     91233    175.57
                         92233    180.84     92234    179.45
                         92235    180.88     92236    179.50
                         92237    180.40     92238    181.31
                         92239    180.40     92240    180.40
                         93237    183.67     94238    186.65
                         94239    189.44     94240    186.36
                         94241    188.99     94242    185.98
                         94243    187.48     95241    190.83
                         95242    190.54     95243    190.25
                         96242    190.49     96244    190.49
                         other    180.00

 the following compilation options were used:
     cheap
     dec
     plot
     mcplot
     default datapath: C:\Users\Tollah\Desktop\prompt gamma\mncpdata
                       c:\Progra~1\LANL\MCNP5\data
1cross-section tables                                                                    print table 100

     table    length

                         tables from file actia

   1001.62c    5202  1-h-1 at 293.6K from endf-vi.8 njoy99.50                          mat 125      12/05/01
   7014.62c   67462  7-n-14 at 293.6K from endf-vi.8 njoy99.50                         mat 725      12/05/01
   8016.62c  170541  8-o-16 at 293.6K from endf-vi.8 njoy99.50                         mat 825      12/05/01
  26056.62c  230655  26-fe-56 at 293.6K from endf-vi.8 njoy99.50                       mat2631      12/20/01

                         tables from file endf66a
```

```
   6000.66c   44688  6-c-0 at 293.6K from endf-vi.6 njoy99.50                                  mat 600      07/13/01

                       tables from file rmccsa

  18000.35c    2182      endl85                                                               (  18)       11/01/85
                     temperature = 0.0000E+00 adjusted to 2.5300E-08

                       tables from file tmccs

   poly.01t   11544  hydrogen in polyethylene at 300 degrees kelvin                    1001     0     010/22/85

  total      532274

 warning. neutron energy cutoff is below some cross-section tables.

 comment.    1 cross sections modified by free gas thermal treatment.
1assignment of s(a,b) data to nuclides.                                                        print table 102
       mat        nuclide         s(a,b)
         3       1001.62c       poly.01t

 ***************************************************************************************************************
 dump no.    1 on file runtp21      nps =           0     coll =              0     ctm =        0.00   nrn =                0

         3 warning messages so far.
1   starting mcrun.      cp0 =  0.85         print table 110

      MCNP5 AmBe input deck, flux profiling

     nps    x          y          z       cell   surf     u          v          w        energy     weight      time

      1  2.099E-01 -1.272E+00  2.177E+00     1      0  5.166E-01  5.185E-01  6.814E-01  6.310E+00  1.000E+00  0.000E+00
      2  5.422E-02 -1.712E-01 -1.929E-01     1      0 -8.244E-02 -9.427E-01 -3.233E-01  7.449E-01  1.000E+00  0.000E+00
      3 -1.142E+00  4.730E-01 -9.649E-01     1      0 -6.367E-01  4.540E-01 -6.233E-01  6.562E+00  1.000E+00  0.000E+00
      4 -8.101E-01  3.888E-01 -2.095E+00     1      0 -9.848E-01 -1.736E-01 -7.957E-03  8.488E+00  1.000E+00  0.000E+00
      5  3.491E-01  1.359E-01 -2.032E+00     1      0  9.284E-01  2.974E-01  2.228E-01  3.165E+00  1.000E+00  0.000E+00
      6 -7.028E-01 -7.112E-01  2.024E+00     1      0 -6.936E-01  6.748E-01  2.520E-01  4.561E+00  1.000E+00  0.000E+00
      7  7.359E-01 -7.801E-01 -2.044E+00     1      0  3.703E-02  9.959E-01  8.298E-02  7.112E+00  1.000E+00  0.000E+00
      8 -5.210E-01  1.081E+00 -1.426E+00     1      0 -8.157E-01 -5.283E-01 -2.355E-01  2.799E+00  1.000E+00  0.000E+00
      9 -1.256E+00  4.554E-01 -5.872E-01     1      0 -5.711E-01 -8.174E-01 -7.528E-02  8.054E+00  1.000E+00  0.000E+00
     10 -5.600E-01  7.263E-01  2.191E+00     1      0 -1.764E-01  2.394E-01  9.548E-01  2.655E+00  1.000E+00  0.000E+00
     11  5.418E-01 -6.242E-01 -3.128E-01     1      0 -4.723E-01  5.705E-01  6.719E-01  1.300E-01  1.000E+00  0.000E+00
     12  5.545E-01 -7.585E-01  5.511E-01     1      0  4.851E-01  8.694E-01 -9.375E-02  4.256E+00  1.000E+00  0.000E+00
     13  5.030E-01 -4.919E-01  9.519E-01     1      0  1.374E-01  3.418E-02  9.899E-01  9.199E+00  1.000E+00  0.000E+00
     14 -8.438E-01  2.205E-01 -1.561E+00     1      0  5.931E-01 -7.669E-01  2.451E-01  8.114E+00  1.000E+00  0.000E+00
     15 -9.545E-01 -9.299E-01 -2.374E+00     1      0 -4.013E-01 -1.894E-01 -8.961E-01  9.476E-01  1.000E+00  0.000E+00
```

```
    16  1.058E+00  1.063E+00  2.422E+00     1      0 -1.418E-01  9.037E-01 -4.040E-01  4.345E+00  1.000E+00  0.000E+00
    17 -1.431E-01  2.952E-01  4.987E-01     1      0 -9.929E-01 -1.165E-01 -2.391E-02  5.223E+00  1.000E+00  0.000E+00
    18 -7.080E-01 -9.759E-01 -8.780E-01     1      0  5.765E-01 -5.180E-01 -6.319E-01  5.554E+00  1.000E+00  0.000E+00
    19 -2.030E-01  1.003E+00  2.034E-02     1      0  1.294E-01  9.826E-01 -1.336E-01  6.187E+00  1.000E+00  0.000E+00
    20 -1.206E-01  1.370E+00 -1.916E+00     1      0  3.339E-01 -9.410E-01 -5.451E-02  4.373E+00  1.000E+00  0.000E+00
    21 -5.244E-01 -1.250E+00  6.512E-02     1      0  5.795E-01  3.499E-01 -7.360E-01  3.059E+00  1.000E+00  0.000E+00
    22  9.379E-01 -1.887E-01 -2.901E-01     1      0  1.029E-01  2.800E-01  9.545E-01  3.053E+00  1.000E+00  0.000E+00
    23 -6.952E-01  1.095E+00 -6.074E-01     1      0  7.976E-01  5.383E-01  2.722E-01  3.203E+00  1.000E+00  0.000E+00
    24 -8.253E-01 -8.552E-01 -2.097E+00     1      0  2.162E-01 -9.717E-01  9.501E-02  9.114E+00  1.000E+00  0.000E+00
    25 -6.992E-01 -6.316E-01 -2.269E+00     1      0  8.598E-01  1.098E-01 -4.988E-01  3.980E+00  1.000E+00  0.000E+00
    26  6.325E-01 -5.209E-01 -1.372E+00     1      0  5.269E-01  8.425E-01 -1.124E-01  4.200E+00  1.000E+00  0.000E+00
    27 -7.273E-01 -1.078E+00  9.545E-01     1      0 -3.163E-01 -9.343E-01 -1.645E-01  1.052E+01  1.000E+00  0.000E+00
    28 -1.007E+00 -5.857E-01  1.692E+00     1      0 -1.635E-03  8.397E-01 -5.431E-01  6.604E+00  1.000E+00  0.000E+00
    29 -1.557E-01  7.887E-01 -3.304E-01     1      0  8.756E-01  2.382E-01  4.203E-01  2.804E+00  1.000E+00  0.000E+00
    30 -8.891E-02 -1.390E-01 -1.357E+00     1      0 -7.427E-01  4.420E-01 -5.031E-01  2.918E+00  1.000E+00  0.000E+00
    31 -1.203E+00 -9.928E-02 -8.629E-01     1      0  6.721E-01  4.360E-01 -5.984E-01  8.352E+00  1.000E+00  0.000E+00
    32  4.742E-01  7.898E-01 -1.876E+00     1      0  5.889E-01 -2.806E-01  7.579E-01  6.214E+00  1.000E+00  0.000E+00
    33  9.393E-01  1.181E-01 -1.801E+00     1      0 -1.759E-01 -9.841E-01 -2.470E-02  4.915E+00  1.000E+00  0.000E+00
    34 -9.067E-01 -1.086E+00 -9.384E-01     1      0 -9.046E-01 -2.333E-01  3.568E-01  7.022E-01  1.000E+00  0.000E+00
    35  1.341E+00 -1.248E-01  9.722E-01     1      0  2.208E-01 -6.396E-01 -7.363E-01  3.675E+00  1.000E+00  0.000E+00
    36 -4.565E-01  1.051E-01 -4.304E-01     1      0 -2.326E-01  2.109E-01 -9.494E-01  1.010E+01  1.000E+00  0.000E+00
    37 -1.451E+00  3.481E-01  1.900E+00     1      0  4.104E-01  4.585E-01 -7.882E-01  2.504E+00  1.000E+00  0.000E+00
    38  5.241E-01  1.008E+00 -1.769E+00     1      0 -1.280E-01 -5.422E-01 -8.304E-01  5.272E+00  1.000E+00  0.000E+00
    39 -1.328E+00  2.147E-01 -1.898E+00     1      0  9.969E-01  7.838E-02  9.892E-03  3.241E+00  1.000E+00  0.000E+00
    40  5.028E-01  4.677E-01  1.620E+00     1      0 -7.220E-01 -3.510E-01  5.963E-01  4.446E+00  1.000E+00  0.000E+00
    41  3.725E-02  7.696E-01 -1.023E+00     1      0 -6.721E-02 -6.602E-01  7.481E-01  7.835E+00  1.000E+00  0.000E+00
    42 -4.592E-01  2.278E-01 -2.291E+00     1      0 -2.972E-01 -8.971E-01  3.268E-01  8.024E+00  1.000E+00  0.000E+00
    43 -1.146E+00  7.127E-01  1.944E+00     1      0 -8.588E-01  5.123E-01  9.803E-03  3.626E+00  1.000E+00  0.000E+00
    44  8.313E-01 -1.042E+00 -4.102E-01     1      0  7.015E-01  5.832E-01  4.096E-01  7.900E+00  1.000E+00  0.000E+00
    45  1.046E-01  9.383E-01 -5.458E-01     1      0 -5.448E-01 -3.639E-01  7.555E-01  2.364E+00  1.000E+00  0.000E+00
    46  2.730E-01  5.203E-01 -8.464E-01     1      0 -5.343E-01 -2.166E-01  8.171E-01  8.023E+00  1.000E+00  0.000E+00
    47 -5.950E-01 -1.280E+00  1.534E+00     1      0  1.474E-01 -9.044E-01 -4.005E-01  1.214E+00  1.000E+00  0.000E+00
    48 -7.378E-01 -1.237E+00  2.591E-02     1      0 -7.856E-01  2.032E-01 -5.845E-01  5.127E+00  1.000E+00  0.000E+00
    49  3.171E-01  1.236E+00 -2.269E+00     1      0 -7.230E-01 -6.785E-01  1.298E-01  2.279E+00  1.000E+00  0.000E+00
    50  2.071E-01 -5.832E-01  3.345E-01     1      0  4.058E-01 -5.934E-01 -6.951E-01  8.490E-02  1.000E+00  0.000E+00

 ************************************************************************************************************************
 dump no.    2 on file runtp21      nps =     4530636     coll =     1533475700     ctm =       60.00   nrn =       12325639268

1problem summary
      run terminated when     5000000  particle histories were done.
+                                                                                                    09/03/14 14:05:40
      MCNP5 AmBe input deck, flux profiling                                                 probid =  09/03/14 13:58:22
0
 neutron creation    tracks      weight        energy            neutron loss        tracks      weight        energy
```

		(per source particle)				(per source particle)	
source	5000000	1.0000E+00	4.1585E+00	escape	518181	8.4354E-02	2.1150E-01
				energy cutoff	0	0.	0.
				time cutoff	0	0.	0.
weight window	0	0.	0.	weight window	0	0.	0.
cell importance	0	0.	0.	cell importance	0	0.	0.
weight cutoff	0	2.2273E-01	1.1614E-08	weight cutoff	4481819	2.2278E-01	1.4770E-08
e or t importance	0	0.	0.	e or t importance	0	0.	0.
dxtran	0	0.	0.	dxtran	0	0.	0.
forced collisions	0	0.	0.	forced collisions	0	0.	0.
exp. transform	0	0.	0.	exp. transform	0	0.	0.
upscattering	0	0.	9.0603E-07	downscattering	0	0.	3.9015E+00
photonuclear	0	0.	0.	capture	0	9.1559E-01	4.5494E-02
(n,xn)	0	0.	0.	loss to (n,xn)	0	0.	0.
prompt fission	0	0.	0.	loss to fission	0	0.	0.
delayed fission	0	0.	0.				
total	5000000	1.2227E+00	4.1585E+00	total	5000000	1.2227E+00	4.1585E+00

number of neutrons banked	0	average time of (shakes)		cutoffs	
neutron tracks per source particle	1.0000E+00	escape	3.1072E+03	tco	1.0000E+33
neutron collisions per source particle	3.3848E+02	capture	1.6186E+04	eco	0.0000E+00
total neutron collisions	1692383003	capture or escape	1.5083E+04	wc1	-5.0000E-01
net multiplication	1.0000E+00 0.0000	any termination	1.8522E+04	wc2	-2.5000E-01

computer time so far in this run	67.07 minutes	maximum number ever in bank	0
computer time in mcrun	66.22 minutes	bank overflows to backup file	0
source particles per minute	7.5503E+04		
random numbers generated	13602974167	most random numbers used was	24749 in history 4394135

range of sampled source weights = 1.0000E+00 to 1.0000E+00

source efficiency = 0.8333 in cell 1

1source distribution frequency tables print table 170

the expected values below do not include the effect of the rejection loop which samples position.

source distribution 1 for erg

Am-Be SPECTRUM (ISO 8529)

		number			weight		
n	source value	sampled	expected	sampled/expected	sampled	expected	sampled/expected
1	1.10000E-01	1.4439E-02	1.4397E-02	1.0029E+00	1.4439E-02	1.4397E-02	1.0029E+00
2	3.30000E-01	3.3491E-02	3.3393E-02	1.0029E+00	3.3491E-02	3.3393E-02	1.0029E+00

3	5.40000E-01	3.1224E-02	3.1294E-02	9.9777E-01	3.1224E-02	3.1294E-02	9.9777E-01
4	7.50000E-01	2.8061E-02	2.8094E-02	9.9881E-01	2.8061E-02	2.8094E-02	9.9881E-01
5	9.70000E-01	2.4957E-02	2.4995E-02	9.9850E-01	2.4957E-02	2.4995E-02	9.9850E-01
6	1.18000E+00	2.1287E-02	2.1396E-02	9.9492E-01	2.1287E-02	2.1396E-02	9.9492E-01
7	1.40000E+00	1.9711E-02	1.9796E-02	9.9569E-01	1.9711E-02	1.9796E-02	9.9569E-01
8	1.61000E+00	1.7516E-02	1.7496E-02	1.0011E+00	1.7516E-02	1.7496E-02	1.0011E+00
9	1.82000E+00	1.9249E-02	1.9196E-02	1.0028E+00	1.9249E-02	1.9196E-02	1.0028E+00
10	2.04000E+00	2.2343E-02	2.2295E-02	1.0021E+00	2.2343E-02	2.2295E-02	1.0021E+00
11	2.25000E+00	2.1461E-02	2.1496E-02	9.9841E-01	2.1461E-02	2.1496E-02	9.9841E-01
12	2.47000E+00	2.2466E-02	2.2495E-02	9.9871E-01	2.2466E-02	2.2495E-02	9.9871E-01
13	2.68000E+00	2.2781E-02	2.2795E-02	9.9939E-01	2.2781E-02	2.2795E-02	9.9939E-01
14	2.90000E+00	2.9492E-02	2.9494E-02	9.9994E-01	2.9492E-02	2.9494E-02	9.9994E-01
15	3.11000E+00	3.5605E-02	3.5593E-02	1.0003E+00	3.5605E-02	3.5593E-02	1.0003E+00
16	3.32000E+00	3.7042E-02	3.6893E-02	1.0040E+00	3.7042E-02	3.6893E-02	1.0040E+00
17	3.54000E+00	3.4537E-02	3.4593E-02	9.9839E-01	3.4537E-02	3.4593E-02	9.9839E-01
18	3.75000E+00	3.0757E-02	3.0694E-02	1.0020E+00	3.0757E-02	3.0694E-02	1.0020E+00
19	3.97000E+00	2.9982E-02	2.9994E-02	9.9959E-01	2.9982E-02	2.9994E-02	9.9959E-01
20	4.18000E+00	2.6842E-02	2.6895E-02	9.9804E-01	2.6842E-02	2.6895E-02	9.9804E-01
21	4.39000E+00	2.8544E-02	2.8594E-02	9.9824E-01	2.8544E-02	2.8594E-02	9.9824E-01
22	4.61000E+00	3.1732E-02	3.1794E-02	9.9806E-01	3.1732E-02	3.1794E-02	9.9806E-01
23	4.82000E+00	3.0812E-02	3.0694E-02	1.0038E+00	3.0812E-02	3.0694E-02	1.0038E+00
24	5.04000E+00	3.3347E-02	3.3293E-02	1.0016E+00	3.3347E-02	3.3293E-02	1.0016E+00
25	5.25000E+00	3.0259E-02	3.0394E-02	9.9556E-01	3.0259E-02	3.0394E-02	9.9556E-01
26	5.47000E+00	2.7428E-02	2.7394E-02	1.0012E+00	2.7428E-02	2.7394E-02	1.0012E+00
27	5.68000E+00	2.3201E-02	2.3295E-02	9.9597E-01	2.3201E-02	2.3295E-02	9.9597E-01
28	5.89000E+00	2.0573E-02	2.0596E-02	9.9887E-01	2.0573E-02	2.0596E-02	9.9887E-01
29	6.11000E+00	1.8217E-02	1.8196E-02	1.0011E+00	1.8217E-02	1.8196E-02	1.0011E+00
30	6.32000E+00	1.7723E-02	1.7696E-02	1.0015E+00	1.7723E-02	1.7696E-02	1.0015E+00
31	6.54000E+00	2.0376E-02	2.0396E-02	9.9901E-01	2.0376E-02	2.0396E-02	9.9901E-01
32	6.75000E+00	1.8230E-02	1.8296E-02	9.9638E-01	1.8230E-02	1.8296E-02	9.9638E-01
33	6.96000E+00	1.6270E-02	1.6297E-02	9.9837E-01	1.6270E-02	1.6297E-02	9.9837E-01
34	7.18000E+00	1.6759E-02	1.6697E-02	1.0038E+00	1.6759E-02	1.6697E-02	1.0038E+00
35	7.39000E+00	1.6881E-02	1.6797E-02	1.0050E+00	1.6881E-02	1.6797E-02	1.0050E+00
36	7.61000E+00	1.8905E-02	1.8796E-02	1.0058E+00	1.8905E-02	1.8796E-02	1.0058E+00
37	7.82000E+00	1.8377E-02	1.8396E-02	9.9897E-01	1.8377E-02	1.8396E-02	9.9897E-01
38	8.03000E+00	1.6861E-02	1.6897E-02	9.9792E-01	1.6861E-02	1.6897E-02	9.9792E-01
39	8.25000E+00	1.4401E-02	1.4397E-02	1.0003E+00	1.4401E-02	1.4397E-02	1.0003E+00
40	8.46000E+00	9.6430E-03	9.6780E-03	9.9638E-01	9.6430E-03	9.6780E-03	9.9638E-01
41	8.68000E+00	6.5450E-03	6.5187E-03	1.0040E+00	6.5450E-03	6.5187E-03	1.0040E+00
42	8.89000E+00	4.2394E-03	4.2591E-03	9.9537E-01	4.2394E-03	4.2591E-03	9.9537E-01
43	9.11000E+00	3.7064E-03	3.6693E-03	1.0101E+00	3.7064E-03	3.6693E-03	1.0101E+00
44	9.32000E+00	3.8116E-03	3.8092E-03	1.0006E+00	3.8116E-03	3.8092E-03	1.0006E+00
45	9.53000E+00	5.0212E-03	5.0590E-03	9.9253E-01	5.0212E-03	5.0590E-03	9.9253E-01
46	9.75000E+00	6.2908E-03	6.2487E-03	1.0067E+00	6.2908E-03	6.2487E-03	1.0067E+00
47	9.96000E+00	5.5666E-03	5.5189E-03	1.0086E+00	5.5666E-03	5.5189E-03	1.0086E+00

48	1.01800E+01	4.6964E-03	4.6791E-03	1.0037E+00	4.6964E-03	4.6791E-03	1.0037E+00
49	1.03900E+01	3.6722E-03	3.6992E-03	9.9269E-01	3.6722E-03	3.6992E-03	9.9269E-01
50	1.06000E+01	2.8040E-03	2.7794E-03	1.0088E+00	2.8040E-03	2.7794E-03	1.0088E+00
51	1.08200E+01	1.5020E-03	1.5097E-03	9.9490E-01	1.5020E-03	1.5097E-03	9.9490E-01
52	1.10300E+01	3.6120E-04	3.6293E-04	9.9524E-01	3.6120E-04	3.6293E-04	9.9524E-01
total		1.0000E+00	1.0000E+00	1.0000E+00	1.0000E+00	1.0000E+00	1.0000E+00

1neutron activity in each cell print table 126

	cell	tracks entering	population	collisions	collisions * weight (per history)	number weighted energy	flux weighted energy	average track weight (relative)	average track mfp (cm)
1	1	6130845	5000000	0	0.0000E+00	3.1678E-03	3.4471E+00	9.1439E-01	0.0000E+00
2	2	8438239	5000000	2103	2.5522E-04	5.9909E-04	2.0380E+00	7.4858E-01	7.6148E+03
3	3	9880241	4999996	1690134337	1.7296E+02	1.0769E-04	7.2316E-01	5.9595E-01	1.0864E+00
4	4	648237	563553	425580	5.2340E-02	6.4264E-04	1.7571E+00	7.4891E-01	4.6567E+00
6	7	9835776	4995862	1818109	2.3806E-01	1.0138E-03	2.5035E+00	8.0814E-01	4.2303E+00
7	21	253554	168837	46	5.2970E-06	1.8290E-04	1.0337E+00	6.7429E-01	5.0653E+03
8	22	256836	186233	63	7.8696E-06	2.3415E-04	1.2314E+00	6.9541E-01	5.5699E+03
9	23	252287	187937	45	6.1460E-06	2.5352E-04	1.2920E+00	7.0192E-01	5.7249E+03
10	6	237727	179815	44	5.1727E-06	2.2512E-04	1.2000E+00	6.8819E-01	5.4832E+03
11	8	207279	157599	45	4.9140E-06	1.7299E-04	9.9756E-01	6.6405E-01	4.9655E+03
12	9	168626	127811	34	3.5593E-06	1.3529E-04	8.3666E-01	6.4105E-01	4.5400E+03
13	10	132142	99766	26	3.2669E-06	1.1159E-04	7.2423E-01	6.1812E-01	4.2337E+03
14	11	101966	76842	18	1.8467E-06	9.6438E-05	6.4466E-01	6.0460E-01	4.0179E+03
15	12	78627	58909	18	2.1379E-06	8.6225E-05	5.9879E-01	5.9096E-01	3.8814E+03
16	13	59656	44694	19	1.8988E-06	8.1597E-05	5.7634E-01	5.8137E-01	3.8085E+03
17	14	45032	33798	4	3.5043E-07	7.8651E-05	5.6374E-01	5.7542E-01	3.7600E+03
18	15	33775	25423	4	2.9507E-07	7.7302E-05	5.5604E-01	5.7126E-01	3.7408E+03
19	16	24725	18882	4	5.4933E-07	8.1373E-05	5.8341E-01	5.7141E-01	3.8152E+03
20	17	17782	13912	0	0.0000E+00	8.3670E-05	5.9172E-01	5.7230E-01	3.8480E+03
21	18	12286	10044	1	1.9937E-07	9.9144E-05	6.8058E-01	5.7460E-01	4.0871E+03
22	19	7737	6952	2	1.7276E-07	1.3442E-04	8.5532E-01	6.0204E-01	4.5613E+03
23	20	4237215	882752	2501	2.9035E-04	1.7439E-04	1.0146E+00	6.5915E-01	4.9991E+03
total		41060590	22839617	1692383003	1.7325E+02				

1neutron weight balance in each cell print table 130

cell index	1	2	3	4	6	7	8	9	10
cell number	1	2	3	4	7	21	22	23	6
external events:									
entering	1.5345E-01	1.4510E+00	1.6282E+00	1.0112E-01	1.6200E+00	3.4067E-02	3.4636E-02	3.4165E-02	3.2286E-02
source	1.0000E+00	0.0000E+00	0.0000E+00	0.0000E+00	0.0000E+00	0.0000E+00	0.0000E+00	0.0000E+00	0.0000E+00
energy cutoff	0.0000E+00	0.0000E+00	0.0000E+00	0.0000E+00	0.0000E+00	0.0000E+00	0.0000E+00	0.0000E+00	0.0000E+00
time cutoff	0.0000E+00	0.0000E+00	0.0000E+00	0.0000E+00	0.0000E+00	0.0000E+00	0.0000E+00	0.0000E+00	0.0000E+00

exiting	-1.1535E+00	-1.4510E+00	-7.3529E-01	-9.6990E-02	-1.6015E+00	-3.4066E-02	-3.4635E-02	-3.4164E-02	-3.2285E-02
total	0.0000E+00	2.2188E-05	8.9295E-01	4.1271E-03	1.8508E-02	5.5993E-07	8.1372E-07	5.1487E-07	4.9777E-07
variance reduction events:									
weight window	0.0000E+00	0.0000E+00	0.0000E+00	0.0000E+00	0.0000E+00	0.0000E+00	0.0000E+00	0.0000E+00	0.0000E+00
cell importance	0.0000E+00	0.0000E+00	0.0000E+00	0.0000E+00	0.0000E+00	0.0000E+00	0.0000E+00	0.0000E+00	0.0000E+00
weight cutoff	0.0000E+00	1.2556E-06	-7.5654E-05	1.0011E-05	8.1090E-06	-3.7747E-08	6.5073E-09	8.1451E-09	9.0225E-09
e or t importance	0.0000E+00	0.0000E+00	0.0000E+00	0.0000E+00	0.0000E+00	0.0000E+00	0.0000E+00	0.0000E+00	0.0000E+00
dxtran	0.0000E+00	0.0000E+00	0.0000E+00	0.0000E+00	0.0000E+00	0.0000E+00	0.0000E+00	0.0000E+00	0.0000E+00
forced collisions	0.0000E+00	0.0000E+00	0.0000E+00	0.0000E+00	0.0000E+00	0.0000E+00	0.0000E+00	0.0000E+00	0.0000E+00
exp. transform	0.0000E+00	0.0000E+00	0.0000E+00	0.0000E+00	0.0000E+00	0.0000E+00	0.0000E+00	0.0000E+00	0.0000E+00
total	0.0000E+00	1.2556E-06	-7.5654E-05	1.0011E-05	8.1090E-06	-3.7747E-08	6.5073E-09	8.1451E-09	9.0225E-09
physical events:									
capture	0.0000E+00	-2.3443E-05	-8.9288E-01	-4.1371E-03	-1.8516E-02	-5.2218E-07	-8.2023E-07	-5.2302E-07	-5.0680E-07
(n,xn)	0.0000E+00	0.0000E+00	0.0000E+00	0.0000E+00	0.0000E+00	0.0000E+00	0.0000E+00	0.0000E+00	0.0000E+00
loss to (n,xn)	0.0000E+00	0.0000E+00	0.0000E+00	0.0000E+00	0.0000E+00	0.0000E+00	0.0000E+00	0.0000E+00	0.0000E+00
fission	0.0000E+00	0.0000E+00	0.0000E+00	0.0000E+00	0.0000E+00	0.0000E+00	0.0000E+00	0.0000E+00	0.0000E+00
loss to fission	0.0000E+00	0.0000E+00	0.0000E+00	0.0000E+00	0.0000E+00	0.0000E+00	0.0000E+00	0.0000E+00	0.0000E+00
photonuclear	0.0000E+00	0.0000E+00	0.0000E+00	0.0000E+00	0.0000E+00	0.0000E+00	0.0000E+00	0.0000E+00	0.0000E+00
total	0.0000E+00	-2.3443E-05	-8.9288E-01	-4.1371E-03	-1.8516E-02	-5.2218E-07	-8.2023E-07	-5.2302E-07	-5.0680E-07
total	0.0000E+00	0.0000E+00	0.0000E+00	0.0000E+00	0.0000E+00	0.0000E+00	0.0000E+00	0.0000E+00	0.0000E+00
cell index	11	12	13	14	15	16	17	18	19
cell number	8	9	10	11	12	13	14	15	16
external events:									
entering	2.7912E-02	2.2136E-02	1.6830E-02	1.2695E-02	9.5774E-03	7.1613E-03	5.3401E-03	3.9872E-03	2.9211E-03
source	0.0000E+00	0.0000E+00	0.0000E+00	0.0000E+00	0.0000E+00	0.0000E+00	0.0000E+00	0.0000E+00	0.0000E+00
energy cutoff	0.0000E+00	0.0000E+00	0.0000E+00	0.0000E+00	0.0000E+00	0.0000E+00	0.0000E+00	0.0000E+00	0.0000E+00
time cutoff	0.0000E+00	0.0000E+00	0.0000E+00	0.0000E+00	0.0000E+00	0.0000E+00	0.0000E+00	0.0000E+00	0.0000E+00
exiting	-2.7911E-02	-2.2136E-02	-1.6830E-02	-1.2695E-02	-9.5773E-03	-7.1611E-03	-5.3401E-03	-3.9872E-03	-2.9210E-03
total	4.2244E-07	4.4290E-07	3.1806E-07	1.6810E-07	1.0356E-07	1.9023E-07	-6.2826E-09	4.3054E-08	8.1186E-08
variance reduction events:									
weight window	0.0000E+00	0.0000E+00	0.0000E+00	0.0000E+00	0.0000E+00	0.0000E+00	0.0000E+00	0.0000E+00	0.0000E+00
cell importance	0.0000E+00	0.0000E+00	0.0000E+00	0.0000E+00	0.0000E+00	0.0000E+00	0.0000E+00	0.0000E+00	0.0000E+00
weight cutoff	1.6413E-07	-4.5056E-08	-3.8557E-08	0.0000E+00	5.5066E-08	1.0330E-08	6.5694E-08	0.0000E+00	-4.4329E-08
e or t importance	0.0000E+00	0.0000E+00	0.0000E+00	0.0000E+00	0.0000E+00	0.0000E+00	0.0000E+00	0.0000E+00	0.0000E+00
dxtran	0.0000E+00	0.0000E+00	0.0000E+00	0.0000E+00	0.0000E+00	0.0000E+00	0.0000E+00	0.0000E+00	0.0000E+00

```
forced collisions  0.0000E+00  0.0000E+00  0.0000E+00  0.0000E+00  0.0000E+00  0.0000E+00  0.0000E+00  0.0000E+00  0.0000E+00
   exp. transform  0.0000E+00  0.0000E+00  0.0000E+00  0.0000E+00  0.0000E+00  0.0000E+00  0.0000E+00  0.0000E+00  0.0000E+00
                   ----------  ----------  ----------  ----------  ----------  ----------  ----------  ----------  ----------
            total  1.6413E-07 -4.5056E-08 -3.8557E-08  0.0000E+00  5.5066E-08  1.0330E-08  6.5694E-08  0.0000E+00 -4.4329E-08

physical events:
          capture -5.8656E-07 -3.9785E-07 -2.7951E-07 -1.6810E-07 -1.5862E-07 -2.0056E-07 -5.9412E-08 -4.3054E-08 -3.6857E-08
           (n,xn)  0.0000E+00  0.0000E+00  0.0000E+00  0.0000E+00  0.0000E+00  0.0000E+00  0.0000E+00  0.0000E+00  0.0000E+00
   loss to (n,xn)  0.0000E+00  0.0000E+00  0.0000E+00  0.0000E+00  0.0000E+00  0.0000E+00  0.0000E+00  0.0000E+00  0.0000E+00
          fission  0.0000E+00  0.0000E+00  0.0000E+00  0.0000E+00  0.0000E+00  0.0000E+00  0.0000E+00  0.0000E+00  0.0000E+00
  loss to fission  0.0000E+00  0.0000E+00  0.0000E+00  0.0000E+00  0.0000E+00  0.0000E+00  0.0000E+00  0.0000E+00  0.0000E+00
     photonuclear  0.0000E+00  0.0000E+00  0.0000E+00  0.0000E+00  0.0000E+00  0.0000E+00  0.0000E+00  0.0000E+00  0.0000E+00
                   ----------  ----------  ----------  ----------  ----------  ----------  ----------  ----------  ----------
            total -5.8656E-07 -3.9785E-07 -2.7951E-07 -1.6810E-07 -1.5862E-07 -2.0056E-07 -5.9412E-08 -4.3054E-08 -3.6857E-08

                   ----------  ----------  ----------  ----------  ----------  ----------  ----------  ----------  ----------
            total  0.0000E+00  0.0000E+00  0.0000E+00  0.0000E+00  0.0000E+00  0.0000E+00  0.0000E+00  0.0000E+00  0.0000E+00

       cell index       20          21          22          23
      cell number       17          18          19          20       total

external events:
         entering  2.1006E-03  1.4647E-03  9.5866E-04  5.5889E-01  5.7610E+00
           source  0.0000E+00  0.0000E+00  0.0000E+00  0.0000E+00  1.0000E+00
    energy cutoff  0.0000E+00  0.0000E+00  0.0000E+00  0.0000E+00  0.0000E+00
      time cutoff  0.0000E+00  0.0000E+00  0.0000E+00  0.0000E+00  0.0000E+00
          exiting -2.1006E-03 -1.4647E-03 -9.5865E-04 -5.5886E-01 -5.8454E+00
                   ----------  ----------  ----------  ----------  ----------
            total  0.0000E+00  4.7755E-09  1.1293E-08  2.9600E-05  9.1565E-01

variance reduction events:
    weight window  0.0000E+00  0.0000E+00  0.0000E+00  0.0000E+00  0.0000E+00
  cell importance  0.0000E+00  0.0000E+00  0.0000E+00  0.0000E+00  0.0000E+00
    weight cutoff  0.0000E+00  0.0000E+00  0.0000E+00 -2.4158E-07 -5.6367E-05
e or t importance  0.0000E+00  0.0000E+00  0.0000E+00  0.0000E+00  0.0000E+00
           dxtran  0.0000E+00  0.0000E+00  0.0000E+00  0.0000E+00  0.0000E+00
forced collisions  0.0000E+00  0.0000E+00  0.0000E+00  0.0000E+00  0.0000E+00
   exp. transform  0.0000E+00  0.0000E+00  0.0000E+00  0.0000E+00  0.0000E+00
                   ----------  ----------  ----------  ----------  ----------
            total  0.0000E+00  0.0000E+00  0.0000E+00 -2.4158E-07 -5.6367E-05

physical events:
          capture  0.0000E+00 -4.7755E-09 -1.1293E-08 -2.9359E-05 -9.1559E-01
           (n,xn)  0.0000E+00  0.0000E+00  0.0000E+00  0.0000E+00  0.0000E+00
   loss to (n,xn)  0.0000E+00  0.0000E+00  0.0000E+00  0.0000E+00  0.0000E+00
```

fission	0.0000E+00	0.0000E+00	0.0000E+00	0.0000E+00	0.0000E+00
loss to fission	0.0000E+00	0.0000E+00	0.0000E+00	0.0000E+00	0.0000E+00
photonuclear	0.0000E+00	0.0000E+00	0.0000E+00	0.0000E+00	0.0000E+00
total	0.0000E+00	-4.7755E-09	-1.1293E-08	-2.9359E-05	-9.1559E-01
total	0.0000E+00	0.0000E+00	0.0000E+00	0.0000E+00	0.0000E+00

1neutron activity of each nuclide in each cell, per source particle print table 140

cell index	cell name	nuclides	atom fraction	total collisions	collisions * weight	wgt. lost to capture	wgt. gain by fission	wgt. gain by (n,xn)	photons produced	photon wgt produced	avg photon energy
2	2	6000.66c	1.50E-04	0	0.0000E+00	0.0000E+00	0.0000E+00	0.0000E+00	0	0.0000E+00	0.0000E+00
		7014.62c	7.84E-01	1871	2.2179E-04	2.3017E-05	0.0000E+00	0.0000E+00	0	0.0000E+00	0.0000E+00
		8016.62c	2.11E-01	229	3.3050E-05	2.8700E-07	0.0000E+00	0.0000E+00	0	0.0000E+00	0.0000E+00
		18000.35c	4.67E-03	3	3.7925E-07	1.3947E-07	0.0000E+00	0.0000E+00	0	0.0000E+00	0.0000E+00
3	3	1001.62c	6.75E-01	1602639875	1.6313E+02	8.8369E-01	0.0000E+00	0.0000E+00	0	0.0000E+00	0.0000E+00
		6000.66c	3.25E-01	87494462	9.8226E+00	9.1885E-03	0.0000E+00	0.0000E+00	0	0.0000E+00	0.0000E+00
4	4	26056.62c	1.00E+00	425580	5.2340E-02	4.1371E-03	0.0000E+00	0.0000E+00	0	0.0000E+00	0.0000E+00
6	7	26056.62c	1.00E+00	1818109	2.3806E-01	1.8516E-02	0.0000E+00	0.0000E+00	0	0.0000E+00	0.0000E+00
7	21	6000.66c	1.50E-04	0	0.0000E+00	0.0000E+00	0.0000E+00	0.0000E+00	0	0.0000E+00	0.0000E+00
		7014.62c	7.84E-01	41	4.7063E-06	5.2217E-07	0.0000E+00	0.0000E+00	0	0.0000E+00	0.0000E+00
		8016.62c	2.11E-01	5	5.9074E-07	1.3855E-11	0.0000E+00	0.0000E+00	0	0.0000E+00	0.0000E+00
		18000.35c	4.67E-03	0	0.0000E+00	0.0000E+00	0.0000E+00	0.0000E+00	0	0.0000E+00	0.0000E+00
8	22	6000.66c	1.50E-04	0	0.0000E+00	0.0000E+00	0.0000E+00	0.0000E+00	0	0.0000E+00	0.0000E+00
		7014.62c	7.84E-01	54	6.6092E-06	8.2019E-07	0.0000E+00	0.0000E+00	0	0.0000E+00	0.0000E+00
		8016.62c	2.11E-01	9	1.2604E-06	3.7568E-11	0.0000E+00	0.0000E+00	0	0.0000E+00	0.0000E+00
		18000.35c	4.67E-03	0	0.0000E+00	0.0000E+00	0.0000E+00	0.0000E+00	0	0.0000E+00	0.0000E+00
9	23	6000.66c	1.50E-04	0	0.0000E+00	0.0000E+00	0.0000E+00	0.0000E+00	0	0.0000E+00	0.0000E+00
		7014.62c	7.84E-01	41	5.4405E-06	5.2301E-07	0.0000E+00	0.0000E+00	0	0.0000E+00	0.0000E+00
		8016.62c	2.11E-01	4	7.0551E-07	4.8447E-12	0.0000E+00	0.0000E+00	0	0.0000E+00	0.0000E+00
		18000.35c	4.67E-03	0	0.0000E+00	0.0000E+00	0.0000E+00	0.0000E+00	0	0.0000E+00	0.0000E+00
10	6	6000.66c	1.50E-04	0	0.0000E+00	0.0000E+00	0.0000E+00	0.0000E+00	0	0.0000E+00	0.0000E+00
		7014.62c	7.84E-01	37	4.4867E-06	5.0677E-07	0.0000E+00	0.0000E+00	0	0.0000E+00	0.0000E+00
		8016.62c	2.11E-01	7	6.8598E-07	2.7840E-11	0.0000E+00	0.0000E+00	0	0.0000E+00	0.0000E+00
		18000.35c	4.67E-03	0	0.0000E+00	0.0000E+00	0.0000E+00	0.0000E+00	0	0.0000E+00	0.0000E+00

11	8	6000.66c	1.50E-04	0	0.0000E+00	0.0000E+00	0.0000E+00	0.0000E+00	0	0.0000E+00	0.0000E+00
		7014.62c	7.84E-01	41	4.4608E-06	5.8655E-07	0.0000E+00	0.0000E+00	0	0.0000E+00	0.0000E+00
		8016.62c	2.11E-01	4	4.5325E-07	7.1517E-12	0.0000E+00	0.0000E+00	0	0.0000E+00	0.0000E+00
		18000.35c	4.67E-03	0	0.0000E+00	0.0000E+00	0.0000E+00	0.0000E+00	0	0.0000E+00	0.0000E+00
12	9	6000.66c	1.50E-04	0	0.0000E+00	0.0000E+00	0.0000E+00	0.0000E+00	0	0.0000E+00	0.0000E+00
		7014.62c	7.84E-01	30	3.1395E-06	3.9783E-07	0.0000E+00	0.0000E+00	0	0.0000E+00	0.0000E+00
		8016.62c	2.11E-01	4	4.1973E-07	1.4712E-11	0.0000E+00	0.0000E+00	0	0.0000E+00	0.0000E+00
		18000.35c	4.67E-03	0	0.0000E+00	0.0000E+00	0.0000E+00	0.0000E+00	0	0.0000E+00	0.0000E+00
13	10	6000.66c	1.50E-04	0	0.0000E+00	0.0000E+00	0.0000E+00	0.0000E+00	0	0.0000E+00	0.0000E+00
		7014.62c	7.84E-01	23	2.8273E-06	2.7950E-07	0.0000E+00	0.0000E+00	0	0.0000E+00	0.0000E+00
		8016.62c	2.11E-01	3	4.3959E-07	1.2885E-11	0.0000E+00	0.0000E+00	0	0.0000E+00	0.0000E+00
		18000.35c	4.67E-03	0	0.0000E+00	0.0000E+00	0.0000E+00	0.0000E+00	0	0.0000E+00	0.0000E+00
14	11	6000.66c	1.50E-04	0	0.0000E+00	0.0000E+00	0.0000E+00	0.0000E+00	0	0.0000E+00	0.0000E+00
		7014.62c	7.84E-01	15	1.5097E-06	1.6809E-07	0.0000E+00	0.0000E+00	0	0.0000E+00	0.0000E+00
		8016.62c	2.11E-01	3	3.3695E-07	1.4555E-11	0.0000E+00	0.0000E+00	0	0.0000E+00	0.0000E+00
		18000.35c	4.67E-03	0	0.0000E+00	0.0000E+00	0.0000E+00	0.0000E+00	0	0.0000E+00	0.0000E+00
15	12	6000.66c	1.50E-04	0	0.0000E+00	0.0000E+00	0.0000E+00	0.0000E+00	0	0.0000E+00	0.0000E+00
		7014.62c	7.84E-01	17	1.9399E-06	1.5862E-07	0.0000E+00	0.0000E+00	0	0.0000E+00	0.0000E+00
		8016.62c	2.11E-01	1	1.9796E-07	3.1742E-12	0.0000E+00	0.0000E+00	0	0.0000E+00	0.0000E+00
		18000.35c	4.67E-03	0	0.0000E+00	0.0000E+00	0.0000E+00	0.0000E+00	0	0.0000E+00	0.0000E+00
16	13	6000.66c	1.50E-04	0	0.0000E+00	0.0000E+00	0.0000E+00	0.0000E+00	0	0.0000E+00	0.0000E+00
		7014.62c	7.84E-01	18	1.8404E-06	2.0055E-07	0.0000E+00	0.0000E+00	0	0.0000E+00	0.0000E+00
		8016.62c	2.11E-01	1	5.8348E-08	3.6701E-12	0.0000E+00	0.0000E+00	0	0.0000E+00	0.0000E+00
		18000.35c	4.67E-03	0	0.0000E+00	0.0000E+00	0.0000E+00	0.0000E+00	0	0.0000E+00	0.0000E+00
17	14	6000.66c	1.50E-04	0	0.0000E+00	0.0000E+00	0.0000E+00	0.0000E+00	0	0.0000E+00	0.0000E+00
		7014.62c	7.84E-01	4	3.5043E-07	5.9412E-08	0.0000E+00	0.0000E+00	0	0.0000E+00	0.0000E+00
		8016.62c	2.11E-01	0	0.0000E+00	0.0000E+00	0.0000E+00	0.0000E+00	0	0.0000E+00	0.0000E+00
		18000.35c	4.67E-03	0	0.0000E+00	0.0000E+00	0.0000E+00	0.0000E+00	0	0.0000E+00	0.0000E+00
18	15	6000.66c	1.50E-04	0	0.0000E+00	0.0000E+00	0.0000E+00	0.0000E+00	0	0.0000E+00	0.0000E+00
		7014.62c	7.84E-01	3	2.4030E-07	4.3052E-08	0.0000E+00	0.0000E+00	0	0.0000E+00	0.0000E+00
		8016.62c	2.11E-01	1	5.4772E-08	2.2557E-12	0.0000E+00	0.0000E+00	0	0.0000E+00	0.0000E+00
		18000.35c	4.67E-03	0	0.0000E+00	0.0000E+00	0.0000E+00	0.0000E+00	0	0.0000E+00	0.0000E+00
19	16	6000.66c	1.50E-04	0	0.0000E+00	0.0000E+00	0.0000E+00	0.0000E+00	0	0.0000E+00	0.0000E+00
		7014.62c	7.84E-01	4	5.4933E-07	3.6857E-08	0.0000E+00	0.0000E+00	0	0.0000E+00	0.0000E+00
		8016.62c	2.11E-01	0	0.0000E+00	0.0000E+00	0.0000E+00	0.0000E+00	0	0.0000E+00	0.0000E+00
		18000.35c	4.67E-03	0	0.0000E+00	0.0000E+00	0.0000E+00	0.0000E+00	0	0.0000E+00	0.0000E+00

20	17	6000.66c	1.50E-04	0	0.0000E+00	0.0000E+00	0.0000E+00	0.0000E+00	0	0.0000E+00	0.0000E+00
		7014.62c	7.84E-01	0	0.0000E+00	0.0000E+00	0.0000E+00	0.0000E+00	0	0.0000E+00	0.0000E+00
		8016.62c	2.11E-01	0	0.0000E+00	0.0000E+00	0.0000E+00	0.0000E+00	0	0.0000E+00	0.0000E+00
		18000.35c	4.67E-03	0	0.0000E+00	0.0000E+00	0.0000E+00	0.0000E+00	0	0.0000E+00	0.0000E+00
21	18	6000.66c	1.50E-04	0	0.0000E+00	0.0000E+00	0.0000E+00	0.0000E+00	0	0.0000E+00	0.0000E+00
		7014.62c	7.84E-01	1	1.9937E-07	4.7755E-09	0.0000E+00	0.0000E+00	0	0.0000E+00	0.0000E+00
		8016.62c	2.11E-01	0	0.0000E+00	0.0000E+00	0.0000E+00	0.0000E+00	0	0.0000E+00	0.0000E+00
		18000.35c	4.67E-03	0	0.0000E+00	0.0000E+00	0.0000E+00	0.0000E+00	0	0.0000E+00	0.0000E+00
22	19	6000.66c	1.50E-04	0	0.0000E+00	0.0000E+00	0.0000E+00	0.0000E+00	0	0.0000E+00	0.0000E+00
		7014.62c	7.84E-01	1	9.5242E-08	1.1288E-08	0.0000E+00	0.0000E+00	0	0.0000E+00	0.0000E+00
		8016.62c	2.11E-01	1	7.7520E-08	4.2705E-12	0.0000E+00	0.0000E+00	0	0.0000E+00	0.0000E+00
		18000.35c	4.67E-03	0	0.0000E+00	0.0000E+00	0.0000E+00	0.0000E+00	0	0.0000E+00	0.0000E+00
23	20	6000.66c	1.50E-04	0	0.0000E+00	0.0000E+00	0.0000E+00	0.0000E+00	0	0.0000E+00	0.0000E+00
		7014.62c	7.84E-01	2292	2.6433E-04	2.9285E-05	0.0000E+00	0.0000E+00	0	0.0000E+00	0.0000E+00
		8016.62c	2.11E-01	208	2.5972E-05	5.2012E-08	0.0000E+00	0.0000E+00	0	0.0000E+00	0.0000E+00
		18000.35c	4.67E-03	1	5.2327E-08	2.1225E-08	0.0000E+00	0.0000E+00	0	0.0000E+00	0.0000E+00
total				1692383003	1.7325E+02	9.1559E-01	0.0000E+00	0.0000E+00	0	0.0000E+00	0.0000E+00

total over all cells by nuclide	total collisions	collisions * weight	wgt. lost to capture	wgt. gain by fission	wgt. gain by (n,xn)	photons produced	photon wgt produced	avg photon energy
1001.62c	1602639875	1.6313E+02	8.8369E-01	0.0000E+00	0.0000E+00	0	0.0000E+00	0.0000E+00
6000.66c	87494462	9.8226E+00	9.1885E-03	0.0000E+00	0.0000E+00	0	0.0000E+00	0.0000E+00
7014.62c	4493	5.2452E-04	5.6621E-05	0.0000E+00	0.0000E+00	0	0.0000E+00	0.0000E+00
8016.62c	480	6.4303E-05	3.3916E-07	0.0000E+00	0.0000E+00	0	0.0000E+00	0.0000E+00
18000.35c	4	4.3158E-07	1.6069E-07	0.0000E+00	0.0000E+00	0	0.0000E+00	0.0000E+00
26056.62c	2243689	2.9040E-01	2.2654E-02	0.0000E+00	0.0000E+00	0	0.0000E+00	0.0000E+00

1tally 4 nps = 5000000
tally type 4 track length estimate of particle flux. units 1/cm**2
tally for neutrons

volumes

cell:	21	22	23	6	8	9	10
	2.12058E+00	2.12058E+00	2.12058E+00	2.12058E+00	2.12058E+00	2.12058E+00	2.12058E+00
cell:	11	12	13	14	15	16	17
	2.12058E+00	2.12058E+00	2.12058E+00	2.12058E+00	2.12058E+00	2.12058E+00	2.12058E+00
cell:	18	19					
	2.12058E+00	2.12058E+00					

```
cell  21
     energy
   5.0000E-07   4.39870E-03 0.0044
   5.0000E-01   1.55976E-03 0.0073
   1.2000E+01   2.19539E-03 0.0056
     total      8.15385E-03 0.0032

cell  22
     energy
   5.0000E-07   4.53135E-03 0.0042
   5.0000E-01   1.74796E-03 0.0070
   1.2000E+01   2.88284E-03 0.0061
     total      9.16215E-03 0.0032

cell  23
     energy
   5.0000E-07   4.40976E-03 0.0042
   5.0000E-01   1.78426E-03 0.0070
   1.2000E+01   3.00894E-03 0.0060
     total      9.20297E-03 0.0032

cell  6
     energy
   5.0000E-07   4.06819E-03 0.0043
   5.0000E-01   1.54496E-03 0.0073
   1.2000E+01   2.47369E-03 0.0058
     total      8.08685E-03 0.0032

cell  8
     energy
   5.0000E-07   3.52491E-03 0.0046
   5.0000E-01   1.20581E-03 0.0081
   1.2000E+01   1.66536E-03 0.0058
     total      6.39608E-03 0.0034

cell  9
     energy
   5.0000E-07   2.92643E-03 0.0050
   5.0000E-01   8.76957E-04 0.0093
   1.2000E+01   1.09242E-03 0.0066
     total      4.89581E-03 0.0038

cell  10
     energy
   5.0000E-07   2.31586E-03 0.0055
```

```
   5.0000E-01   6.15468E-04 0.0109
   1.2000E+01   7.18875E-04 0.0080
     total      3.65020E-03 0.0043

cell  11
     energy
   5.0000E-07   1.79745E-03 0.0062
   5.0000E-01   4.48267E-04 0.0129
   1.2000E+01   4.86256E-04 0.0095
     total      2.73198E-03 0.0050

cell  12
     energy
   5.0000E-07   1.40199E-03 0.0070
   5.0000E-01   3.15736E-04 0.0149
   1.2000E+01   3.41777E-04 0.0113
     total      2.05950E-03 0.0057

cell  13
     energy
   5.0000E-07   1.04873E-03 0.0080
   5.0000E-01   2.27445E-04 0.0172
   1.2000E+01   2.40935E-04 0.0133
     total      1.51711E-03 0.0065

cell  14
     energy
   5.0000E-07   7.88715E-04 0.0091
   5.0000E-01   1.64375E-04 0.0207
   1.2000E+01   1.74995E-04 0.0152
     total      1.12809E-03 0.0076

cell  15
     energy
   5.0000E-07   5.84983E-04 0.0105
   5.0000E-01   1.23150E-04 0.0238
   1.2000E+01   1.26944E-04 0.0175
     total      8.35077E-04 0.0087
cell  16
     energy
   5.0000E-07   4.25622E-04 0.0124
   5.0000E-01   8.55377E-05 0.0276
   1.2000E+01   9.94247E-05 0.0206
     total      6.10585E-04 0.0102
```

```
 cell  17
      energy
    5.0000E-07   2.99212E-04 0.0146
    5.0000E-01   6.52226E-05 0.0314
    1.2000E+01   7.14704E-05 0.0233
      total      4.35905E-04 0.0120

 cell  18
      energy
    5.0000E-07   1.98589E-04 0.0174
    5.0000E-01   4.40705E-05 0.0379
    1.2000E+01   5.49825E-05 0.0270
      total      2.97642E-04 0.0141

 cell  19
      energy
    5.0000E-07   1.10076E-04 0.0209
    5.0000E-01   3.10563E-05 0.0445
    1.2000E+01   4.18406E-05 0.0315
      total      1.82973E-04 0.0164
 ================================================================================================================================
           results of 10 statistical checks for the estimated answer for the tally fluctuation chart (tfc) bin of tally   4

 tfc bin     --mean--      ---------relative error---------      ----variance of the variance----      --figure of merit--     -pdf-
 behavior    behavior      value   decrease   decrease rate      value   decrease   decrease rate       value     behavior     slope

 desired      random       <0.10      yes      1/sqrt(nps)       <0.10      yes        1/nps           constant    random      >3.00
 observed     random        0.00      yes          yes            0.00      yes         yes            constant    random      10.00
 passed?        yes          yes      yes          yes              yes      yes         yes               yes        yes         yes
 ================================================================================================================================

 this tally meets the statistical criteria used to form confidence intervals: check the tally fluctuation chart to verify.
 the results in other bins associated with this tally may not meet these statistical criteria.

 ----- estimated confidence intervals:  -----

 estimated asymmetric confidence interval(1,2,3 sigma): 8.1278E-03 to 8.1801E-03; 8.1017E-03 to 8.2062E-03; 8.0755E-03 to 8.2323E-03
 estimated  symmetric confidence interval(1,2,3 sigma): 8.1277E-03 to 8.1800E-03; 8.1016E-03 to 8.2061E-03; 8.0755E-03 to 8.2322E-03

1analysis of the results in the tally fluctuation chart bin (tfc) for tally   4 with nps =     5000000  print table 160

 normed average tally per history  = 8.15385E-03          unnormed average tally per history  = 1.72908E-02
 estimated tally relative error    = 0.0032               estimated variance of the variance  = 0.0000
 relative error from zero tallies  = 0.0024               relative error from nonzero scores  = 0.0021
```

```
 number of nonzero history tallies =      168837          efficiency for the nonzero tallies  = 0.0338
 history number of largest  tally  =     1654199          largest  unnormalized history tally = 8.39372E+00
 (largest  tally)/(average tally)  = 4.85443E+02          (largest  tally)/(avg nonzero tally)= 1.63921E+01

 (confidence interval shift)/mean  = 0.0000               shifted confidence interval center  = 8.15392E-03

 if the largest  history score sampled so far were to occur on the next history, the tfc bin quantities would change as follows:

      estimated quantities           value at nps           value at nps+1          value(nps+1)/value(nps)-1.

      mean                            8.15385E-03             8.15464E-03                   0.000097
      relative error                  3.20480E-03             3.20596E-03                   0.000360
      variance of the variance        4.20176E-05             4.27742E-05                   0.018008
      shifted center                  8.15392E-03             8.15392E-03                   0.000000
      figure of merit                 1.47024E+03             1.46918E+03                  -0.000719

 the estimated slope of the 200 largest  tallies starting at  3.46091E+00 appears to be decreasing at least exponentially.
 the large score tail of the empirical history score probability density function appears to have no unsampled regions.

 fom = (histories/minute)*(f(x) signal-to-noise ratio)**2 = (7.550E+04)*( 1.395E-01)**2 = (7.550E+04)*(1.947E-02) = 1.470E+03

1unnormed tally density for tally   4            nonzero tally mean(m) = 5.121E-01   nps =     5000000  print table 161

 abscissa              ordinate   log plot of tally probability density function in tally fluctuation chart bin(d=decade,slope=10.0)
  tally  number num den log den:d-------------d---------------d--------------d--------------d---------------d--------------d--------
 2.00-06      1 2.72-01  -0.566 **************|***************|**************|**************|***************|**************|********
 3.16-06      0 0.00+00   0.000               |               |              |              |               |              |
 5.01-06      0 0.00+00   0.000               |               |              |              |               |              |
 7.94-06      0 0.00+00   0.000               |               |              |              |               |              |
 1.26-05      1 4.30-02  -1.366 **************|***************|**************|**************|***************|***********   |
 2.00-05      0 0.00+00   0.000               |               |              |              |               |              |
 3.16-05      0 0.00+00   0.000               |               |              |              |               |              |
 5.01-05      2 2.16-02  -1.665 **************|***************|**************|**************|***************|******        |
 7.94-05      6 4.09-02  -1.388 **************|***************|**************|**************|***************|**********    |
 1.26-04      3 1.29-02  -1.889 **************|***************|**************|**************|***************|***           |
 2.00-04      5 1.36-02  -1.867 **************|***************|**************|**************|***************|***           |
 3.16-04     11 1.89-02  -1.725 **************|***************|**************|**************|***************|*****         |
 5.01-04     14 1.51-02  -1.820 **************|***************|**************|**************|***************|****          |
 7.94-04     24 1.64-02  -1.786 **************|***************|**************|**************|***************|****          |
 1.26-03     45 1.94-02  -1.713 **************|***************|**************|**************|***************|*****         |
 2.00-03     63 1.71-02  -1.767 **************|***************|**************|**************|***************|*****         |
 3.16-03     88 1.51-02  -1.822 **************|***************|**************|**************|***************|****          |
 5.01-03    152 1.64-02  -1.784 **************|***************|**************|**************|***************|****          |
 7.94-03    261 1.78-02  -1.749 **************|***************|**************|**************|***************|*****         |
 1.26-02    385 1.66-02  -1.781 **************|***************|**************|**************|***************|****          |
```

```
 2.00-02    605 1.64-02  -1.784 **************|***************|**************|**************|***************|****          |
 3.16-02   1027 1.76-02  -1.754 **************|***************|**************|**************|***************|*****         |
 5.01-02   1622 1.75-02  -1.756 **************|***************|**************|**************|***************|*****         |
 7.94-02   2767 1.89-02  -1.724 **************|***************|**************|**************|***************|*****         |
 1.26-01  10428 4.49-02  -1.348 **************|***************|**************|**************|***************|***********   |
 2.00-01  17106 4.65-02  -1.333 **************|***************|**************|**************|***************|***********   |
 3.16-01  25423 4.36-02  -1.361 **************|***************|**************|**************|***************|***********   |
 5.01-01  48261 5.22-02  -1.282 **************|***************|**************|**************|***************|***********   |
 7.94-01  32886 2.24-02  -1.649 mmmmmmmmmmmmmmm|mmmmmmmmmmmmmmmm|mmmmmmmmmmmmmmmm|mmmmmmmmmmmmmmmm|mmmmmmmmmmmmmmmm|mmmmmm        |
 1.26+00  17550 7.55-03  -2.122 **************|***************|**************|**************|***************|              |
 2.00+00   7233 1.96-03  -2.707 **************|***************|**************|**************|******         |              |
 3.16+00   2532 4.34-04  -3.363 **************|***************|**************|***********    |               |              |
 5.01+00    318 3.44-05  -4.464 **************|***************|*********     |               |               |              |
 7.94+00     17 1.16-06  -5.936 **************|***            |              |               |               |              |
 1.00+01      1 9.72-08  -7.012 *             |               |              |               |               |              |
  total  168837 3.38-02         d-------------d---------------d--------------d--------------d---------------d--------------d--------
1cumulative tally number for tally   4           nonzero tally mean(m) = 5.121E-01   nps =     5000000  print table 162

   abscissa     cum   ordinate    plot of the cumulative number of tallies in the tally fluctuation chart bin from 0 to 100 percent
    tally      number  cum pct:--------10--------20--------30--------40--------50--------60--------70--------80--------90-------100
 1.99526E-06        1    0.001|         |         |         |         |         |         |         |         |         |         |
 3.16228E-06        1    0.001|         |         |         |         |         |         |         |         |         |         |
 5.01188E-06        1    0.001|         |         |         |         |         |         |         |         |         |         |
 7.94329E-06        1    0.001|         |         |         |         |         |         |         |         |         |         |
 1.25893E-05        2    0.001|         |         |         |         |         |         |         |         |         |         |
 1.99526E-05        2    0.001|         |         |         |         |         |         |         |         |         |         |
 3.16228E-05        2    0.001|         |         |         |         |         |         |         |         |         |         |
 5.01188E-05        4    0.002|         |         |         |         |         |         |         |         |         |         |
 7.94329E-05       10    0.006|         |         |         |         |         |         |         |         |         |         |
 1.25893E-04       13    0.008|         |         |         |         |         |         |         |         |         |         |
 1.99526E-04       18    0.011|         |         |         |         |         |         |         |         |         |         |
 3.16228E-04       29    0.017|         |         |         |         |         |         |         |         |         |         |
 5.01188E-04       43    0.025|         |         |         |         |         |         |         |         |         |         |
 7.94329E-04       67    0.040|         |         |         |         |         |         |         |         |         |         |
 1.25893E-03      112    0.066|         |         |         |         |         |         |         |         |         |         |
 1.99526E-03      175    0.104|         |         |         |         |         |         |         |         |         |         |
 3.16228E-03      263    0.156|         |         |         |         |         |         |         |         |         |         |
 5.01188E-03      415    0.246|         |         |         |         |         |         |         |         |         |         |
 7.94329E-03      676    0.400|         |         |         |         |         |         |         |         |         |         |
 1.25893E-02     1061    0.628|*        |         |         |         |         |         |         |         |         |         |
 1.99526E-02     1666    0.987|*        |         |         |         |         |         |         |         |         |         |
 3.16228E-02     2693    1.595|**       |         |         |         |         |         |         |         |         |         |
 5.01188E-02     4315    2.556|***      |         |         |         |         |         |         |         |         |         |
 7.94329E-02     7082    4.195|****     |         |         |         |         |         |         |         |         |         |
 1.25893E-01    17510   10.371|*********|         |         |         |         |         |         |         |         |         |
```

```
 1.99526E-01    34616   20.503|*********|*********|*        |         |         |         |         |         |         |
 3.16228E-01    60039   35.560|*********|*********|*********|******   |         |         |         |         |         |
 5.01188E-01   108300   64.145|*********|*********|*********|*********|*********|*********|****     |         |         |
 7.94329E-01   141186   83.623|mmmmmmmmmm|mmmmmmmmmm|mmmmmmmmmm|mmmmmmmmmm|mmmmmmmmmm|mmmmmmmmmm|mmmmmmmmmm|mmmm     |         |
 1.25893E+00   158736   94.017|*********|*********|*********|*********|*********|*********|*********|*********|*********|****     |
 1.99526E+00   165969   98.301|*********|*********|*********|*********|*********|*********|*********|*********|*********|******** |
 3.16228E+00   168501   99.801|*********|*********|*********|*********|*********|*********|*********|*********|*********|*********|
 5.01188E+00   168819   99.989|*********|*********|*********|*********|*********|*********|*********|*********|*********|*********|
 7.94329E+00   168836   99.999|*********|*********|*********|*********|*********|*********|*********|*********|*********|*********|
 1.00000E+01   168837  100.000|*********|*********|*********|*********|*********|*********|*********|*********|*********|*********|
    total      168837  100.000:--------10--------20--------30--------40--------50--------60--------70--------80--------90-------100

1cumulative unnormed tally for tally   4         nonzero tally mean(m) = 5.121E-01   nps =   5000000    print table 162

   abscissa     cum    ordinate                plot of the cumulative tally in the tally fluctuation chart bin from 0 to 100 percent
    tally    tally/nps  cum pct:--------10--------20--------30--------40--------50--------60--------70--------80--------90-------100
 1.995E-06  2.885E-13    0.000|         |         |         |         |         |         |         |         |         |         |
 3.162E-06  2.885E-13    0.000|         |         |         |         |         |         |         |         |         |         |
 5.012E-06  2.885E-13    0.000|         |         |         |         |         |         |         |         |         |         |
 7.943E-06  2.885E-13    0.000|         |         |         |         |         |         |         |         |         |         |
 1.259E-05  2.336E-12    0.000|         |         |         |         |         |         |         |         |         |         |
 1.995E-05  2.336E-12    0.000|         |         |         |         |         |         |         |         |         |         |
 3.162E-05  2.336E-12    0.000|         |         |         |         |         |         |         |         |         |         |
 5.012E-05  1.800E-11    0.000|         |         |         |         |         |         |         |         |         |         |
 7.943E-05  9.950E-11    0.000|         |         |         |         |         |         |         |         |         |         |
 1.259E-04  1.565E-10    0.000|         |         |         |         |         |         |         |         |         |         |
 1.995E-04  3.124E-10    0.000|         |         |         |         |         |         |         |         |         |         |
 3.162E-04  9.002E-10    0.000|         |         |         |         |         |         |         |         |         |         |
 5.012E-04  2.000E-09    0.000|         |         |         |         |         |         |         |         |         |         |
 7.943E-04  5.073E-09    0.000|         |         |         |         |         |         |         |         |         |         |
 1.259E-03  1.471E-08    0.000|         |         |         |         |         |         |         |         |         |         |
 1.995E-03  3.524E-08    0.000|         |         |         |         |         |         |         |         |         |         |
 3.162E-03  8.073E-08    0.000|         |         |         |         |         |         |         |         |         |         |
 5.012E-03  2.062E-07    0.001|         |         |         |         |         |         |         |         |         |         |
 7.943E-03  5.455E-07    0.003|         |         |         |         |         |         |         |         |         |         |
 1.259E-02  1.326E-06    0.008|         |         |         |         |         |         |         |         |         |         |
 1.995E-02  3.303E-06    0.019|         |         |         |         |         |         |         |         |         |         |
 3.162E-02  8.602E-06    0.050|         |         |         |         |         |         |         |         |         |         |
 5.012E-02  2.182E-05    0.126|         |         |         |         |         |         |         |         |         |         |
 7.943E-02  5.804E-05    0.336|         |         |         |         |         |         |         |         |         |         |
 1.259E-01  2.750E-04    1.591|**       |         |         |         |         |         |         |         |         |         |
 1.995E-01  8.274E-04    4.785|*****    |         |         |         |         |         |         |         |         |         |
 3.162E-01  2.152E-03   12.444|*********|**       |         |         |         |         |         |         |         |         |
 5.012E-01  6.030E-03   34.874|*********|*********|*********|*****    |         |         |         |         |         |         |
 7.943E-01  1.014E-02   58.631|mmmmmmmmmm|mmmmmmmmmm|mmmmmmmmmm|mmmmmmmmmm|mmmmmmmmmm|mmmmmmmmmm|         |         |         |         |
```

```
 1.259E+00  1.357E-02   78.470|*********|*********|*********|*********|*********|*********|********* |         |         |
 1.995E+00  1.579E-02   91.344|*********|*********|*********|*********|*********|*********|*********|*********|*        |
 3.162E+00  1.704E-02   98.524|*********|*********|*********|*********|*********|*********|*********|*********|*********|
 5.012E+00  1.727E-02   99.883|*********|*********|*********|*********|*********|*********|*********|*********|*********|
 7.943E+00  1.729E-02   99.990|*********|*********|*********|*********|*********|*********|*********|*********|*********|
 1.000E+01  1.729E-02  100.000|*********|*********|*********|*********|*********|*********|*********|*********|*********|
   total  1.72908E-02  100.000:--------10--------20--------30--------40--------50--------60--------70--------80--------90-------100

1status of the statistical checks used to form confidence intervals for the mean for each tally bin

 tally   result of statistical checks for the tfc bin (the first check not passed is listed) and error magnitude check for all bins

     4   passed the 10 statistical checks for the tally fluctuation chart bin result
         passed all bin error check:    64 tally bins all have relative errors less than 0.10 with no zero bins

 the 10 statistical checks are only for the tally fluctuation chart bin and do not apply to other tally bins.

1tally fluctuation charts

                     tally    4
         nps      mean     error   vov  slope    fom
       256000   8.2635E-03 0.0142 0.0008 10.0    1439
       512000   8.2151E-03 0.0100 0.0004 10.0    1461
       768000   8.2146E-03 0.0082 0.0003 10.0    1456
      1024000   8.1643E-03 0.0071 0.0002  8.2    1462
      1280000   8.1329E-03 0.0063 0.0002  5.0    1467
      1536000   8.1308E-03 0.0058 0.0001  4.8    1468
      1792000   8.1050E-03 0.0054 0.0001  5.0    1459
      2048000   8.1041E-03 0.0050 0.0001 10.0    1459
      2304000   8.1062E-03 0.0047 0.0001 10.0    1455
      2560000   8.1020E-03 0.0045 0.0001 10.0    1459
      2816000   8.1126E-03 0.0043 0.0001 10.0    1463
      3072000   8.1237E-03 0.0041 0.0001 10.0    1465
      3328000   8.1208E-03 0.0039 0.0001 10.0    1464
      3584000   8.1231E-03 0.0038 0.0001 10.0    1466
      3840000   8.1313E-03 0.0037 0.0001 10.0    1467
      4096000   8.1331E-03 0.0035 0.0001 10.0    1468
      4352000   8.1342E-03 0.0034 0.0000 10.0    1468
      4608000   8.1384E-03 0.0033 0.0000 10.0    1467
      4864000   8.1462E-03 0.0033 0.0000 10.0    1470
      5000000   8.1538E-03 0.0032 0.0000 10.0    1470

 ************************************************************************************************************************
 dump no.    3 on file runtp21      nps =     5000000     coll =     1692383003     ctm =       66.22   nrn =       13602974167
```

```
          3 warning messages so far.

     run terminated when     5000000  particle histories were done.

     computer time =   67.07 minutes

     mcnp     version 5     11112005                     09/03/14 14:05:40                     probid =  09/03/14 13:58:22
```

Tally results for site 1

```
1tally   4        nps =     5000000
           tally type 4    track length estimate of particle flux.      units   1/cm**2
           tally for  neutrons

           volumes
                   cell:       6            8            9           10           11           12           13
                         2.12058E+00  2.12058E+00  2.12058E+00  2.12058E+00  2.12058E+00  2.12058E+00  2.12058E+00
                   cell:      14           15           16           17           18           19
                         2.12058E+00  2.12058E+00  2.12058E+00  2.12058E+00  2.12058E+00  2.12058E+00

 cell  6
      energy
    5.0000E-07   4.69731E-03 0.0037
    5.0000E-01   3.93647E-03 0.0042
    1.2000E+01   1.95079E-02 0.0015
      total      2.81416E-02 0.0014

 cell  8
      energy
    5.0000E-07   3.98886E-03 0.0040
    5.0000E-01   2.31866E-03 0.0054
    1.2000E+01   5.10380E-03 0.0026
      total      1.14113E-02 0.0022

 cell  9
      energy
    5.0000E-07   3.16721E-03 0.0044
    5.0000E-01   1.59694E-03 0.0065
    1.2000E+01   2.62540E-03 0.0037
      total      7.38954E-03 0.0027
```

```
cell  10
     energy
   5.0000E-07   2.40278E-03 0.0050
   5.0000E-01   1.09694E-03 0.0077
   1.2000E+01   1.64296E-03 0.0046
     total      5.14268E-03 0.0033

cell  11
     energy
   5.0000E-07   1.81032E-03 0.0057
   5.0000E-01   7.56502E-04 0.0092
   1.2000E+01   1.14459E-03 0.0055
     total      3.71141E-03 0.0038

cell  12
     energy
   5.0000E-07   1.32547E-03 0.0066
   5.0000E-01   5.22054E-04 0.0110
   1.2000E+01   8.41170E-04 0.0065
     total      2.68870E-03 0.0045

cell  13
     energy
   5.0000E-07   9.49872E-04 0.0077
   5.0000E-01   3.78393E-04 0.0131
   1.2000E+01   6.38036E-04 0.0074
     total      1.96630E-03 0.0052

cell  14
     energy
   5.0000E-07   6.80287E-04 0.0089
   5.0000E-01   2.64992E-04 0.0153
   1.2000E+01   4.87452E-04 0.0085
     total      1.43273E-03 0.0059

cell  15
     energy
   5.0000E-07   4.92232E-04 0.0105
   5.0000E-01   1.83793E-04 0.0181
   1.2000E+01   3.79263E-04 0.0094
     total      1.05529E-03 0.0069

cell  16
     energy
   5.0000E-07   3.52033E-04 0.0124
```

```
   5.0000E-01   1.31669E-04 0.0207
   1.2000E+01   3.03533E-04 0.0105
     total      7.87236E-04 0.0078

 cell  17
      energy
   5.0000E-07   2.40505E-04 0.0152
   5.0000E-01   9.89879E-05 0.0242
   1.2000E+01   2.43885E-04 0.0115
     total      5.83378E-04 0.0090

 cell  18
      energy
   5.0000E-07   1.56089E-04 0.0182
   5.0000E-01   7.44446E-05 0.0278
   1.2000E+01   2.01997E-04 0.0125
     total      4.32530E-04 0.0101

 cell  19
      energy
   5.0000E-07   8.61149E-05 0.0216
   5.0000E-01   4.76895E-05 0.0321
   1.2000E+01   1.65939E-04 0.0137
     total      2.99743E-04 0.0111
 ============================================================================================================================
          results of 10 statistical checks for the estimated answer for the tally fluctuation chart (tfc) bin of tally   4

 tfc bin     --mean--      ---------relative error---------      ----variance of the variance----      --figure of merit--     -pdf-
 behavior    behavior      value   decrease   decrease rate      value   decrease   decrease rate       value     behavior     slope

 desired      random       <0.10      yes      1/sqrt(nps)       <0.10      yes        1/nps          constant    random      >3.00
 observed     random        0.00      yes          yes            0.00      yes         yes           constant    random      10.00
 passed?        yes          yes      yes          yes              yes      yes         yes              yes        yes         yes
 ============================================================================================================================
```

Tally results for site 3

```
1tally   4        nps =     5000000
           tally type 4    track length estimate of particle flux.      units   1/cm**2
           tally for  neutrons

           volumes
                   cell:      21           22           23           6            8            9           10
```

```
                    2.12058E+00  2.12058E+00  2.12058E+00  2.12058E+00  2.12058E+00  2.12058E+00  2.12058E+00
               cell:      11           12           13           14           15           16           17
                    2.12058E+00  2.12058E+00  2.12058E+00  2.12058E+00  2.12058E+00  2.12058E+00  2.12058E+00
               cell:      18           19
                    2.12058E+00  2.12058E+00

cell  21
     energy
   5.0000E-07   1.85778E-03 0.0066
   5.0000E-01   3.93417E-04 0.0143
   1.2000E+01   4.47405E-04 0.0144
     total      2.69861E-03 0.0056

cell  22
     energy
   5.0000E-07   1.92256E-03 0.0062
   5.0000E-01   4.34501E-04 0.0139
   1.2000E+01   5.03187E-04 0.0153
     total      2.86025E-03 0.0055

cell  23
     energy
   5.0000E-07   1.90889E-03 0.0061
   5.0000E-01   4.43064E-04 0.0138
   1.2000E+01   4.88710E-04 0.0158
     total      2.84066E-03 0.0055

cell  6
     energy
   5.0000E-07   1.78296E-03 0.0063
   5.0000E-01   4.05975E-04 0.0142
   1.2000E+01   4.76004E-04 0.0148
     total      2.66494E-03 0.0055

cell  8
     energy
   5.0000E-07   1.57400E-03 0.0067
   5.0000E-01   3.44913E-04 0.0152
   1.2000E+01   3.90652E-04 0.0142
     total      2.30956E-03 0.0057

cell  9
     energy
   5.0000E-07   1.34320E-03 0.0073
   5.0000E-01   2.74284E-04 0.0170
```

```
   1.2000E+01   3.09146E-04 0.0149
     total      1.92663E-03 0.0062

cell  10
     energy
   5.0000E-07   1.10106E-03 0.0079
   5.0000E-01   2.15645E-04 0.0188
   1.2000E+01   2.35757E-04 0.0162
     total      1.55246E-03 0.0068

cell  11
     energy
   5.0000E-07   8.62244E-04 0.0088
   5.0000E-01   1.65087E-04 0.0211
   1.2000E+01   1.73521E-04 0.0175
     total      1.20085E-03 0.0075

cell  12
     energy
   5.0000E-07   6.68680E-04 0.0099
   5.0000E-01   1.16787E-04 0.0250
   1.2000E+01   1.22204E-04 0.0213
     total      9.07671E-04 0.0086

cell  13
     energy
   5.0000E-07   5.13779E-04 0.0112
   5.0000E-01   8.74317E-05 0.0285
   1.2000E+01   9.06796E-05 0.0238
     total      6.91890E-04 0.0097

cell  14
     energy
   5.0000E-07   3.82701E-04 0.0129
   5.0000E-01   6.95758E-05 0.0335
   1.2000E+01   6.46899E-05 0.0276
     total      5.16966E-04 0.0112

cell  15
     energy
   5.0000E-07   2.88611E-04 0.0151
   5.0000E-01   4.85210E-05 0.0407
   1.2000E+01   4.81359E-05 0.0322
     total      3.85268E-04 0.0133
```

```
 cell  16
      energy
    5.0000E-07   2.15239E-04 0.0168
    5.0000E-01   3.34220E-05 0.0445
    1.2000E+01   3.42232E-05 0.0377
      total      2.82884E-04 0.0148

 cell  17
      energy
    5.0000E-07   1.52513E-04 0.0200
    5.0000E-01   2.69073E-05 0.0501
    1.2000E+01   2.42621E-05 0.0396
      total      2.03683E-04 0.0173

 cell  18
      energy
    5.0000E-07   1.01948E-04 0.0234
    5.0000E-01   1.85648E-05 0.0613
    1.2000E+01   1.90328E-05 0.0507
      total      1.39546E-04 0.0203

 cell  19
      energy
    5.0000E-07   5.57541E-05 0.0293
    5.0000E-01   1.22074E-05 0.0716
    1.2000E+01   1.45508E-05 0.0577
      total      8.25124E-05 0.0249
 ============================================================================================================================================
           results of 10 statistical checks for the estimated answer for the tally fluctuation chart (tfc) bin of tally   4
 tfc bin     --mean--      ---------relative error---------      ----variance of the variance----      --figure of merit--     -pdf-
 behavior    behavior      value   decrease   decrease rate      value   decrease   decrease rate       value     behavior     slope

 desired      random       <0.10      yes      1/sqrt(nps)       <0.10      yes        1/nps           constant    random      >3.00
 observed     random        0.01      yes          yes            0.00      yes         yes            constant    random       4.11
 passed?        yes          yes      yes          yes              yes      yes         yes               yes        yes         yes
 ============================================================================================================================================
```

Tally results for site 4

```
1tally   4        nps =     5000000
           tally type 4    track length estimate of particle flux.      units   1/cm**2
           tally for  neutrons
           volumes
```

```
                cell:      21          22          23           6           8           9          10
                      2.12058E+00 2.12058E+00 2.12058E+00 2.12058E+00 2.12058E+00 2.12058E+00 2.12058E+00
                cell:      11          12          13          14          15          16          17
                      2.12058E+00 2.12058E+00 2.12058E+00 2.12058E+00 2.12058E+00 2.12058E+00 2.12058E+00
                cell:      18          19
                      2.12058E+00 2.12058E+00

cell  21
     energy
   5.0000E-07   5.79782E-04 0.0115
   5.0000E-01   1.16427E-04 0.0267
   1.2000E+01   1.23007E-04 0.0285
     total      8.19216E-04 0.0102

cell  22
     energy
   5.0000E-07   6.05688E-04 0.0109
   5.0000E-01   1.18414E-04 0.0266
   1.2000E+01   1.31829E-04 0.0303
     total      8.55930E-04 0.0099

cell  23
     energy
   5.0000E-07   5.97311E-04 0.0109
   5.0000E-01   1.17348E-04 0.0265
   1.2000E+01   1.32576E-04 0.0303
     total      8.47235E-04 0.0099

cell  6
     energy
   5.0000E-07   5.71380E-04 0.0108
   5.0000E-01   1.09356E-04 0.0270
   1.2000E+01   1.19996E-04 0.0301
     total      8.00732E-04 0.0098

cell  8
     energy
   5.0000E-07   5.25671E-04 0.0114
   5.0000E-01   1.12583E-04 0.0279
   1.2000E+01   1.10095E-04 0.0282
     total      7.48348E-04 0.0101

cell  9
     energy
   5.0000E-07   4.61037E-04 0.0122
```

```
   5.0000E-01   8.81480E-05 0.0305
   1.2000E+01   9.54914E-05 0.0289
     total      6.44676E-04 0.0108

cell  10
     energy
   5.0000E-07   3.86677E-04 0.0132
   5.0000E-01   7.60727E-05 0.0327
   1.2000E+01   8.47046E-05 0.0292
     total      5.47454E-04 0.0115

cell  11
     energy
   5.0000E-07   3.21984E-04 0.0144
   5.0000E-01   6.15678E-05 0.0355
   1.2000E+01   6.50473E-05 0.0316
     total      4.48599E-04 0.0125

cell  12
     energy
   5.0000E-07   2.58694E-04 0.0161
   5.0000E-01   4.52142E-05 0.0396
   1.2000E+01   5.06457E-05 0.0358
     total      3.54554E-04 0.0140

cell  13
     energy
   5.0000E-07   2.08313E-04 0.0180
   5.0000E-01   3.51844E-05 0.0462
   1.2000E+01   3.94961E-05 0.0387
     total      2.82994E-04 0.0157

cell  14
     energy
   5.0000E-07   1.56538E-04 0.0201
   5.0000E-01   2.58292E-05 0.0515
   1.2000E+01   2.90616E-05 0.0443
     total      2.11429E-04 0.0176

cell  15
     energy
   5.0000E-07   1.21530E-04 0.0229
   5.0000E-01   2.25162E-05 0.0588
   1.2000E+01   2.45126E-05 0.0515
     total      1.68559E-04 0.0202
```

```
cell  16
     energy
   5.0000E-07   9.30073E-05 0.0264
   5.0000E-01   1.57673E-05 0.0674
   1.2000E+01   1.63243E-05 0.0532
     total      1.25099E-04 0.0228

cell  17
     energy
   5.0000E-07   6.52621E-05 0.0298
   5.0000E-01   1.17706E-05 0.0838
   1.2000E+01   1.31643E-05 0.0634
     total      9.01971E-05 0.0264

cell  18
     energy
   5.0000E-07   4.57918E-05 0.0359
   5.0000E-01   7.66015E-06 0.0962
   1.2000E+01   9.89520E-06 0.0703
     total      6.33472E-05 0.0308

cell  19
     energy
   5.0000E-07   2.58593E-05 0.0437
   5.0000E-01   4.31673E-06 0.1094
   1.2000E+01   7.01700E-06 0.0804
     total      3.71931E-05 0.0363
```

results of 10 statistical checks for the estimated answer for the tally fluctuation chart (tfc) bin of tally 4

tfc bin behavior	--mean-- behavior	---------relative error--------- value	decrease	decrease rate	----variance of the variance---- value	decrease	decrease rate	--figure of merit-- value	behavior	-pdf- slope
desired	random	<0.10	yes	1/sqrt(nps)	<0.10	yes	1/nps	constant	random	>3.00
observed	random	0.01	yes	yes	0.00	yes	yes	constant	random	10.00
passed?	yes	yes	yes	yes	yes	yes	yes	yes	yes	yes

Appendix B

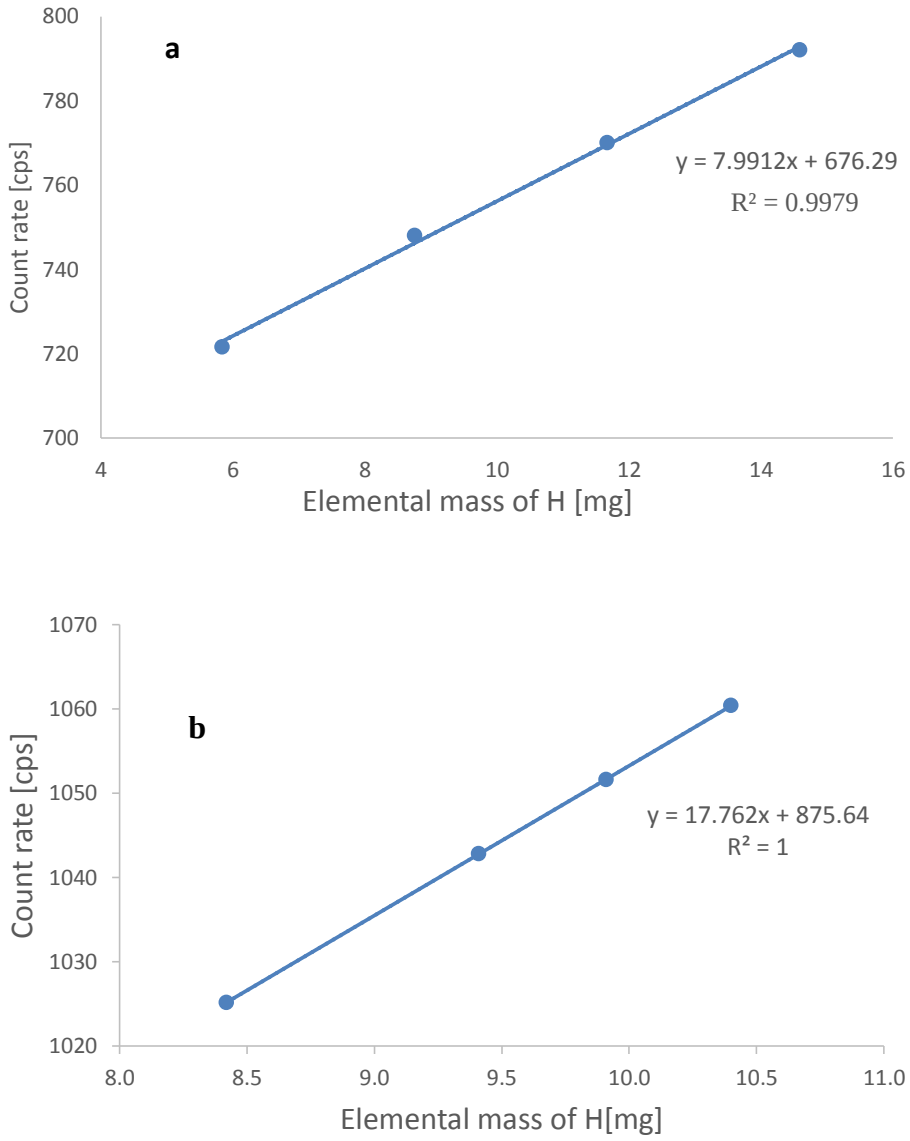

Figure 6.1. The sensitivity curve of hydrogen concentration values against the peak area at 2223keV a) for configuration A and b) for configuration B

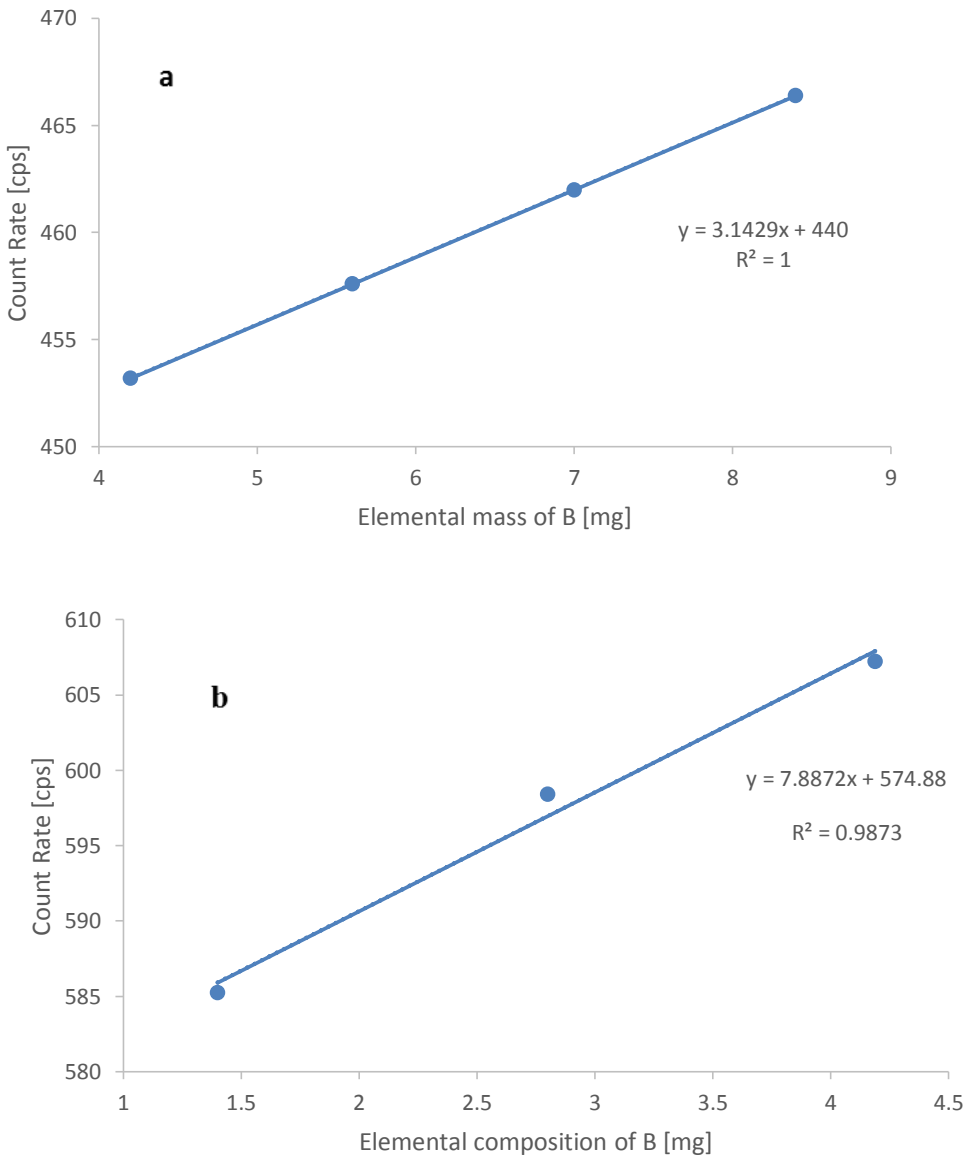

Figure 6.2. The sensitivity curve of boron concentration values against the peak area at 478 keV a) for configuration A and b) for configuration B

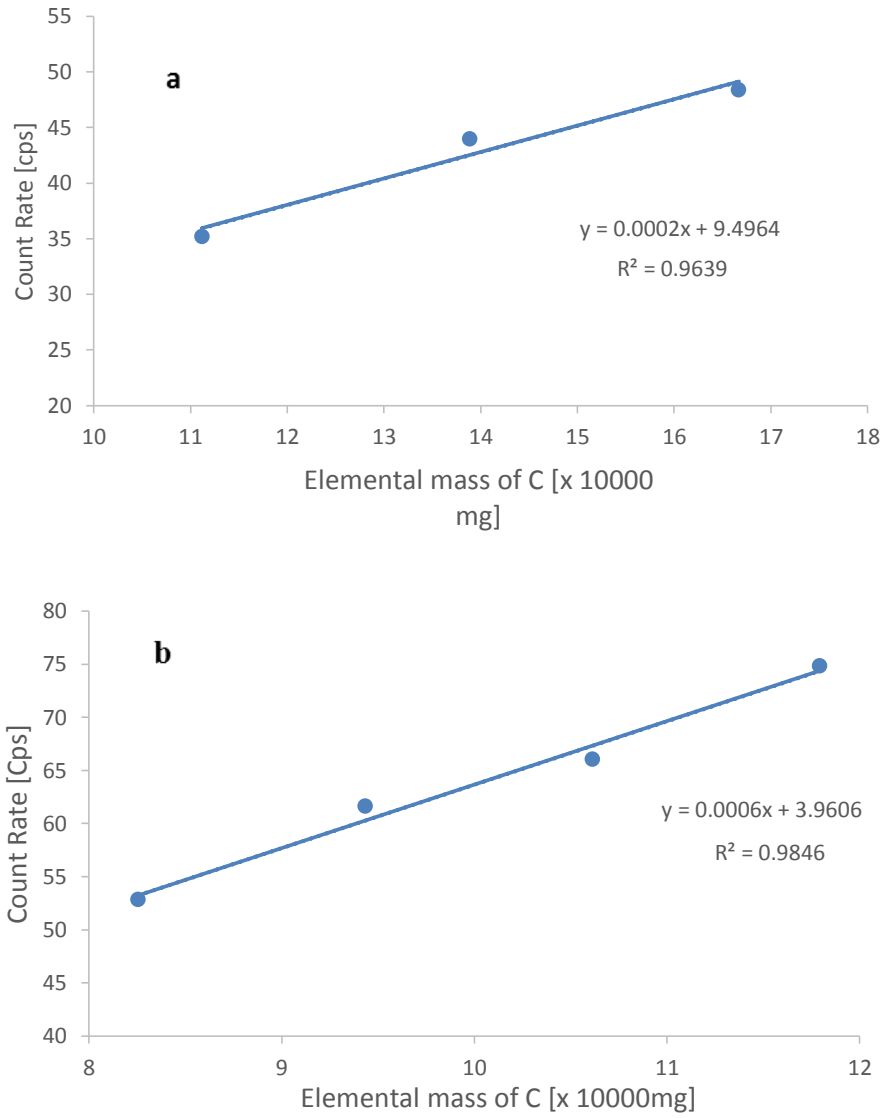

Figure 6.3. The sensitivity curve of carbon concentration values against the peak area at 1261 keV a) for configuration A and b) for configuration B

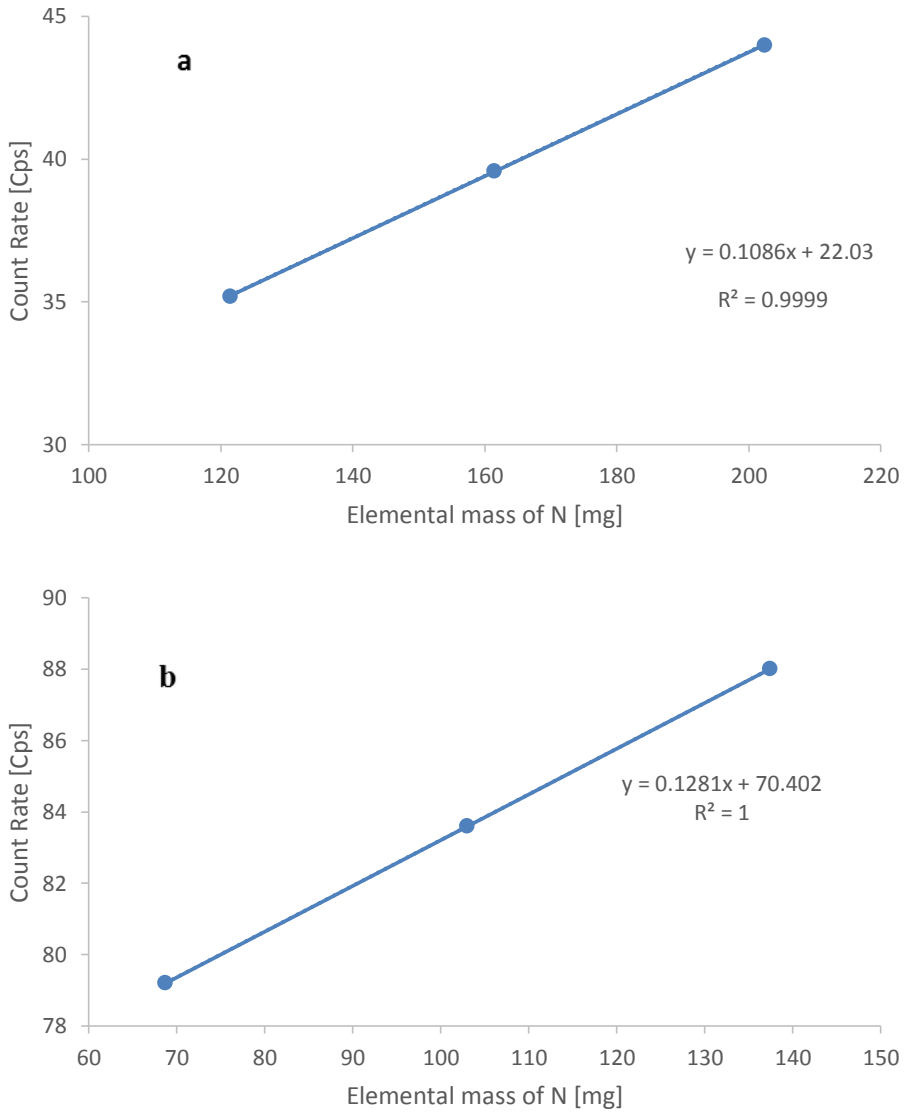

Figure 6.4. The sensitivity curve of nitrogen concentration values against the peak area at 1885 keV a) for configuration A and b) for configuration B

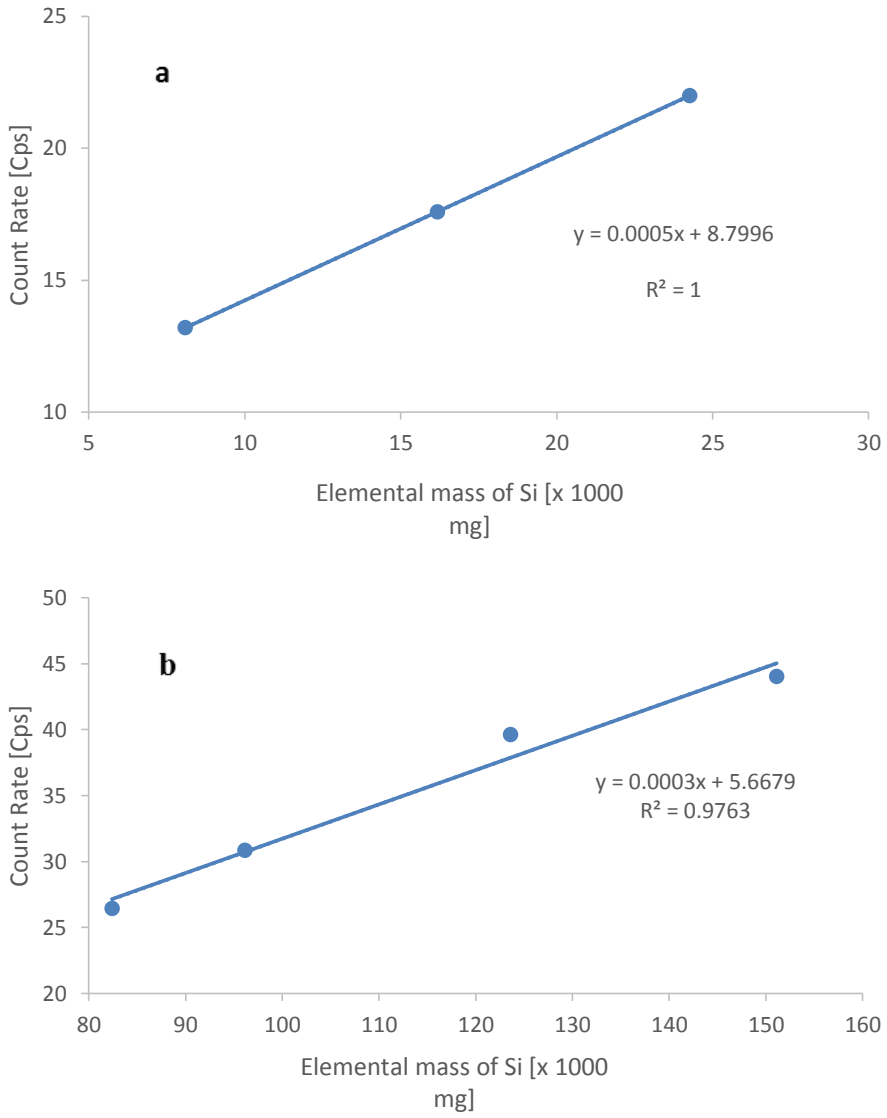

Figure 6.5. The sensitivity curve of silicon concentration values against the peak area at 3539 keV a) for configuration A and b) for configuration B

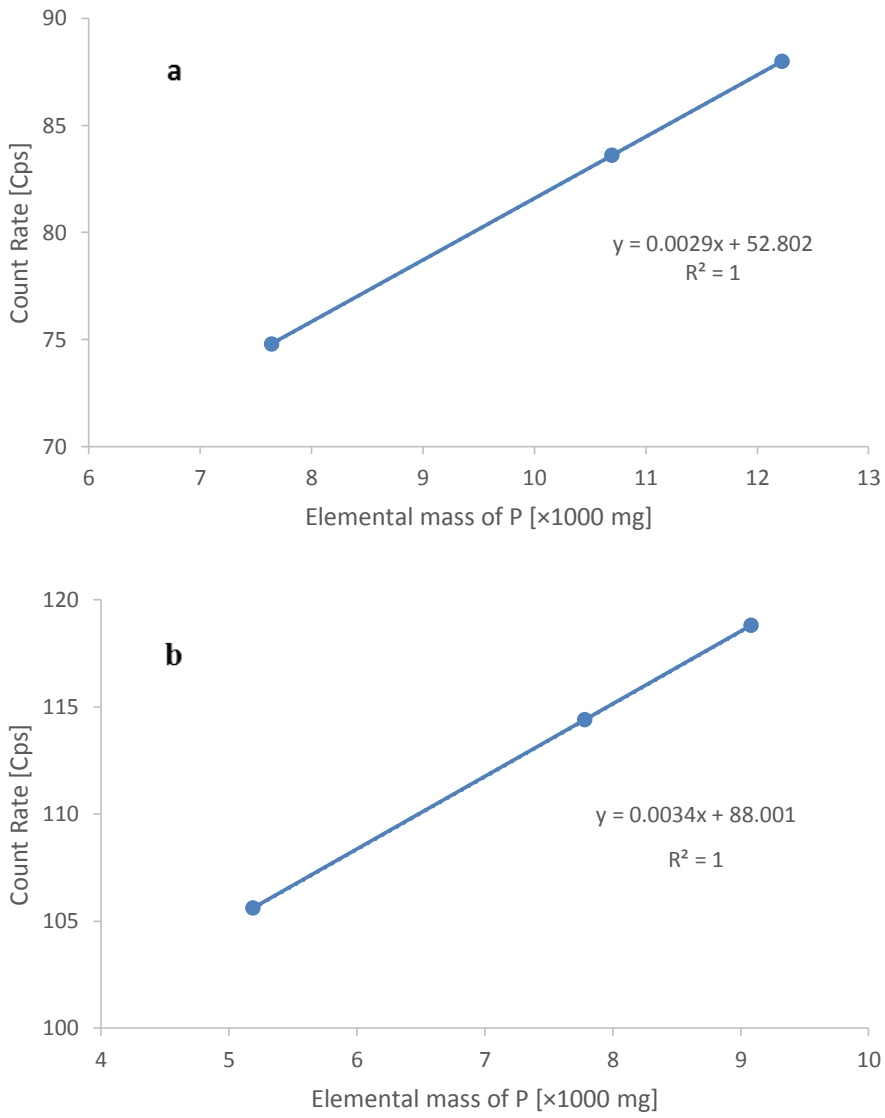

Figure 6.6. The sensitivity curve of phosphorus concentration values against the peak area at 638 keV a) for configuration A and b) for configuration B